# LONG-TERM SUBSURFACE DRAINAGE EFFECTS ON SOIL PHYSICAL AND HYDRAULIC PROPERTIES

by

**Daniel Welage**

**A Thesis**

*Submitted to the Faculty of Purdue University*

*In Partial Fulfillment of the Requirements for the degree of*

**Master of Science**


Department of Agronomy

West Lafayette, Indiana

August 2020

**THE PURDUE UNIVERSITY GRADUATE SCHOOL**

**STATEMENT OF COMMITTEE APPROVAL**

**Dr. Eileen J. Kladivko, Chair**

Department of Agronomy

**Dr. Jason P. Ackerson**

Department of Agronomy

**Dr. Laura C. Bowling**

Department of Agronomy

**Approved by:**

Dr. Ronald F. Turco

# ACKNOWLEDGMENTS

I would like to thank my major professor, Dr. Eileen Kladivko, for her support, advice, and guidance during my graduate studies. Thank you for giving me this opportunity and for helping me become a better researcher, student, and person. I would also like to thank the members of my committee, Dr. Jason Ackerson and Dr. Laura Bowling, for their time and feedback on my project. Thank you to the entire Agronomy department for your assistance during my time at Purdue.

Thank you to my fellow graduate students in the Kladivko lab, Kevin Mitchell and Caleb Smith, for your help with field and lab work, support, and friendship. Thank you to Stacy Zuber and Amanda Modglin for assistance with field work. I would also like to thank Dena Anderson for her help with the soil profile descriptions, Dr. Daniel Hirmas for his help with the soil pit sampling, and the entire SEPAC crew for their many years of dedicated work on this project. Last but not least, I want to thank my family and friends for their love and support throughout my college career.

This project was supported in part by the Purdue Agricultural Research Programs, and USDA National Institute of Food and Agriculture, Hatch project 87887.

# TABLE OF CONTENTS

LIST OF TABLES ..... 5
LIST OF FIGURES ..... 8
ABSTRACT ..... 12
CHAPTER 1. LITERATURE REVIEW ..... 13
1.1 Introduction ..... 13
1.2 Water Retention and Bulk Density ..... 14
1.3 Water Flow ..... 17
1.4 Soil Structure and Morphological Development ..... 22
1.5 Research Objectives and Hypotheses ..... 24
CHAPTER 2. METHODS ..... 25
2.1 Site Description ..... 25
2.2 Soil Profile Descriptions ..... 27
2.3 Bulk Density ..... 27
2.4 Water Retention ..... 28
2.5 Saturated Hydraulic Conductivity ..... 29
2.6 Statistical Analysis ..... 31
CHAPTER 3. RESULTS AND DISCUSSION ..... 32
3.1 Soil Profile Descriptions ..... 32
3.2 Bulk Density ..... 47
3.3 Total Porosity ..... 55
3.4 Water Retention ..... 61
3.4.1 Samples from 0-5 cm, 5-15 cm, and 15-30 cm ..... 61
3.4.2 Samples from soil pit horizons ..... 63
3.4.3 Water Retention Summary ..... 64
3.5 Saturated Hydraulic Conductivity ..... 83
3.6 Summary ..... 90
CHAPTER 4. CONCLUSIONS AND FUTURE WORK ..... 93
REFERENCES ..... 96
APPENDIX AUGER HOLE METHOD ..... 104

# LIST OF TABLES

Table 2.1. Horizon (Depth) for core samples from each soil pit. ..... 28

Table 3.1. Soil profile description of the 5 m Block 1 soil pit. ..... 35

Table 3.2. Soil profile description of the 5 m Block 2 soil pit. ..... 38

Table 3.3. Soil profile description of the 40 m Block 1 soil pit. ..... 41

Table 3.4. Soil profile description of the 40 m Block 2 soil pit. ..... 44

Table 3.5. Soil bulk density (g $cm^{-3}$) at multiple depths, sampled with the short core method. Each value represents the mean of both blocks and 8 subplots (n=16). Values within the same depth that contain the same letter are not significantly different as determined by an LSMeans test ($p \leq 0.10$). Standard deviations are presented in parentheses. ..... 50

Table 3.6. Soil bulk density (g $cm^{-3}$), sampled with the hydraulic probe. Each value represents the mean of both blocks and 8 subplots (n=16). Values within the same depth that contain the same letter are not significantly different as determined by an LSMeans test ($p \leq 0.10$). Standard deviations are presented in parentheses. ..... 51

Table 3.7. Soil pit bulk density (g $cm^{-3}$). Each value represents the mean of both blocks and 5 subsamples (n=10). Values within the same horizon that contain the same letter are not significantly different as determined by an LSMeans test ($p \leq 0.10$). Standard deviations are presented in parentheses. ..... 53

Table 3.8. Soil total porosity ($cm^3$ $cm^{-3}$). Each value represents the mean of both blocks and 8 subplots (n=16). Values within the same depth that contain the same letter are not significantly different as determined by an LSMeans test ($p \leq 0.10$). Standard deviations are presented in parentheses. ..... 56

Table 3.9. Total porosity ($cm^3$ $cm^{-3}$) from the hydraulic probe samples. Each value represents the mean of both blocks and 8 subplots (n=16). Values within the same depth that contain the same letter are not significantly different as determined by an LSMeans test ($p \leq 0.10$). Standard deviations are presented in parentheses. ..... 57

Table 3.10. Soil pit total porosity ($cm^3$ $cm^{-3}$). Each value represents the mean of both blocks and 5 subsamples (n=10). Values within the same horizon that contain the same letter are not significantly different as determined by an LSMeans test ($p \leq 0.10$). Standard deviations are presented in parentheses. ..... 59

Table 3.11. Volumetric water contents ($cm^3$ $cm^{-3}$) at 0-5 cm at multiple water potentials. Each value represents the mean of both blocks and 8 subplots (n=16). Values within the same water potential that contain the same letter are not significantly different as determined by an LSMeans test ($p \leq 0.10$). Standard deviations are presented in parentheses. ..... 65

Table 3.12. Volumetric water contents ($cm^3$ $cm^{-3}$) at 5-15 cm at multiple water potentials. Each value represents the mean of both blocks and 8 subplots (n=16). Values within the same water

potential that contain the same letter are not significantly different as determined by an LSMeans test ($p \leq 0.10$). Standard deviations are presented in parentheses. ..... 68

Table 3.13. Volumetric water contents ($cm^3\ cm^{-3}$) at 15-30 cm at multiple water potential. Each value represents the mean of both blocks and 8 subplots (n=16). Values within the same water potential that contain the same letter are not significantly different as determined by an LSMeans test ($p \leq 0.10$). Standard deviations are presented in parentheses. ..... 69

Table 3.14. Water holding capacity ($cm^3\ cm^{-3}$) at 0-5 cm, 5-15 cm, and 15-30 cm. Each value represents the mean of both blocks and 8 subplots (n=16). Values within the same depth that contain the same letter are not significantly different as determined by an LSMeans test ($p \leq 0.10$). Standard deviations are presented in parentheses. ..... 71

Table 3.15. Soil pit volumetric water contents ($cm^3\ cm^{-3}$) in the Ap2 horizon at multiple water potentials. Each value represents the mean of both blocks and 5 subsamples (n=10). Values within the same water potential that contain the same letter are not significantly different as determined by an LSMeans test ($p \leq 0.10$). Standard deviations are presented in parentheses. ..... 73

Table 3.16. Soil pit volumetric water contents ($cm^3\ cm^{-3}$) in the Btg1 horizon at multiple water potentials. Each value represents the mean of both blocks and 5 subsamples (n=10). Values within the same water potential that contain the same letter are not significantly different as determined by an LSMeans test ($p \leq 0.10$). Standard deviations are presented in parentheses. ..... 75

Table 3.17. Soil pit volumetric water contents ($cm^3\ cm^{-3}$) in the Btg1/Btg2 horizon at multiple water potentials. Each value represents the mean of both blocks and 5 subsamples (n=10). Values within the same water potential that contain the same letter are not significantly different as determined by an LSMeans test ($p \leq 0.10$). Standard deviations are presented in parentheses. .... 78

Table 3.18. Soil pit volumetric water contents ($cm^3\ cm^{-3}$) in the Btg2/Bt/Btg3 horizon at multiple water potentials. Each value represents the mean of both blocks and 5 subsamples (n=10). Values within the same water potential that contain the same letter are not significantly different as determined by an LSMeans test ($p \leq 0.10$). Standard deviations are presented in parentheses. .... 79

Table 3.19. Soil pit gravimetric water contents ($g\ g^{-1}$) in the Ap1, Ap2, Btg1/Btg2, and Btg2/Bt/Btg3 horizons at -1500 kPa water potential. Each value represents the mean of both blocks and 2 subsamples (n=4). Values within the same depth that contain the same letter are not significantly different as determined by an LSMeans test ($p \leq 0.10$). Standard deviations are presented in parentheses. ..... 82

Table 3.20. Auger hole method Ksat ($cm\ day^{-1}$). Statistical analyses were not performed on the data due to measurements only taken in the 40 m treatment. ..... 87

Table 3.21. Saturated hydraulic conductivity ($cm\ day^{-1}$) measured with the Guelph permeameter at a depth of 63.5 cm. Each value represents the mean of both blocks and 5 subsamples (n=10). Values that contain the same letter are not significantly different as determined by an LSMeans test ($p \leq 0.10$). Standard deviations are presented in parentheses. ..... 87

Table 3.22. Saturated hydraulic conductivity ($cm\ day^{-1}$) measured by the slug test. Statistical analyses were not performed on the data due to the high variation and recognizing that differences among treatments would not be detected. ..... 88

Table 3.23. Arithmetic mean, standard deviation (SD), and inter-quartile range (IQR) of saturated hydraulic conductivity (cm $day^{-1}$) measured using the constant head method on the soil pit cores. Each value represents both blocks and 5 subsamples (n=10). ..... 89

Table 3.24. Statistical analysis of saturated hydraulic conductivity data presented in the previous table. Data were transformed for the analysis but are presented in back-transformed units (cm $day^{-1}$). LSMeans are presented. Each value represents the mean of both blocks and 5 subsamples (n=10). Values within the same horizon that contain the same letter are not significantly different as determined by an LSMeans test ($p \leq 0.10$). ..... 89

# LIST OF FIGURES

Figure 2.1. Plot diagram of the SEPAC drainage experimental site. ..... 26

Figure 3.1. Soil profile of the 5 m Block 1 soil pit. ..... 37

Figure 3.2. Soil profile of the 5 m Block 2 soil pit. ..... 40

Figure 3.3. Soil profile of the 40 m Block 1 soil pit. ..... 43

Figure 3.4. Soil profile of the 40 m Block 2 soil pit. ..... 46

Figure 3.5. Soil bulk density (g $cm^{-3}$) at multiple depths, sampled with the short core method. Each data point represents the mean of both blocks and 8 subplots (n=16). Data points within the same depth that contain the same letter are not significantly different as determined by an LSMeans test ($p \leq 0.10$). Data points that do not contain a letter are not significantly different than any other point within that depth. ..... 50

Figure 3.6. Soil bulk density sampled with the short core method spacing*block effect at 0-5 cm depth increment. Each value represents the mean of 8 subplots (n=8). Values that contain the same letter are not significantly different as determined by an LSMeans test ($p \leq 0.10$). ..... 51

Figure 3.7. Soil bulk density (g $cm^{-3}$), sampled with the hydraulic probe. Each data point represents the mean of both blocks and 8 subplots (n=16). Data points within the same depth that contain the same letter are not significantly different as determined by an LSMeans test ($p \leq 0.10$). Data points that do not contain a letter are not significantly different than any other point within that depth.52

Figure 3.8. Soil bulk density sampled with the hydraulic probe, spacing*block effect at 75-100 cm. Each value represents the mean of 8 subplots (n=8). Values that contain the same letter are not significantly different as determined by an LSMeans test ($p \leq 0.10$). ..... 52

Figure 3.9. Soil pit bulk density (g $cm^{-3}$). Each data point represents the mean of both blocks and 5 subsamples (n=10). Data points within the same horizon that contain the same letter are not significantly different as determined by an LSMeans test ($p \leq 0.10$). Data points that do not contain a letter are not significantly different than any other point within that horizon. ..... 53

Figure 3.10. Soil pit bulk density spacing*block effect in the Btg1 horizon. Each value represents the mean of 5 subsamples (n=5). Values that contain the same letter are not significantly different as determined by an LSMeans test ($p \leq 0.10$). ..... 54

Figure 3.11. Soil total porosity ($cm^3$ $cm^{-3}$). Each data point represents the mean of both blocks and 8 subplots (n=16). Data points within the same depth that contain the same letter are not significantly different as determined by an LSMeans test ($p \leq 0.10$). Data points that do not contain a letter are not significantly different than any other point within that depth. ..... 56

Figure 3.12. Soil total porosity spacing*block effect at 0-5 cm depth increment. Each value represents the mean of 8 subplots (n=8). Values that contain the same letter are not significantly different as determined by an LSMeans test ($p \leq 0.10$). ..... 57

Figure 3.13. Total porosity ($cm^3$ $cm^{-3}$) from the hydraulic probe samples. Each data point represents the mean of both blocks and 8 subplots (n=16). Data points within the same depth that contain the same letter are not significantly different as determined by an LSMeans test ($p \leq 0.10$). Data points that do not contain a letter are not significantly different than any other point within that depth. ..... 58

Figure 3.14. Total porosity from the hydraulic probe samples, spacing*block effect at 75-100 cm. Each value represents the mean of 8 subplots (n=8). Values that contain the same letter are not significantly different as determined by an LSMeans test ($p \leq 0.10$). ..... 58

Figure 3.15. Soil pit total porosity ($cm^3$ $cm^{-3}$). Each data point represents the mean of both blocks and 5 subsamples (n=10). Data points within the same horizon that contain the same letter are not significantly different as determined by an LSMeans test ($p \leq 0.10$). Data points that do not contain a letter are not significantly different than any other point within that horizon. ..... 59

Figure 3.16. Soil pit total porosity spacing*block effect in the Btg1 horizon. Each value represents the mean of 5 subsamples (n=5). Values that contain the same letter are not significantly different as determined by an LSMeans test ($p \leq 0.10$). ..... 60

Figure 3.17. Water retention curves at 0-5 cm at multiple water potentials. Each data point represents the mean of both blocks and 8 subplots (n=16). Data points within the same water potential that contain the same letter are not significantly different as determined by an LSMeans test ($p \leq 0.10$). Data points that do not contain a letter are not significantly different than any other point within that water potential. ..... 65

Figure 3.18. Water retention at -4.9 kPa spacing*block effect at 0-5 cm depth. Each value represents the mean of 8 subplots (n=8). Values that contain the same letter are not significantly different as determined by an LSMeans test ($p \leq 0.10$). ..... 66

Figure 3.19. Water retention at -9.8 kPa spacing*block effect at 0-5 cm depth. Each value represents the mean of 8 subplots (n=8). Values that contain the same letter are not significantly different as determined by an LSMeans test ($p \leq 0.10$). ..... 66

Figure 3.20. Water retention at -33 kPa spacing*block effect at 0-5 cm depth. Each value represents the mean of 8 subplots (n=8). Values that contain the same letter are not significantly different as determined by an LSMeans test ($p \leq 0.10$). ..... 67

Figure 3.21. Water retention at -1500 kPa spacing*block effect at 0-5 cm depth. Each value represents the mean of 8 subplots (n=8). Values that contain the same letter are not significantly different as determined by an LSMeans test ($p \leq 0.10$). ..... 67

Figure 3.22. Water retention curves at 5-15 cm at multiple water potentials. Each data point represents the mean of both blocks and 8 subplots (n=16). Data points within the same water potential that contain the same letter are not significantly different as determined by an LSMeans test ($p \leq 0.10$). Data points that do not contain a letter are not significantly different than any other point within that water potential. ..... 68

Figure 3.23. Water retention at -1500 kPa spacing*block effect at 5-15 cm depth. Each value represents the mean of 8 subplots (n=8). Values that contain the same letter are not significantly different as determined by an LSMeans test ($p \leq 0.10$). ..... 69

Figure 3.24. Water retention curves at 15-30 cm at multiple water potentials. Each data point represents the mean of both blocks and 8 subplots (n=16). Data points within the same water potential that contain the same letter are not significantly different as determined by an LSMeans test ($p \leq 0.10$). Data points that do not contain a letter are not significantly different than any other point within that water potential. ..... 70

Figure 3.25. Water retention at -1500 kPa spacing*block effect at 15-30 cm depth. Each value represents the mean of 8 subplots (n=8). Values that contain the same letter are not significantly different as determined by an LSMeans test ($p \leq 0.10$). ..... 70

Figure 3.26. Water holding capacity ($cm^3\ cm^{-3}$) at 0-5 cm, 5-15 cm, and 15-30 cm. Each data point represents the mean of both blocks and 8 subplots (n=16). Data points within the same depth that contain the same letter are not significantly different as determined by an LSMeans test ($p \leq 0.10$). Data points that do not contain a letter are not significantly different than any other point within that depth. ..... 71

Figure 3.27. Water holding capacity spacing*block effect at 0-5 cm depth. Each value represents the mean of 8 subplots (n=8). Values that contain the same letter are not significantly different as determined by an LSMeans test ($p \leq 0.10$). ..... 72

Figure 3.28. Water holding capacity spacing*block effect at 5-15 cm depth. Each value represents the mean of 8 subplots (n=8). Values that contain the same letter are not significantly different as determined by an LSMeans test ($p \leq 0.10$). ..... 72

Figure 3.29. Water holding capacity spacing*block effect at 15-30 cm depth. Each value represents the mean of 8 subplots (n=8). Values that contain the same letter are not significantly different as determined by an LSMeans test ($p \leq 0.10$). ..... 73

Figure 3.30. Water retention curves in the Ap2 horizon at multiple water potentials. Each data point represents the mean of both blocks and 5 subsamples (n=10). Data points within the same water potential that contain the same letter are not significantly different as determined by an LSMeans test ($p \leq 0.10$). Data points that do not contain a letter are not significantly different than any other point within that water potential. ..... 74

Figure 3.31. Water retention at -33 kPa spacing*block effect in the Ap2 horizon. Each value represents the mean of 5 subsamples (n=5). Values that contain the same letter are not significantly different as determined by an LSMeans test ($p \leq 0.10$). ..... 74

Figure 3.32. Water retention curves in the Btg1 horizon at multiple water potentials. Each data point represents the mean of both blocks and 5 subsamples (n=10). Data points within the same water potential that contain the same letter are not significantly different as determined by an LSMeans test ($p \leq 0.10$). Data points that do not contain a letter are not significantly different than any other point within that water potential. ..... 75

Figure 3.33. Water retention at 0 kPa spacing*block effect in the Btg1 horizon. Each value represents the mean of 5 subsamples (n=5). Values that contain the same letter are not significantly different as determined by an LSMeans test ($p \leq 0.10$). ..... 76

Figure 3.34. Water retention at -2.45 kPa spacing*block effect in the Btg1 horizon. Each value represents the mean of 5 subsamples (n=5). Values that contain the same letter are not significantly different as determined by an LSMeans test ($p \leq 0.10$). ..... 76

Figure 3.35. Water retention at -4.9 kPa spacing*block effect in the Btg1 horizon. Each value represents the mean of 5 subsamples (n=5). Values that contain the same letter are not significantly different as determined by an LSMeans test (p≤0.10). ..... 77

Figure 3.36. Water retention at -9.8 kPa spacing*block effect in the Btg1 horizon. Each value represents the mean of 5 subsamples (n=5). Values that contain the same letter are not significantly different as determined by an LSMeans test (p≤0.10). ..... 77

Figure 3.37. Water retention at -33 kPa spacing*block effect in the Btg1 horizon. Each value represents the mean of 5 subsamples (n=5). Values that contain the same letter are not significantly different as determined by an LSMeans test (p≤0.10). ..... 78

Figure 3.38. Water retention curves in the Btg1/Btg2 horizon at multiple water potentials. Each data point represents the mean of both blocks and 5 subsamples (n=10). Data points within the same water potential that contain the same letter are not significantly different as determined by an LSMeans test (p≤0.10). Data points that do not contain a letter are not significantly different than any other point within that water potential. ..... 79

Figure 3.39. Water retention curves in the Btg2/Bt/Btg3 horizon at multiple water potentials. Each data point represents the mean of both blocks and 5 subsamples (n=10). Data points within the same water potential that contain the same letter are not significantly different as determined by an LSMeans test (p≤0.10). Data points that do not contain a letter are not significantly different than any other point within that water potential. ..... 80

Figure 3.40. Water retention at -4.9 kPa spacing*block effect in the Btg2/Bt/Btg3 horizon. Each value represents the mean of 5 subsamples (n=5). Values that contain the same letter are not significantly different as determined by an LSMeans test (p≤0.10). ..... 80

Figure 3.41. Water retention at -9.8 kPa spacing*block effect in the Btg2/Bt/Btg3 horizon. Each value represents the mean of 5 subsamples (n=5). Values that contain the same letter are not significantly different as determined by an LSMeans test (p≤0.10). ..... 81

Figure 3.42. Water retention at -33 kPa spacing*block effect in the Btg2/Bt/Btg3 horizon. Each value represents the mean of 5 subsamples (n=5). Values that contain the same letter are not significantly different as determined by an LSMeans test (p≤0.10). ..... 81

Figure 3.43. Water retention at -1500 kPa spacing*block effect in the Ap1 horizon. Each value represents the mean of 2 subsamples (n=2). Values that contain the same letter are not significantly different as determined by an LSMeans test (p≤0.10). ..... 82

# ABSTRACT

Subsurface tile drainage is a common management practice implemented by farmers throughout the Midwest in fields that have poorly drained soils. Tile drainage has several benefits including increased productivity, reduced erosion, and increased trafficability. However, relatively little is known about the long-term change of soil properties that may occur as a result of subsurface drainage. Careful monitoring of tile drains at the long-term experimental site at the Southeast Purdue Agricultural Center led to the observation of faster drain flow than in the past, with hydrographs of the flow showing flashier peaks, suggesting that more preferential flow paths have developed over time. The overall goal of this study was to characterize possible evolution of physical and hydraulic properties of this silt loam soil after 35 years of subsurface drainage. Bulk density and water retention were measured in May of 2018 at 0-5 cm, 5-15 cm, and 15-30 cm in all plots and again in July of 2019 in the 5 m and 40 m spacings at four different horizons down to depths of approximately 100 cm, rather than set depth increments. Bulk density results from both sets of sampling show the 5 m spacing to have a significantly lower bulk density than the 40 m spacing in the top 30 cm of soil, although the difference was small. Differences in water retention among treatments were too small to be physically meaningful. Saturated hydraulic conductivity results measured by three different methods were highly variable and no differences were detected. In soils with naturally weak structure, low organic matter, and low clay content, like the soil in this study, the processes responsible for soil aggregation, structure stabilization, and lowering bulk density are inherently slow and may require longer than 35 years of subsurface drainage to produce significant changes in the physical properties measured.

# CHAPTER 1. LITERATURE REVIEW

## 1.1 Introduction

Draining excess water from soils is essential for healthy crop growth. Many soils in the Midwest experience drainage issues and may not be suitable for the annual crops usually grown in this area. Land smoothing or other surface drainage systems may help direct surface water off the field and create a sufficient environment for crop development but in some cases subsurface drainage is also recommended. Subsurface tile drainage decreases soil moisture content in the root zone by lowering the water table. Subsurface drainage has several benefits including increased productivity (Fausey and Lal, 1989), reduced erosion, and increased trafficability (Fausey et al., 1987). Lowering the water table increases the air content in the root zone causing the soil to warm up faster in the spring allowing the plants to begin growing early and vigorously. A major benefit is that field operations may also be allowed to begin earlier in the spring due to the subsurface drainage system removing excess water faster than the natural drainage system resulting in more timely planting and management. Tile drains remove water from beneath the soil surface, making more air-filled space within the soil to store water, which allows for subsequent precipitation to infiltrate rather than runoff and carry sediment with it (Fausey et al., 1987).

Pedogenesis has generally been thought of as a process that occurs slowly over thousands of years. This is true but people often do not think about how humans impact soil evolution through agricultural management practices. Water serves a dual purpose in soil evolution because it is the weathering agent as well as the phase that transports particles and solutes (Montagne et al., 2009). Drainage causes an increased water flux compared to the soil's natural state which can lead to a lower water table depth and changes in the soil's redox status as well as its physical properties such as water retention, aggregation, bulk density, and infiltration capacity. (Montagne et al., 2009). Nearly 50% of all cropland in Indiana, Ohio, and Illinois has subsurface drainage (Sugg, 2007). Even though tile drainage is a widely adopted practice in agriculture, especially in the Midwest, little is known about its long-term effect on soil physical properties. Subsurface drainage is a long-term installation and understanding how it affects soil properties over time will help us improve our management of soil and water.

## 1.2 Water Retention and Bulk Density

While there have been very few studies that have specifically focused on the effect of subsurface drainage on water retention, there are numerous studies that examine soil properties' effects on water retention and several studies that examine effects of drainage on soil properties. Evidence has been published of drainage changing soil structure and color after a period of a few decades (Hayes and Vepraskas, 2000; Montagne et al, 2007) and as few as 10 years (Kapilevich et al., 1991). Frison et al. (2009) measured a significant increase in water retention as distance from the subsurface drain decreased in 20 years. This evidence suggests that drainage can change physical properties of the soil in a relatively short period of time. It is widely accepted that texture, organic matter, bulk density, and structure are the main factors that affect soil water retention (Jamison and Kroth, 1958; Petersen et al., 1968b; Gupta and Larson, 1979; Sharma and Uehara, 1968; Frison et al., 2009) but depending on the situation, certain factors can be more or less influential.

Soil structure has been shown to have a large influence on water retention with water potentials from saturation to -33 kPa, but at water potentials beyond that range, soil texture takes over as the most influential (Sharma and Uehara, 1968). Clays tend to influence water content at -1500 kPa because they hold onto water so tightly while silt is the major influence on water content between -33 and -1500 kPa matric potentials. This range is where water is available to plants and the term available water holding capacity is commonly used. However, in soils with a high water table, like the soil at our experimental site, field capacity is better estimated at -9.8 kPa matric potential rather than -33 kPa, therefore available water holding capacity is calculated as the volumetric water content difference between -9.8 kPa and -1500 kPa matric potential (Franzmeier and Kladivko, 2001). Silt allows pores to form that have adequate dimensions for holding water available to plants. In coarse textured soils, the pores are too large to hold onto water and in finer textured soils, the water is held at too high of tensions for plant use (Petersen et al., 1968a). One study that examined silt loam soil profiles from Missouri found that coarse silt (0.05 to 0.02 mm) increases available water holding capacity more than fine silt (0.02 to 0.002 mm) (Jamison and Kroth, 1958) while another study that looked at silt loam surface and subsoil horizons from Pennsylvania suggests that fine silt increases available water holding capacity more than coarse silt (Petersen et al., 1968b).

The effect of organic matter on available water holding capacity has been, and still is, a controversial topic. Organic matter may influence water holding capacity directly by holding onto water but also indirectly by leading to changes in soil structure. In some studies, organic matter has been shown to increase available water holding capacity in coarse textured soils but not in fine textures (Petersen et al., 1968b, Jamison and Kroth, 1958). Jamison and Kroth (1958) studied 54 soil profiles, most of them being silt loams, spread across 20 different soil series. The authors observed a slight increase in available water holding capacity with an increase in organic matter in a fine textured soil but that increase could have also been attributed to textural changes. In the 54 soil profiles they analyzed, soil surface samples had the most organic matter but generally had higher levels of silt also. These soils had increased available water hold capacity as organic matter and silt content were higher. In one grouping of samples that had high levels of sand and low levels of silt, there was little evidence to support a relationship between organic matter and available water holding capacity. Therefore, Jamison and Kroth concluded that the increase in available water holding capacity in the fine textured soils was most likely caused by the increase in silt. Hudson (1994) claims that Jamison and Kroth's study is inconclusive by criticizing their experimental design. In most of Jamison and Kroth's samples, the organic matter was less than 2% while soil texture and other soil properties were wide-ranging. Hudson (1994) suggests that the larger variation in soil properties than the variation in organic matter obscured any relationship between organic matter and available water holding capacity. Hudson (1994) makes the same claim of inconclusiveness and poor experimental design towards Petersen et al. (1968b). Hollis et al. (1977) studied the influence of organic matter on available water holding capacity in 144 surface and subsurface horizons from England and found a significant positive correlation between organic matter and available water holding capacity that accounted for nearly 50% of the variation. Similarly, Salter et al. (1966) found a significant positive correlation between organic matter and available water holding capacity after inspecting 26 different soils. Hudson (1994) believes Hollis et al. (1977) and Salter et al (1966) had better designed experiments and therefore better results than Jamison and Kroth (1958) and Petersen et al. (1968b) because they used samples with wide ranges of organic matter relative to soil texture and other properties. Hudson (1994) created his own experiment to analyze the effect of organic matter on available water holding capacity in which soils were carefully selected so that the sample-to-sample variation of organic matter content was greater than the variation of silt or clay in each textural class. This would prevent any

relationship between organic matter and available water holding capacity from being obscured by variation in texture. The results showed a positive correlation between organic matter and available water holding capacity in all three texture classes (sand, silt loam, and silty clay loam). Using the National Cooperative Soil Survey Characterization Database to evaluate any effects of organic matter on available water holding capacity, Libohova et al. (2018) found soil organic matter to be weakly correlated with available water holding capacity and the most pronounced effect occurred in sandy soils compared to other textures. Minasny and McBratney (2018) presented similar results that indicated a small effect on soil water content with an increase in organic carbon as well as loams and clays to be affected less than sandy soils. These conflicting results suggest that more research needs to be done on the relationship between organic matter and available water holding capacity.

As the water table is lowered with subsurface drainage, pores open up for air infiltration and increase the soil aeration (Larney et al., 1988). This not only creates a more hospitable environment for root growth but also for biological activity (Frison et al., 2009). Soil structure improves from the biological activity but also from the wetting and drying cycles (Kapilevich et al., 1991; Montagne et al., 2009). Improved structure, as previously stated, has been shown to influence water retention at water potentials from saturation to -33 kPa. Improved or better soil structure refers to an increase in grade, aggregate stability, and a balanced pore size distribution with good connectivity of pores, all of which promote air and water circulation and retention, biological activity, and plant health. Lal and Fausey (1993) studied a field with silt loam and silty clay loam soils in Ohio and found undrained plots to generally have lower bulk densities than drained plots although the difference was not statistically significant. Some other studies in Ohio showed evidence of bulk density decreasing as a result of subsurface drainage: Baker et al. (2004) on a clay loam soil with subirrigation and Hundal et al. (1976) on a silty clay soil. Jia et al. (2008) presented data from a silty clay loam soil in North Dakota that showed no significant difference in bulk density after 5 years of tile drainage. Reeve et al. (1973) reported that in silty soils, bulk density is negatively correlated with available water, air capacity, and retained water capacity. Taking information from these studies suggest that drainage may decrease bulk density and therefore increase the available water capacity. Frison et al. (2009) provided evidence of available water holding capacity being 30% larger at 0.6 meters from the drain compared to 7 meters from the drain in a silty soil in France with subsurface drains spaced 15 meters apart that were installed

20 years prior to the study. However, the authors acknowledge a change in minerology as distance from the tile increases may play a significant role in the available water content differences.

Water retention and available water holding capacity is important for agronomists, agricultural engineers, and soil scientists but determining water retention curves can be time consuming and expensive (Jamison and Kroth, 1958; Gupta and Larson, 1979). Methods and equations have been created to estimate water retention curves within a reasonable error based on basic soil properties that are easy to obtain, such as particle size distribution, organic matter percent, and bulk density, saving people time and money (Gupta and Larson, 1979). However, when analyzing the impact of drainage, bulk density may or may not change. If there is no change in bulk density as a result of drainage, this approach would not predict any changes in water retention because organic matter and texture are fairly constant across the entire field.

### 1.3 Water Flow

Water flow in soils can be represented by several different measurements including infiltration, saturated hydraulic conductivity, and unsaturated hydraulic conductivity. Soil porosity, soil structure, texture, organic matter, and mineralogy are a few factors that can affect saturated hydraulic conductivity (Ksat) (Arshad and Coen, 1992). Not only does the total porosity of the soil affect Ksat and infiltration, but the size and connections of the pores play an important role. Many studies have expressed the major influence of macropores, cracks, and earthworm channels on hydraulic conductivity, infiltration, and preferential flow (Beven and Germann, 1982; Shipitalo et al., 2004; Flury et al., 1994; Bouma, 1991; McCoy et al., 1994; Mbagwu, 1994; Oygarden et al., 1997; Inoue, 1993, Mason et al., 1957). These macropores, if connected, allow water to bypass saturated and unsaturated portions of the soil and penetrate deeper in the profile in a shorter period of time (Flury et al., 1994). Even though macropores may only comprise a small portion of the total soil porosity, they have a very large influence on water flow (Beven and Germann, 1982; Bouma, 1991). Mbagwu (1994) found that macroporosity, followed by bulk density, were the most influential physical properties for Ksat.

Although hydraulic conductivity has been shown to be negatively correlated with bulk density (Mason et al., 1957), bulk density may not always be a good indicator of hydraulic conductivity. Changes in bulk density indicate a difference in total porosity but it does not give information about volume distribution, connectivity, or tortuosity of the pores which can have

large impacts on soil hydraulics (Assouline, 2006). A slight increase in aggregation or compaction may increase or decrease Ksat by orders of magnitude but the total porosity and bulk density may only change very slightly or not at all (Kutílek, 2011).

A handful of studies have investigated the effects of tile drainage on soil hydraulic conductivity and they have reported conflicting results. At a 5 year old tile drainage site in North Dakota with clay loam and silty clay loam soils, Jia et al. (2008) measured saturated hydraulic conductivity at 0.9, 4.0, 7.0, and 10.1 meters from the tile and compared it to an undrained control plot. No significant differences were detected. Hundal et al. (1976) detected a significant increase in saturated hydraulic conductivity due to subsurface drainage on a silty clay soil in north-central Ohio. Chieng and Hughes-Games (1995) also recorded significantly higher Ksat values in tile drained plots compared to drained plots with subirrigation in British Columbia on a silty clay loam soil. The authors did not find a significant difference in Ksat among drained and undrained plots, but they suspect that the higher percentage of sand in the undrained plot soil gave it a high Ksat value. The differences in results among the studies may be partially attributed to the differences in drain spacing and time of measurements after drain installation. The studies done by Jia et al. (2008), Hundal et al. (1976), and Chieng and Hugh-Games (1995) had drain spacings and time lengths of 18.3 m for 5 years, 12 m for 16 years, and 14 m for 8 years, respectively. The studies that reported significant differences had narrower drain spacings as well as longer drainage histories than the study that did not find a significant difference in Ksat. A few experiments have compared soil physical properties of locations directly above tile drains and locations a set distance away from the tile. Petersen et al. (2012) pumped smoke into tile drains and recorded the location of macropores on the surface that were emitting smoke to quantify the number and location of macropores connected to the tile lines. They found nearly all of the smoke emitting macropores to be within a 1 meter band centered above the tile. In southern Ontario, Canada on sandy loam and loam soils, Frey et al. (2012) showed saturated hydraulic conductivity to be greater over the tile drain than it was 1.5 m and 4 m away from the drain after 23 years of drainage. Messing and Wesstrom (2006) analyzed the efficiency of tile drains in the trench backfill zone and at the midplane on 7 different sites in Sweden with “high” and “very high” clay contents. The ages of the drainage systems at the different sites ranged from 2-45 years and the lateral spacings ranged between 14-18 meters. Results show that there are large differences in drainage efficiency between the midplane position and directly above the drain with Ksat values being larger directly over the

drain. These studies show that water flow is most likely not consistent across entire tile drained fields and that the installation process of tile drains decades ago can still have significant effects on water flow today in the trench backfill zone.

The spatial variability of the soil's pore system can cause certain areas to conduct water at higher rates than the surrounding matrix. Preferential flow refers to the rapid transport of soil solution along certain pathways that bypass part of the unsaturated soil matrix leading to soil solution traveling deeper and faster than can be predicted with the application of Richards equation (Simunek et al., 2003; Hendrickx and Flury, 2001; Beven, 2018). Kutilek (2011) categorized preferential flow into three different types: (i) flow in the voids between structural aggregates, (ii) macropore flow (worm or root channels), and (iii) flow due to unstable wetting fronts due to changes in permeability or hydrophobicity. Bouma (1981) has shown that voids and cracks between aggregates are more important for water flow than root or worm channels in a clay soil. But the soil at the experimental site is a poorly structured silt loam soil throughout the profile with an abundance of earthworms so most preferential flow is probably occurring in root and worm channels. Macropore flow starts when the matrix around the macropore is near saturation in order to surpass the water entry potential of the macropore (Hendrickx and Flury, 2001). Water can flow down macropore walls as film flow which means the macropores do not have to be completely full to transport water. A portion of the water will be absorbed into the soil matrix while the rest will percolate downwards (Hendrickx and Flury, 2001).

Preferential flow has been an important area of research for the past 30 years (Jarvis et al., 2016) but finding methods to measure, model, and visualize it has proven to be a challenge. Tracer breakthrough studies have been one of the most utilized techniques for measuring preferential flow in the past and in recent years. These experiments involve applying one or more chemical compounds, usually accompanied with irrigation, to the soil surface of a subsurface drained field or soil columns in a lab, and then monitoring the tile effluent for traces of the applied chemical compound. The time required for the compound to move through the soil and out of the drains as well as the concentration of the compound in the water can be measured. These data can be fitted with models to asses if preferential flow was likely involved in the compounds' transport (Jarvis et al., 2016). Researchers have used tracer breakthrough studies to investigate how preferential flow is affected by several different factors including soil compaction (Mossadeghi-Bjorklund et al., 2016; Mooney and Nipattasuk, 2003), bulk density (Soares et al., 2015; Koestel et al., 2013;

Katuwal et al., 2015), tile drain spacing (Kladivko et al., 1999; Kung et al., 2000), and many others. But one limitation of the tracer breakthrough technique is that it only measures temporal variations in flow and does not measure spatial patterns of the preferential flow. One technique used to investigate preferential flow that does measure spatial patterns is dye staining experiments. This method involves applying a dye with irrigation that will stain the soil upon contact and letting the solution infiltrate and percolate through the soil. After a determined period of time, the soil is excavated to reveal the spatial patterns of water flow through the soil (Allaire et al., 2009). The stained soil can be photographed and preferential flow can be characterized by calculating several statistical indices that can be used to correlate similar flow pattern areas with soil properties and morphology (Bogner et al., 2013; Jarvis et al., 2016). Flury et al. (1994) conducted dye staining experiments on 14 different field sites in Switzerland to compare the susceptibility of different soils to have preferential flow of water. They found evidence of water bypassing the soil matrix at most of the sites, although the extent of bypassing differed. One of the field sites in this experiment was on a silt loam soil with many earthworm channels. Infiltration solution at this site almost completely bypassed the soil matrix without fully wetting it and was channeled into the subsoil (Flury et al., 1994).

Advances in technology have enabled researchers to use noninvasive imaging techniques such as X-ray tomography, magnetic resonance imaging, and neutron radiography to three dimensionally quantify soil macropore properties which have tremendous effects on preferential flow (Jarvis et al., 2016). Sammartino et al. (2015) used a sequence of X-ray scans at time intervals of 5, 10, and 15 minutes to show that a large portion of the macroporosity remained air-filled during preferential flow events and connectivity of macropores is a significant factor in regulating a macropore's activity during preferential flow events. The authors used a set of geometric descriptors to characterize the soil structure and connectivity of macropores. Air entrapment in large pores during saturation events has been documented by Luo and Lin (2009) as well as Luo et al. (2008), both using X-ray tomography, which may help explain why a large fraction of the soil macroporosity does not conduct flow even during ponding events (Jarvis et al., 2016; Sammartino et al., 2015). Noninvasive direct imaging has the potential to provide information on the size and properties of the pores that are active in preferential flow which has not yet been quantified (Jarvis et al., 2016). Models have been used to estimate indirectly the size of pores that are active in preferential flow but major errors can build from these models if they are based on

oversimplified concepts (Hunt et al., 2013). Errors in preferential flow models can also arise from the inability to account for variability in pore connectivity, and changes in pore structure due to freeze-thaw cycles, earthworm activity, tillage, shrink-swell, and hydrophobicity of earthworm and insect burrows (Jarvis et al., 2016). One potential limitation of these noninvasive scanning techniques is getting both a high enough image resolution necessary to measure macropores and a large enough sample size that encompasses the complex connectivity and continuity of the preferential flow network (Jarvis et al., 2016). These technology driven techniques may need more time and advancement in equipment before they are easily accessible and more widely utilized.

Preferential flow at the long-term drainage experimental site in southeast Indiana has been documented in a couple different studies. Kladivko et al. (1999) showed that a small but significant fraction of the pesticides leached out of the soil and into the tile drain water after the first major rain event after pesticide application. The timing of pesticides appearing in the drainage water was consistent with preferential flow movement. More flow and load were observed on the narrow spacing than the wide spacing implying that preferential flow to subsurface tile drains occurs most within close proximity to the drain, although the exact area is unknown. A tracer study was also conducted at the SEPAC drainage site in 1996, 13 years after the tile drains were installed (Kung et al., 2000). Four tracers were sequentially applied and the drainage effluent was intensely monitored. Results show that the first tracer applied had the slowest arrival time and tracers that were applied after the soil was irrigated had much shorter arrival times. This was due to larger pores of the preferential flow paths not being hydraulically active while the top of the soil profile was relatively dry. The fast arrival times of the tracers suggest that preferential flow dictates the leaching of chemicals. These results also indicate that as the soil becomes wetter during a rainfall event, water movement and transport shifts towards larger pores in the preferential flow paths. Soil water content, rate of water addition, soil structure, and relative pore size and connectivity all influence the rate of water moving through macropores (Thomas and Phillips, 1979).

Two different pathways of preferential flow to the tile drains have been hypothesized. One pathway is mostly rapid vertical movement down earthworm and root channels to the water table where it then moves laterally to the tile in the saturated zone. The other pathway consists of diagonal movement from the surface straight towards the tile drain. Evidence of the latter has been presented by Kohne and Gerke (2005) in a bromide tracer study on a loam soil in northern Germany. At the end of the tracer experiment, Kohne and Gerke (2005) took 108 soil samples

from a trench wall transect at six depths and 18 horizontal positions from the drain. Resident bromide concentrations were measured and the data shows diagonal transport of the tracer through the unsaturated zone toward the tile drain whereas models suggest primarily vertical movement in the unsaturated zone followed by lateral movement to the tile drain once it reaches the saturated zone.

Soils with low bulk density and good aggregation may show more preferential flow than soils that are compacted (Flury et al., 1994; Arshad and Coen, 1992). When soils are drained with subsurface tile, the subsoil becomes better aerated which improves biological activity and soil structure (Kapilevich et al., 1991; Montagne et al., 2009). Increased earthworm activity should lead to lower bulk density and more burrows, many of which may be connected to the drains (Shipitalo et al., 2004; Oygarden et al., 1997). These burrows connected to the drains provide water a rapid flow path through the soil. Some studies that investigated differences in the number and density of earthworm burrows directly above tile drains compared to between tile lines found higher numbers and density at the above tile location (Alakukku et al., 2010; Nuutinen et al., 2001; Nuutinen and Butt, 2003) while other studies did not find any variation in earthworm populations in relation to tile location (Frey and Rudolph, 2011). Nuutinen et al. (2003) showed the earthworm burrows to be deepest over top the tile and the authors give a likely explanation of the soil above the drains being better aerated with a lower water table than at the midplane position which creates a beneficial environment for earthworm growth and reproduction. The disagreement in results suggest that tile location is not the only influence on earthworm burrow location.

## 1.4 Soil Structure and Morphological Development

Several studies have focused on how subsurface drainage affects sediment loss and water quality but very few have devoted attention to how it impacts soil development and evolution (Montagne et al., 2009). Hayes and Vepraskas (2000) investigated the morphological changes in a sandy loam soil due to 30 years of drainage by ditching. They found that within 30 meters of the ditch, the water table fluctuated enough to significantly alter the volume of iron masses at depths of 40 to 100 cm. As distance from the ditch increased, the volume of iron masses decreased. Kapilevich et al. (1991) looked along a slope containing three different clay soils that had been subsurface drained for 18 years. Drainage changed the intensity and time period of saturation which altered the redox processes leading to the precipitation of iron oxides. By observations and

profile descriptions, they were able to detect that the subsurface horizons developed a network of cracks and the dense, massive structure prior to drainage transitioned into microaggregates on the surface and columnar structure in the subsurface. They also measured a 20% loss of the clay particle size fraction in one horizon due to eluviation which may have significant impacts.

Some more recent work has been focused on quantitatively measuring soil structure by using a multistripe laser triangulation (MLT) scanner and relating it to water flow (Hirmas, 2013; Eck et al., 2013; Eck et al., 2016). Eck et al. (2013) found that the MLT scanner was able to quantitatively describe soil structure on an exposed profile face that compared well to the soil structure described in the field from a traditional morphological description. This method is advantageous because it is able to continually measure soil structure as a variable and does not force it into a category which allows the user to distinguish subtle changes in structure that are not obvious or simply ignored during a morphological description (Eck et al., 2013). In order for the MLT scanner to examine an undisturbed profile that was free of smears created by tools during excavation, Eck et al. (2013) used a method developed by Hirmas (2013) which involved flash freezing the exposed profile face and then carefully peeling off the frozen soil, leaving a new surface that was much closer to a natural state than the previous smeared profile. This allowed the researchers to gather scans of undisturbed, natural soil surfaces. The MLT scanning was then used by Eck et al. (2016) in a study to determine the relationship between saturated hydraulic conductivity and soil structure where they found 87% of the variation in saturated hydraulic conductivity could be explained by measurements from the MLT scanner when combined with a coefficient of linear extensibility. The authors recognize the potential of this technique in predicting the relationship between soil structure and water flow but state that much more work is needed to apply this to a range of different soil types. Another limitation is the time and labor required for these analyses. Gathering undisturbed samples in large soil trays can be challenging and strenuous as well as time consuming and the preparation, scanning, and analyzing of the samples is much more time consuming than traditional morphological profile descriptions. However, certain areas of study can greatly benefit from the quantitative soil structure measurements that are possible with this method.

## 1.5 Research Objectives and Hypotheses

As discussed in this review, subsurface tile drainage can lead to changes in soil physical and hydraulic properties such as water retention, bulk density, hydraulic conductivity and preferential flow in relatively short periods of time. Researchers have used many different methods to characterize these changes in soil properties and as technology advances and access to new technology improves, innovative methods are becoming more useful in characterizing phenomenon such as preferential flow that have previously been hard to quantify. A greater understanding of how subsurface drains affect soil properties and water movement can lead to improved management and conservation of soil and water resources. Therefore, the objectives of this study were to: (i) observe changes in soil structural development under different drainage intensities, (ii) measure bulk density and water retention at different depths and drain spacings, (iii) and measure the soils ability to allow water flow (saturated hydraulic conductivity) with different drain spacings after 35 years of drainage. The hypotheses for this study include the following: (i) soil structure will improve at the midplane by an increase in grade as drain spacing decreases, (ii) bulk density will decrease at the midplane as the drain spacing decreases, (iii)water retention will increase at the midplane as the drain spacing decreases, (iv) and saturated hydraulic conductivity will be higher at the midplane in the narrower drain spacings.

# CHAPTER 2. METHODS

## 2.1 Site Description

The SEPAC drainage experimental site is located at the Southeast Purdue Agricultural Center (SEPAC) in Jennings County, near Butlerville, Indiana. The site has been described in detail by Kladivko et al. (1991, 1999, 2004, 2005). The Clermont silt loam soil (fine silty, mixed, superactive, mesic Typic Glossaqualfs) has a low organic matter, light gray surface with about 1% slope. The soil is poorly structured, poorly drained, slowly permeable, and has a borderline fragipan at 120 cm depth. In 1983, subsurface drains (10 cm diam.) were installed at 5, 10, and 20 meter spacings at a depth of 75 cm. Each spacing experiment has three drain lines with the outside lines acting as a shared drain between adjacent treatments (Figure 1). Each spacing was replicated in two blocks separated by 40 meters. Each drain spacing plot is divided into 8 subplots for sampling purposes with all samples and measurements taken at the midplane position. These subplots are on the east and west side of the center tile at distances of 22.9 m, 61 m, 83.8 m, and 106.7 m from the north end of the field. From 1984 through 1993, the field was in continuous corn using conventional tillage which consisted of using a chisel plow to a 20- to 25-cm depth in the spring followed by one or two passes with a disc or field cultivator. Beginning in 1994, the field transitioned to a no-till, corn-soybean rotation with cover crops. Soybeans were planted in both 2018 and 2019. Crop and fertility management was performed based on good agronomic practices and did not differ among treatments.

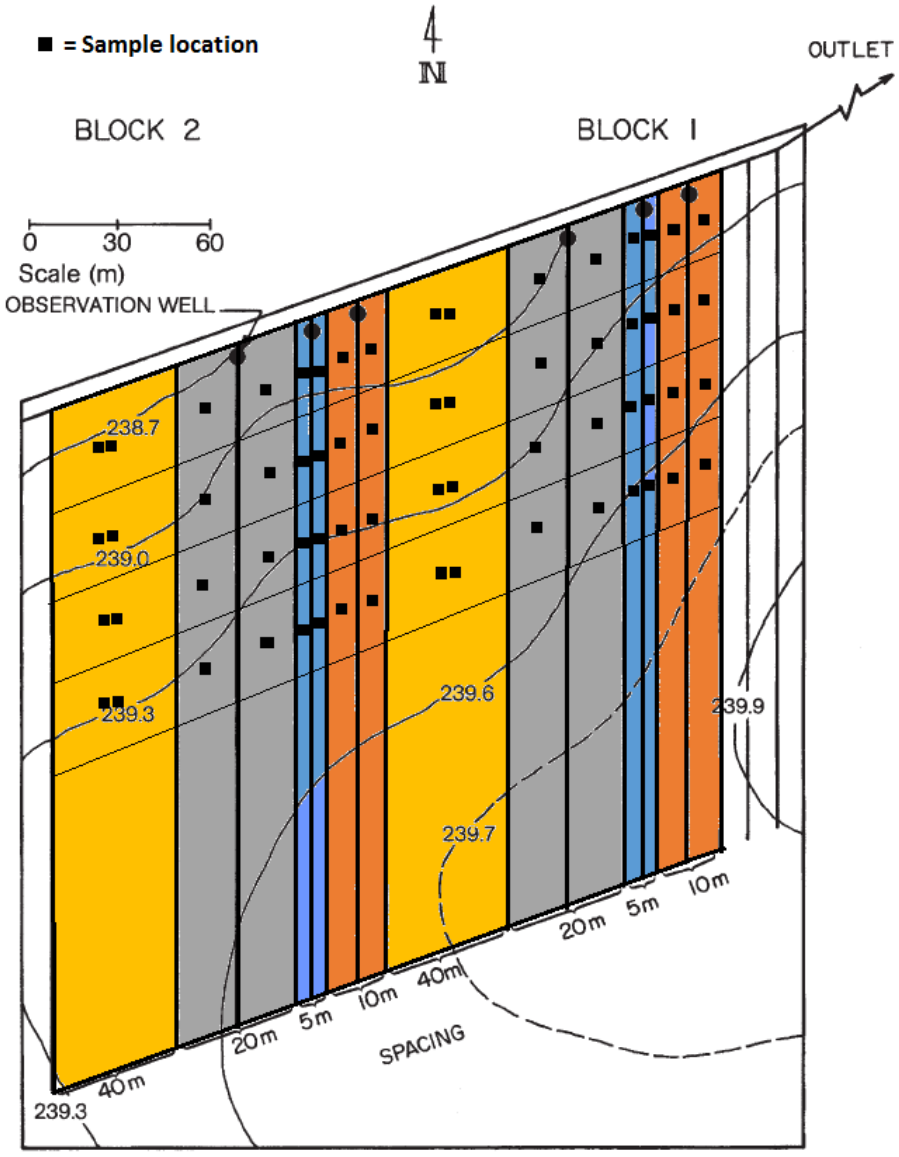


Figure 2.1. Plot diagram of the SEPAC drainage experimental site.

## 2.2 Soil Profile Descriptions

In July 2019, soil pits approximately 1 m deep were dug at the southern end of the experimental site in the 5 m and 40 m treatments in both blocks. Before samples for bulk density, water retention, and saturated hydraulic conductivity were taken from the soil, soil profile descriptions of each pit were done by Dena Anderson, USDA NRCS Resource Soil Scientist, and Dr. Jason Ackerson, Assistant Professor of Agronomy at Purdue University. Photographs of each soil profile were taken as well. Once the soil profile descriptions were complete, core samples were taken from respective horizons for water retention, bulk density, and Ksat measurements.

## 2.3 Bulk Density

Bulk density was measured three times. The first set of bulk density samples were taken at shallow depths which allowed us to characterize bulk density near the surface but these samples were also used for water retention measurements. The second set of bulk density measurements were collected down to 100 cm and the third set was sampled from soil pits which allowed us to sample individual soil horizons rather than sampling at set depth increments. The first bulk density samples were taken in May of 2018 using the short core method described by Grossman and Reinsch (2002) using a 3 cm tall core 5.4 cm in diameter for the 0-5 cm depth and 6 cm tall cores for the 5-15 cm and 15-30 cm depth. Samples were taken approximately in the center of the depth interval to represent that depth increment. These are the same cores used for water retention. After water retention data had been collected from the cores, they were oven dried, weighed, and bulk density was calculated. All three depths were sampled in each subplot, resulting in 24 cores (3 depths x 8 subplots) per drain spacing plot (24 cores x 8 plots = 192 cores total).

The second set of bulk density measurements collected samples from 0-15, 15-30, 30-50, 50-75, and 75-100 cm depths in May of 2018. A core was taken with a Giddings hydraulic probe 5.2 cm in diameter that was immediately cut into the respective depth ranges and all the soil from each respective depth range was carefully collected in paper bags. One hydraulic probe core was taken in each subplot. The samples were air dried and weighed. Samples from 2E and 2W subplots were put in the oven and dried to obtain the air-dry moisture content so a conversion could be made between air dry weight and oven dry weight and bulk density calculated.

The third set of bulk density measurements were sampled from soil pits using the short core method (Grossman and Reinsch, 2002). Cores with dimensions of 6 cm height and 5.4 cm diameter were used to sample the soil profiles in similar horizons rather than at set depth increments. Samples were taken in the Ap2 horizon as well as multiple B horizons. Exact sampling horizon and depth for each soil pit are listed in Table 1. Five cores were taken per horizon in each soil pit. These cores were used to measure bulk density, water retention, and saturated hydraulic conductivity. After water retention and saturated hydraulic conductivity measurements were finished on the cores, they were oven dried and weighed to calculate bulk density.

Table 2.1. Horizon (Depth) for core samples from each soil pit.

| **5 m Block 1** | **40 m Block 1** | **5 m Block 2** | **40 m Block 2** |
|---|---|---|---|
| Ap2 (15 cm) | Ap2 (15 cm) | Ap2 (8-20 cm) | Ap2 (13-25 cm) |
| Btg1 (28 cm) | Btg1 (30 cm) | Btg1 (27-36 cm) | Btg1 (25-35 cm) |
| Btg1 (41 cm) | Btg1 (41 cm) | Btg2 (36-69 cm) | Btg2 (35-56 cm) |
| Btg2 (76 cm) | Btg2 (71 cm) | Bt (69-101 cm) | Btg3 (56-84 cm) |

## 2.4 Water Retention

Water retention was measured using sand tables and pressure pot methods described by Dane and Hopmans (2002a, 2002b). The same 0-5, 5-15, and 15-30 cm depth cores used for bulk density as well as the bulk density cores from the soil pits were used for water retention at saturation, -4.9, -9.8, and -33 kPa. The cores from the soil pits were additionally measured at -2.45 kPa. An air-dry bulk sample that was crushed to pass through a 2 mm sieve was used for measurements at -1500 kPa. Cores were soaked until they reached saturation, weighed, and placed on sand tables. After they equilibrated, they were weighed again to measure -2.45 kPa (only soil pit cores), -4.9 kPa, and -9.8 kPa water retention. Cores were then transferred to pressure pots and allowed to equilibrate at -33 kPa and weighed. The cores were then oven dried to obtain a dry weight for bulk density measurements. The crushed and sieved bulk samples were placed in pressure pots and allowed to equilibrate at -1500 kPa. After getting the equilibrated weights, the -1500 kPa samples were oven dried and weighed again. The -1500 kPa gravimetric water contents were multiplied by the bulk density to obtain volumetric water contents. Water holding capacity (WHC) was calculated as the difference between -9.8 and -1500 kPa.

## 2.5 Saturated Hydraulic Conductivity

Saturated Hydraulic Conductivity (Ksat) was measured using the auger-hole method as described by Amoozegar (2002), a Guelph Permeameter as described by Reynolds and Elrick (1986), the Slug Test as described by Bouwer and Rice (1976), and the Laboratory Constant Head Method as described by Klute and Dirksen (1986). Measurements using the auger-hole method were taken in March of 2019 only in the 40 m control treatment due to the water table receding too deep in the 5, 10, and 20 m plots. The 40 m control was the only treatment where the water table was high enough to take measurements. A cylindrical hole with a diameter of 9 cm was dug to a depth of 100 cm and a cylindrical screen made of ¼ inch-mesh hardware cloth was inserted into the hole to prevent the sides from collapsing (See Appendix Fig. A.1). Four holes were dug in each block and 2 reps were measured in each hole. The water table was allowed to rise to static level and then the water was pumped out of the hole. A tape measure with a float attached to the end was placed in the hole and the rate of water rise was measured until the water had risen 25% of the initial water depth (Appendix Table A.1). In order to calculate Ksat, a shape factor needed to be calculated for each set of measurements. According to van Beers (1958), soil layers more than 10-15 cm below the bottom of the hole have negligible influence on the rate of water rise in the hole which means the fragipan approximately 20 cm below the hole will not influence our measurements and Equation 1 in the appendix can be used to calculate the shape factor. The shape factor was multiplied by the rate of rise of water in the hole to calculate Ksat.

The Ksat measurements with the Guelph Permeameter (Appendix Tables A.2, A.3, A.4, Fig. A.2) were taken in mid-August 2019. The Guelph Permeameter apparatus was assembled according to instructions provided by the manufacturer, Soilmoisture Equipment Corp. A 63.5 cm deep, 6 cm diameter borehole was prepared using a soil auger and a sizing auger to ensure the bottom of the hole was flat. A well prep brush was used to remove any smearing on the walls that occurred during excavation with the soil auger. The Guelph Permeameter was lowered into the hole, being careful not to knock any debris off the walls down into the hole, until it was resting on the bottom of the borehole. The tripod bushing on the Guelph Permeameter apparatus was lowered into the top of the well hole to provide stability. The tripod was placed adjacent to the apparatus and tied to it with rope to provide extra stability. Once the apparatus was stabilized, the reservoir valve was adjusted to connect both the inner and outer reservoirs and they were filled with water. The air inlet tip was then raised to establish a well head height of 10 cm. Once the initial bubbling

from filling the well stopped, the reservoir valve was adjusted to use only the inner reservoir. The initial water level in the reservoir was recorded and readings were taken every two minutes until the rate of change was consistent for three consecutive measurements, indicating a steady-state had been reached. After the 10 cm well head height had reached a steady-state, the inner and outer reservoirs were connected and the air inlet tip was raised to establish a well head height of 25 cm. After the initial bubbling from filling the well stopped, the initial water level in the reservoir was recorded and measurements were taken every two minutes until steady-state was reached. Five holes were used in both the 5 m spacing and 40 m spacing in each block. The Ksat was calculated using the Guelph Permeameter K-sat Calculator spreadsheet provided by Soilmoisture Equipment Corp. which uses equations presented by Reynolds and Elrick (1986). Due to the double head method calculation producing negative values, each borehole had the single head analysis applied to each head and the resulting saturated hydraulic conductivity values were averaged.

The Slug Test (Appendix Table A.5) was performed on two 1.5 m deep, 2.54 cm diameter wells in each plot at the northern end of the experimental site. In March 2019, the static water level in the wells was measured and then water was pumped out of the wells to a depth of 100 cm and the rate of rise was measured with a water level sensor. Two reps were measured in each well for one of the 10 m plots, and both 20 and 40 m plots. The water level in the 5 m plots and one of the 10 m plots was below 100 cm so measurements were not taken. Hydraulic conductivity was calculated using Hvorselve's (1951) expression of hydraulic conductivity with a radius of the well equal to 1.27 cm, radius of the well boring equal to 3.81 cm, and length of perforated zone equal to 150 cm minus the static water level. In order to acquire the TO value, HT/HO vs time was plotted on a semi log graph with HT/HO on the log Y axis. A straight line was fitted to the data and the equation of the line was used to estimate TO as the time when HT/HO = 0.37.

The Laboratory Constant Head Method (Klute and Dirksen, 1986) was performed on the cores taken from the soil pits (5 m and 40 m treatments) in July 2019. An additional empty core of the same dimensions was taped on top of the soil cores to provide room for the head of water and a piece of filter paper was placed on the soil surface to prevent surface disturbance. An apparatus was constructed in the lab that supplied a constant head of water to the cores and allowed the resulting flux of water to be measured. The percolate was captured in a beaker and weighed every hour or sooner depending on how much water was accumulating. The weight of the water was converted to a volume using a density of 1 g $cm^{-3}$. A constant head was applied to the cores

for three hours or until 8 measurements were taken. Darcy's Law was used to calculate Ksat for each measurement and the average over approximately the final hour or the last 3 measurements was used as the steady-state Ksat.

## 2.6 Statistical Analysis

Statistical analyses were performed using SAS Version 9.4 software (SAS Institute Inc., Cary, NC.). Data was checked for normality and homogeneity of variance using the MIXED procedure and a Box-Cox transformation in the TRANSREG procedure was used to see if a transformation was needed. The soil pit Ksat data were $Y^{0.25}$ transformed for the Ap2 and Btg1 horizons, $Y^{-0.5}$ transformed for the Btg1/Btg2 horizon, and log transformed for the Btg2/Bt/Btg3 horizon. Results are presented in back-transformed units. All depths, horizons, and water potentials were analyzed separately. Statistical analyses were not performed on the auger-hole method data or slug test Ksat data. All measurements were analyzed as a randomized complete block experimental design using the GLIMMIX procedure. Data from the soil cores at 0-5, 5-15, and 15-30 cm as well as the bulk density data taken with the hydraulic probe are comprised of two blocks and four treatments while the soil pit data and Guelph permeameter data are comprised of two blocks and two spacings. An LSMeans separation test was performed on all significant effects ($p \leq 0.10$).

# CHAPTER 3. RESULTS AND DISCUSSION

## 3.1 Soil Profile Descriptions

Soil profile descriptions were done on the 5 m and 40 m treatments in both Block 1 and 2 to a depth of approximately 100 cm before the soil pit cores for bulk density, water retention, and Ksat were taken (Tables 3.1, 3.2, 3.3, and 3.4, Figures 3.1, 3.2, 3.3, and 3.4). Generally, the soil was a silt loam texture down to 56-69 cm before gaining enough clay to be a silty clay loam. Larney et al. (1988) conducted experiments at this same site and provided some inherent properties of the soil. The authors had slightly lower clay percentage estimations than in our profile descriptions, resulting in a silt loam texture extending beyond 1 m deep. Near the surface, the structure was weak platy before transitioning to weak subangular blocky further down in the profile. Generally, a plow pan was detected in the lower part of the Ap2 horizon and upper part of the B horizon around 25-30 cm below the surface. The surface Ap1 horizon generally had a matrix color of 10YR 4/2 or 4/3, and the Ap2 horizon generally had a matrix color of 10YR 5/3 or 5/4. The Btg horizons generally had a matrix color of 10YR 7/1 or 7/2 except for the 40 m pit in Block 2. The 40 m Block 2 pit face had higher chroma colors in the area where the profile description and samples were taken resulting in matrix colors of 10YR 6/4 and 5/6 in the lower B horizons. However, the surrounding pit face outside the sampling area had a lower chroma and would have been classified as gleyed so it was decided to classify these horizons as Btg to better match the surrounding soil. Another general observation from the field that was not documented in the profile description was the abundance of earthworms. Many large earthworms were observed in both treatments and blocks with burrows being exposed nearly the full depth of the soil pit. More earthworms and burrows were observed in the 5 m treatments than the 40 m treatments. This may be attributed to a more well-drained and better aerated environment in the narrow spacing compared to the wider spacing which would be beneficial for earthworm growth and reproduction. Several studies have found higher numbers and density of earthworms directly above tile drains, which is better aerated, than further away from the drains (Alakukku et al., 2010; Nuutinen et al., 2001; Nuutinen and Butt, 2003).

A difference between the Block 1 profiles and the Block 2 profiles caused a difference in the Btg horizon designations. In Block 1, both the 5 m and 40 m treatments had a Btg1 horizon

that ranged from approximately 28 cm down to around 65 cm. In Block 2, both in the 5 m and 40 m treatments, this same Btg horizon had enough change in structure and/or color partially down the horizon to separate it into two horizons, Btg1 and Btg2. All four pits had another Btg horizon below these horizons resulting in Block 1 labeling it as Btg2 and Block 2 labeling it as Btg3. However, this Btg3 horizon in the 5 m Block 2 profile had a matrix color of 10YR 6/3 which means it is one chroma too high and slightly too brown to be gleyed and receive the "g" subordinate distinction. Therefore, it was characterized as a Bt horizon. When taking soil core samples, Block 2 was sampled in the Btg1 and Btg2 horizons and Block 1 was sampled in the upper part and lower part of the large Btg1 horizon to correspond with the Btg1 and Btg2 horizons in Block 2.

A few small differences among treatments were detected with the soil profile descriptions. In Block 2, the Ap2 horizon of the 40 m spacing had weak thick platy structure parting to weak subangular blocky structure. The 5 m spacing did not have dominant platy structure and instead had weak very coarse subangular blocky structure parting to weak medium subangular blocky structure. However, this small difference in structure was not evident in Block 1. Structure throughout the B horizons was fairly consistent across treatments. Kapilevich et al. (1991) was able to observe in profile descriptions a network of cracks develop in the subsurface horizons. The authors were also able to detect the dense, massive structure transform into a columnar structure in the subsurface horizons after 18 years of subsurface drainage. At the SEPAC site, there was also a small difference in redoximorphic concentration abundance among treatments. In Block 1, the 40 m spacing had a 5-10% higher concentration abundance than the 5 m spacing. In Block 2, the 40 m spacing had a 5-20% higher concentration abundance than the 5 m spacing. Also, the concentrations in the 40 m profile generally had a slightly more reddish hue than the concentrations in the 5 m profiles. These results contrast the idea of more iron being oxidized in a drained soil than an undrained soil due to better aeration. Hayes and Vepraskas (2000) provided evidence of redoximorphic concentrations increasing in the Bt horizons as the distance from a drainage ditch decreased. When the soil is saturated, soil microbes use up all the remaining oxygen during respiration and eventually have to use iron as their electron acceptor. This reduces the iron and makes it soluble. The iron is then washed away from the soil and the natural gray color of the soil minerals are revealed. Once the soil drains and oxygen is reintroduced, the iron is then oxidized, turning it red which forms the redoximorphic concentrations. Following this idea, there should be more redoximorphic concentrations in the 5 m treatment than the 40 m treatment due to better

aeration in the 5 m spacing. However, when the soil pits were dug in Block 2, the 40 m spacing pit had much more red color in the area where samples and the profile description were taken than in the other areas of the pit. This random variation in the soil explains the 5-20% difference in concentration abundance between the 5 m and 40 m spacings in Block 2. In Block 1, the difference in concentration abundance was only 5-10%. The Ap2 and Btg2 horizons in the 40 m spacing had 5% more concentrations than the 5 m spacing and the Btg1 horizon had 10% more concentrations in the 40 m spacing than the 5 m spacing. When considering the qualitative approach of soil profile descriptions and the estimation instead of direct measurement of redoximorphic feature abundance, as well as the natural soil variability, a 5% and 10% difference in concentration abundance is probably not significant.

Table 3.1. Soil profile description of the 5 m Block 1 soil pit.

| Depth [cm] | | Horizon | Boundary | | Texture | | Structure | Consistence | Matrix Color |
|---|---|---|---|---|---|---|---|---|---|
| Upper | Lower | | Dist. | Topo. | Class | Clay [%] | | | |
| 0 | 6 | Ap1 | Clear | Smooth | SiL | 15 | Weak thin platy parting to weak med./co. GR | Friable | 10YR 4/3or2 |
| 6 | 15 | Ap2 | Clear | Smooth | SiL | 15 | Mod med./thick platy | Firm | 10YR 5/4 |
| 15 | 28 | Ap2 | Abrupt | Smooth | SiL | 17 | Weak thick platy parting to mod. med./co. SBK | Very Firm | 10YR 5/4 |
| 28 | 65 | Btg1 | Clear | Wavy | SiL | 22 | Weak med./co. SBK | Firm | 10YR 7/2 |
| 65 | 109 | Btg2 | Clear | Wavy | SiCL | 29 | Mod. med./co. SBK | Firm | 10YR 7/1 |
| 109 | 119+ | 2Btg | -- | -- | -- | -- | -- | -- | -- |

Dist. = Distinctness, Topo. = Topography, Mod. = Moderate, Med. = Medium, Co. = Coarse, GR = Granular, SBK = Subangular blocky

Table 3.1 continued.

| Horizon | Concentrations | | Depletions | | FeMN Concretions | | Notes |
|---|---|---|---|---|---|---|---|
| | Color | Abundance [%] | Color | Abundance [%] | Size | Abundance [%] | |
| Ap1 | -- | -- | -- | -- | -- | -- | -- |
| Ap2 | 10YR 5/8 | 1-2 | -- | -- | -- | -- | 10YR 6/3 mottles due to tillage or bioturbation |
| Ap2 | 7.5YR 4/6 | 15 | 10YR 6/1 | 10 | Fine /V. Fine | 1-2 | "Plow Pan" |
| Btg1 | 7.5YR or 10YR 5/8 | 20 | -- | -- | V. Fine | 1-2 | Few discontinuous clay films (10YR 6/2), many fine organic coats in root channels, upper 5-10cm very firm ("plow pan") |
| Btg2 | 5YR 4/6, 7.5YR 5/8 | 25, 5 | -- | -- | -- | -- | Many clay films (10YR 6/1) |
| 2Btg | -- | -- | -- | -- | -- | -- | Not described, below pit depth |


Figure 3.1. Soil profile of the 5 m Block 1 soil pit.

Table 3.2. Soil profile description of the 5 m Block 2 soil pit.

| Depth [cm] | | Horizon | Boundary | | Texture | | Structure | Consistence | Matrix Color |
|---|---|---|---|---|---|---|---|---|---|
| Upper | Lower | | Dist. | Topo. | Class | Clay [%] | | | |
| 0 | 8 | Ap1 | Clear | Smooth | SiL | 15 | Weak/Mod. medium plates parting to mod. fine SBK | Friable | 10YR 4/2 |
| 8 | 20 | Ap2 | Clear | Smooth | SiL | 15 | Weak v.co. SKB parting to weak med. SBK | Friable | 10YR 5/3 |
| 20 | 27 | Bg | Clear | Wavy | SiL | 18 | Weak co. SBK | Very Firm | 2.5Y 6/2 |
| 27 | 36 | Btg1 | Gradual | Wavy | SiL | 22 | Weak co. /med. SBK | Firm | 10YR 7/1 |
| 36 | 69 | Btg2 | Clear | Wavy | SiL | 25 | Weak med. SBK | Firm | 10YR 7/2 |
| 69 | 108+ | Bt | -- | -- | SiCL | 28 | Mod. med. SBK | Firm | 10YR 6/3 |

Dist. = Distinctness, Topo. = Topography, Mod. = Moderate, Med. = Medium, Co. = Coarse, GR = Granular, SBK = Subangular blocky

Table 3.2 continued.

| Horizon | Concentrations | | Depletions | | FeMN Concretions | | Notes |
|---|---|---|---|---|---|---|---|
| | Color | Abundance [%] | Color | Abundance [%] | Size | Abundance [%] | |
| Ap1 | 7.5YR 4/6 | 1 | -- | -- | -- | -- | -- |
| Ap2 | 10 YR 6/6 | 3 | 10YR 6/1 | 5 | Fine | 2 | -- |
| Bg | 10YR 7/8 | 12 | -- | -- | Fine | 2 | -- |
| Btg1 | 10YR 6/6, 10YR 5/8 | 15, 5 | -- | -- | Fine | 1 | Few clay films on pore linings |
| Btg2 | 10YR 7/8, 10YR 5/8 | 20, 5 | -- | -- | -- | -- | Few discontinuous clay films (10YR 6/1) |
| Bt | 10YR 5/8 | 20 | 10YR 7/1 | 15 | -- | -- | Clay films (10YR 6/2) |

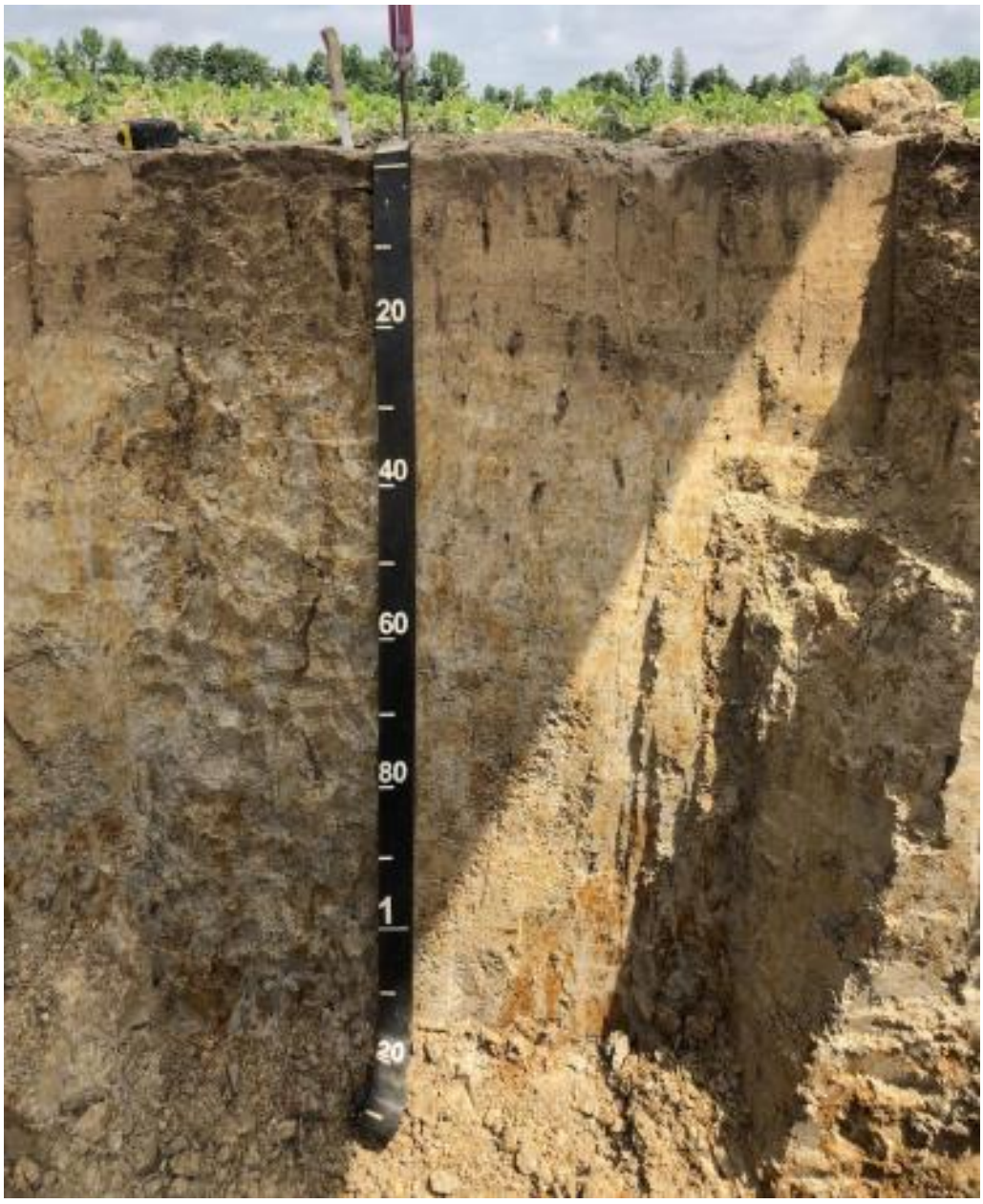


Figure 3.2. Soil profile of the 5 m Block 2 soil pit.

Table 3.3. Soil profile description of the 40 m Block 1 soil pit.

| Depth [cm] | | Horizon | Boundary | | Texture | | Structure | Consistence | Matrix Color |
|---|---|---|---|---|---|---|---|---|---|
| **Upper** | **Lower** | | **Dist.** | **Topo.** | **Class** | **Clay [%]** | | | |
| 0 | 15 | Ap1 | Clear | Smooth | SiL | 15 | Mod. thick platy parting to weak med./fine GR | Friable | 10YR 4/2 |
| 15 | 29 | Ap2 | Abrupt | Smooth | SiL | 17 | Weak thick platy parting to weak co. SBK | Firm | 10YR 6/4 |
| 29 | 64 | Btg1 | Gradual | Wavy | SiL | 24 | Weak med. SBK | Firm | 10YR 7/2 |
| 64 | 100 | Btg2 | Gradual | Wavy | SiCL | 32 | Mod. med. SBK | Firm | 10YR 7/2 |
| 100 | 120+ | 2Btg/2Bx** | -- | -- | -- | -- | -- | -- | -- |
| -- | -- | 2Btg | -- | -- | SiCL | 30 | Weak med. SBK | Firm | 10YR 7/1 |
| -- | -- | 2Bx | -- | -- | SiL | 24 | Weak med. Prismatic | Firm | 10YR 5/6 |

**described below as separate horizons.

Dist. = Distinctness, Topo. = Topography, Mod. = Moderate, Med. = Medium, Co. = Coarse, GR = Granular, SBK = Subangular blocky

Table 3.3 continued.

| Horizon | Concentrations | | Depletions | | FeMN Concretions | | Notes |
|---|---|---|---|---|---|---|---|
| | Color | Abundance [%] | Color | Abundance [%] | Size | Abundance [%] | |
| Ap1 | 7.5YR 5/8 | 2 | -- | -- | -- | -- | Distinct silt coatings on plate faces |
| Ap2 | 7.5YR 5/8 | 10 | 10YR 7/3or2 | 20 | Fine | 2 | Lower 5cm Very firm (upper "plow pan") |
| Btg1 | 7.5YR 5/8, 2.5YR 3/6 | 30, 2-5 | -- | -- | Fine | 1-2 | Few discontinuous clay films, upper 10cm very firm (Plow Pan), 10YR 7/1 or 6/2 organic coatings |
| Btg2 | 7.5YR 5/8, 2.5YR 3/6 | 30, 5 | -- | -- | Fine | 1 | Clay Films (10YR 6/2) |
| 2Btg/2Bx** | -- | -- | -- | -- | -- | -- | **Described Below as separate horizons |
| 2Btg | 10YR 5/6 | 20 | -- | -- | -- | -- | Clay Films (10YR 6/2) |
| 2Bx | -- | -- | -- | -- | -- | -- | Beginning of fragipan prism tips ~25-30% of total horizon (i.e. 25-30% of 2Btg/2Bx), clay films (10YR 4/6), FeMN coats and pore linings |


Figure 3.3. Soil profile of the 40 m Block 1 soil pit.

Table 3.4. Soil profile description of the 40 m Block 2 soil pit.

| Depth [cm] | | Horizon | Boundary | | Texture | | Structure | Consistence | Matrix Color |
|---|---|---|---|---|---|---|---|---|---|
| Upper | Lower | | Dist. | Topo. | Class | Clay [%] | | | |
| 0 | 10 | Ap1 | Clear | Smooth | SiL | 12 | Weak thin platy parting to weak med./fine SBK | Friable | 10YR 4/2 |
| 10 | 25 | Ap2 | Clear | Smooth | SiL | 17 | Weak thick platy parting to weak med. SBK | Firm | 10YR 5/3 |
| 25 | 35 | Btg1 | Gradual | Wavy | SiL | 21 | Weak med./co. SBK | Firm | 10YR 7/1 |
| 35 | 56 | Btg2* | Gradual | Wavy | SiL | 22 | Mod. med./co. SBK | Firm | 10YR 6/4 |
| 56 | 83 | Btg3* | Clear | Wavy | SiCL | 29 | Mod. fine/med. SBK | Firm | 10YR 5/6 |
| 83 | 104+ | 2Btg* | -- | -- | SiCL | 31 | Weak med./co. SBK | Firm | 10YR 5/3 |

*As described in the text, Btg2, Btg3, and 2Btg do not have a low enough chroma to have a "g" subordinate distinction. However, the majority of the pit face (outside the sampling area) would have been classified as Btg so we decided to label these horizons as Btg to better match the surrounding soil.

Dist. = Distinctness, Topo. = Topography, Mod. = Moderate, Med. = Medium, Co. = Coarse, GR = Granular, SBK = Subangular blocky

Table 3.4 continued.

| Horizon | Concentrations | | Depletions | | FeMN Concretions | | Notes |
|---|---|---|---|---|---|---|---|
| | Color | Abundance [%] | Color | Abundance [%] | Size | Abundance [%] | |
| Ap1 | 10YR 5/8 | 3-4 | -- | -- | Fine | 1 | -- |
| Ap2 | 10YR 5/8 | 8-10 | 10YR 6/2 | 15 | V. Fine | 2-3 | -- |
| Btg1 | 10YR 5/6, 5YR 5/8 | 30, 10 | -- | -- | Fine | 3 | Few thick clay films |
| Btg2* | 5YR 5/8 | 30 | -- | -- | Fine | 2-3 | Clay films (10YR 7/1) |
| Btg3* | 7.5YR 5/8, 5YR 5/8 | 25, 5 | -- | -- | Fine | 2 | Clay films (10YR 6/1) 60% of profile |
| 2Btg* | 7.5YR 5/6 | 18-20 | 10YR 6/1 | 40 | Fine | 2 | Clay films, FeMN coats 10-15% |


Figure 3.4. Soil profile of the 40 m Block 2 soil pit.

## 3.2 Bulk Density

The first set of bulk density samples were taken in all four treatments at depths of 0-5, 5-15, and 15-30 cm (Table 3.5, Figure 3.5). The 0-5 cm depth had a significant spacing*block effect (Figure 3.6). Block 1 had no differences among treatments while in Block 2, the 10 m treatment was much higher than all other treatments. This difference in Block 2 caused a spacing effect of the 10 m treatment being higher than all other treatments (Table 3.5). The high bulk density in the 10 m Block 2 plot aligns with other anomalous carbon content and soil fertility data, not presented in this thesis, collected from the same plot. A block effect was also observed at the 0-5 cm depth with Block 2 being higher than Block 1 due to the 10 m plot in Block 2. At 5-15 cm, the 5m spacing had a lower bulk density (1.53 g $cm^{-3}$) than the 10 m, 20 m, and 40 m spacings (1.57 g $cm^{-3}$, 1.56 g $cm^{-3}$, and 1.58 g $cm^{-3}$, respectively). At 15-30 cm, the 5 m spacing had a lower bulk density than the 40 m spacing (1.57 g $cm^{-3}$ and 1.61 g $cm^{-3}$, respectively).

The hydraulic probe bulk density samples were taken on all four treatments at depth increments of 0-15, 15-30, 30-50, 50-75, and 75-100 cm. At the 0-15 cm depth, the 5 m spacing had a lower bulk density (1.46 g $cm^{-3}$) than the 10 m and 20 m spacings (1.54 g $cm^{-3}$ and 1.52 g $cm^{-3}$, respectively) but did not differ from the 40 m spacing (Table 3.6, Figure 3.7). At the 15-30 cm depth, the 5 m spacing was lower than the 40 m spacing (1.61 g $cm^{-3}$ and 1.65 g $cm^{-3}$, respectively). Hundal et al. (1976) found a significant, but small, difference in bulk density at 0-15 cm between tile drained and undrained silty clay soils with the tile drained treatment having a slightly lower bulk density than the undrained. The authors did not find a significant difference at the 15-30 cm depth. No spacing effect, block effect, or spacing*block effect was apparent at the 30-50 cm or 50-75 cm depths. A spacing*block effect was revealed at the 75-100 cm depth where Block 2 had no significant differences but in Block 1, the 40 m spacing was higher than all other treatments (Figure 3.8). There was also a spacing effect at 75-100 cm where the 10 m spacing was lower than the 40 m spacing. Jia et al. (2008) found no significant differences in bulk density among tile drained and undrained silty clay loam fields down to the 1.5 m deep tiles.

The third set of bulk density measurements were taken from the soil pits in the 5 m and 40 m treatments in similar horizons rather than set depth increments. The horizons sampled were Ap2, Btg1, Btg1/Btg2, and Btg2/Bt/Btg3. The 5 m spacing had a lower bulk density (1.59 g $cm^{-3}$) than the 40 m spacing (1.62 g $cm^{-3}$) in the Ap2 horizon (Table 3.7, Figure 3.9). The Btg1 horizon had a spacing*block effect due to the 40 m being lower than the 5 m in Block 1 but no differences in

Block 2 (Figure 3.10). There were no main effects of spacing or block evident in the Btg1 horizon. There were no spacing, block, or spacing*block effects in the Btg1/Btg2 or Btg2/Bt/Btg3 horizons.

Bulk density results from the hydraulic probe samples match well with the first set of bulk density cores. The 0-15 cm values from the hydraulic probe are close to the average of the 0-5 cm and 5-15 cm values from the first set of bulk density cores. The hydraulic probe bulk density values at 15-30 cm are slightly higher than the first set of bulk density core values but they follow the same trends among treatments. The slightly higher bulk density values from the hydraulic probe may have been caused by the plow pan being included in the hydraulic probe sample but not in the 6 cm tall hand cores. The only horizon from the soil pits that can be compared to the first set of bulk density cores is the Ap2 horizon. The depths of the Ap2 horizons correspond fairly well with the 15-30 cm depth increment. The bulk density values of the 15-30 cm depth from the first set of bulk density cores are very similar to the bulk density values for the Ap2 horizons from the soil pit sampling. In all three sets of bulk density measurements, the 5 m spacing was significantly lower than the 40 m spacing at 15-30 cm, although the difference among treatments was small. As the water table is lowered in the 5 m treatment, the increased aeration in the soil provides a more beneficial environment for plant roots and soil organisms. The soil organisms create burrows that decrease bulk density and also excrete compounds that aid in soil aggregation. As aggregation increases and the soil becomes more stable, pore space becomes stable and bulk density decreases. Plant roots also create channels in the soil and excrete compounds that aid in aggregate formation leading to a decrease in bulk density. The 5 m treatment also had significantly lower bulk density than the 40 m treatment in the 5-15 cm depth but not in the 0-5 cm. Not detecting a significant difference in the 0-5 cm depth may have been caused by several environmental variables at the surface covering up any effect of drainage such as wind and water erosion, solar radiation and evaporation drying the surface, foot and wheel traffic compacting the surface, disturbance from planting equipment, freeze-thaw cycles, and many more. Perhaps the reason no significant difference was detected among the 5 m and 40 m spacings in the 0-15 cm depth from the hydraulic probe samples even though there was a 0.04 g $cm^{-3}$ difference was because the 0-5 cm section diluted any differences that occurred in the 5-15 cm section. The top 30 cm of soil in the 5 m treatment spends less time saturated than in the 40 m treatment resulting in more soil organism activity and better root growth. Perhaps we do not see a significant difference in bulk density below 30 cm because the 5 m treatment spends more time saturated at this depth than closer to the surface

and the difference in amount of time saturated between the 5 m and 40 m treatments may not be enough to cause a significant difference. There is also less organic matter to fuel soil organism activity and possibly less roots due to high bulk density which is discussed later. Even though multiple methods were used to measure bulk density at different times, the results were in agreement. It is difficult to compare the bulk density values taken with the hydraulic probe to the soil pit bulk density values because the depths do not align well and most of the hydraulic probe depth increments contain multiple horizons. Bulk density differences among treatments were very small. The maximum difference in a spacing effect was 0.06 g $cm^{-3}$ and most of the time it was less than that. Although these differences are statistically significant, they are most likely not physically significant. A difference that small will probably not change any effects on root penetration, water retention, or air and water infiltration and circulation. For silty soils, a bulk density less than 1.4 g $cm^{-3}$ is ideal for plant growth and bulk densities over 1.65 g $cm^{-3}$ can restrict root growth (USDA, 2008). At the 0-5 cm depth, the bulk density values were generally between 1.4 g $cm^{-3}$ and 1.5 g $cm^{-3}$. However, as depth increases, particularly 15-30 cm and below, the bulk density values tend to be closer to 1.6 g $cm^{-3}$. Although these values are not above the general guideline value of 1.65 g $cm^{-3}$ to severely restrict root growth, they are high enough to have some negative influence on root growth and possibly air and water movement in the soil.

Table 3.5. Soil bulk density (g $cm^{-3}$) at multiple depths, sampled with the short core method. Each value represents the mean of both blocks and 8 subplots (n=16). Values within the same depth that contain the same letter are not significantly different as determined by an LSMeans test ($p \leq 0.10$). Standard deviations are presented in parentheses.

| **Treatment** | **Depth (cm)** | | |
|---|---|---|---|
| | **0-5** | **5-15** | **15-30** |
| **5 m** | 1.40b (0.07) | 1.53b (0.03) | 1.57b (0.04) |
| **10 m** | 1.50a (0.07) | 1.57a (0.03) | 1.59ab (0.03) |
| **20 m** | 1.39b (0.05) | 1.56a (0.04) | 1.59ab (0.04) |
| **40 m** | 1.43b (0.09) | 1.58a (0.03) | 1.61a (0.03) |

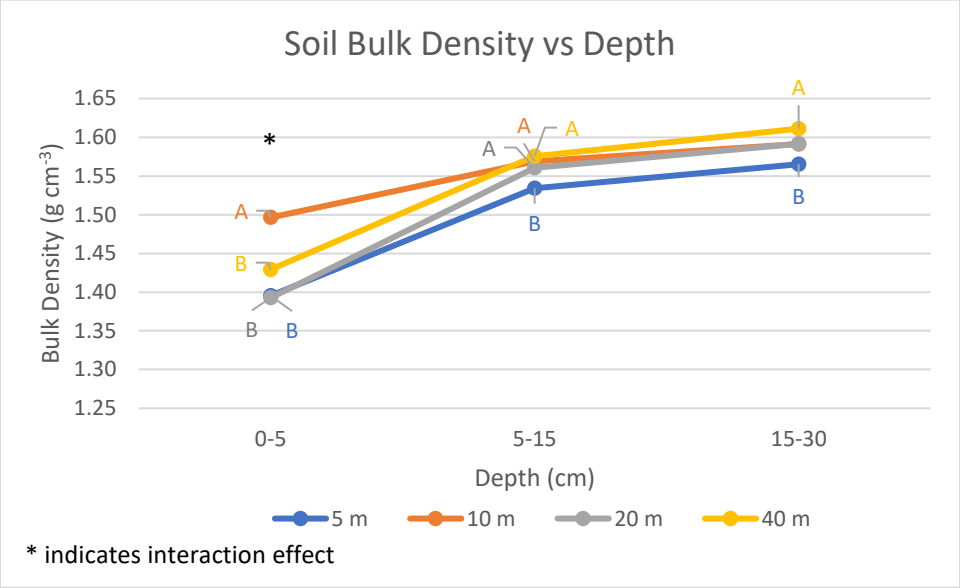


Figure 3.5. Soil bulk density (g $cm^{-3}$) at multiple depths, sampled with the short core method. Each data point represents the mean of both blocks and 8 subplots (n=16). Data points within the same depth that contain the same letter are not significantly different as determined by an LSMeans test ($p \leq 0.10$). Data points that do not contain a letter are not significantly different than any other point within that depth.

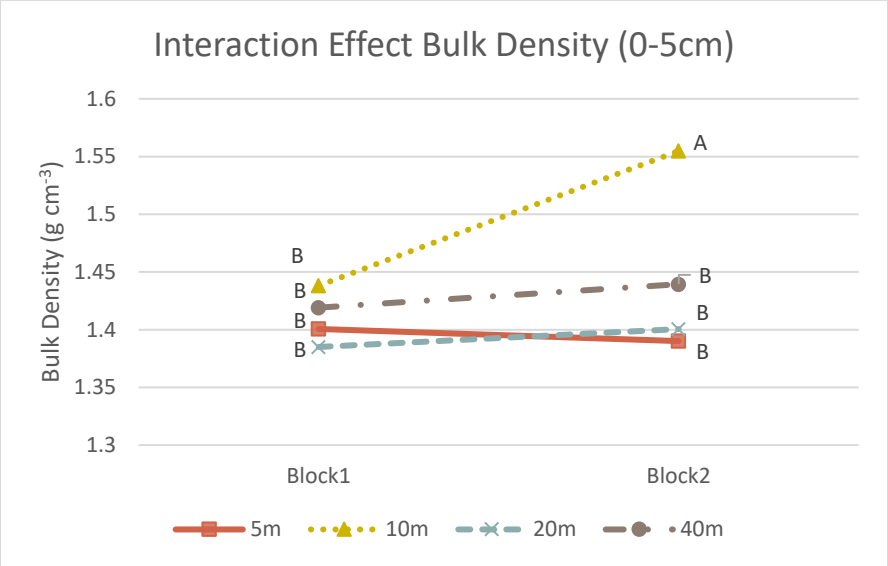


Figure 3.6. Soil bulk density sampled with the short core method spacing*block effect at 0-5 cm depth increment. Each value represents the mean of 8 subplots (n=8). Values that contain the same letter are not significantly different as determined by an LSMeans test ($p \leq 0.10$).

Table 3.6. Soil bulk density (g $cm^{-3}$), sampled with the hydraulic probe. Each value represents the mean of both blocks and 8 subplots (n=16). Values within the same depth that contain the same letter are not significantly different as determined by an LSMeans test ($p \leq 0.10$). Standard deviations are presented in parentheses.

| **Treatment** | **Depth (cm)** | | | | |
|---|---|---|---|---|---|
| | **0-15** | **15-30** | **30-50** | **50-75** | **75-100** |
| **5 m** | 1.46b (0.05) | 1.61b (0.05) | 1.59a (0.06) | 1.57a (0.04) | 1.59ab (0.07) |
| **10 m** | 1.54a (0.04) | 1.63ab (0.04) | 1.59a (0.06) | 1.58a (0.05) | 1.57b (0.05) |
| **20 m** | 1.52a (0.06) | 1.63ab (0.04) | 1.60a (0.05) | 1.58a (0.05) | 1.59ab (0.05) |
| **40 m** | 1.50ab (0.07) | 1.66a (0.04) | 1.62a (0.06) | 1.60a (0.07) | 1.63a (0.05) |

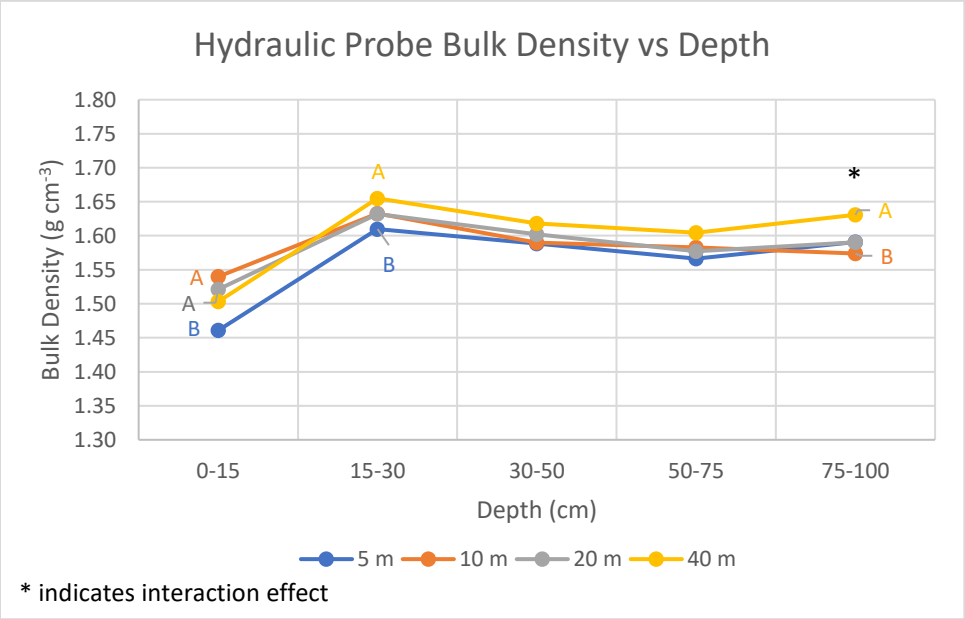


Figure 3.7. Soil bulk density (g $cm^{-3}$), sampled with the hydraulic probe. Each data point represents the mean of both blocks and 8 subplots (n=16). Data points within the same depth that contain the same letter are not significantly different as determined by an LSMeans test ($p \leq 0.10$). Data points that do not contain a letter are not significantly different than any other point within that depth.

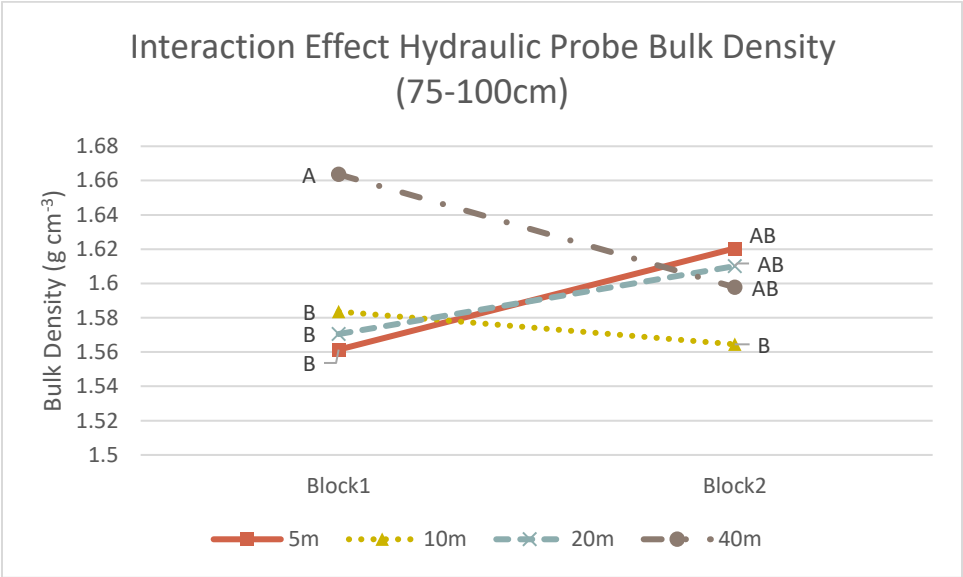


Figure 3.8. Soil bulk density sampled with the hydraulic probe, spacing*block effect at 75-100 cm. Each value represents the mean of 8 subplots (n=8). Values that contain the same letter are not significantly different as determined by an LSMeans test ($p \leq 0.10$).

Table 3.7. Soil pit bulk density (g $cm^{-3}$). Each value represents the mean of both blocks and 5 subsamples (n=10). Values within the same horizon that contain the same letter are not significantly different as determined by an LSMeans test ($p \leq 0.10$). Standard deviations are presented in parentheses.

| **Treatment** | **Horizon** | | | |
|---|---|---|---|---|
| | **Ap2** | **Btg1** | **Btg1/Btg2** | **Btg2/Bt/Btg3** |
| **5 m** | 1.59b (0.03) | 1.63a (0.02) | 1.56a (0.04) | 1.50a (0.04) |
| **40 m** | 1.62a (0.01) | 1.60a (0.07) | 1.56a (0.05) | 1.48a (0.09) |

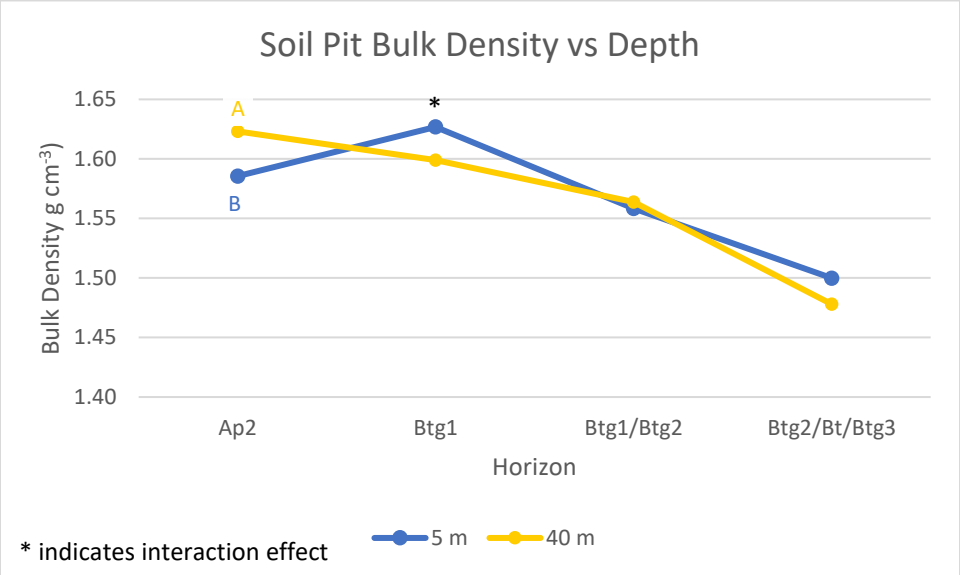


Figure 3.9. Soil pit bulk density (g $cm^{-3}$). Each data point represents the mean of both blocks and 5 subsamples (n=10). Data points within the same horizon that contain the same letter are not significantly different as determined by an LSMeans test ($p \leq 0.10$). Data points that do not contain a letter are not significantly different than any other point within that horizon.

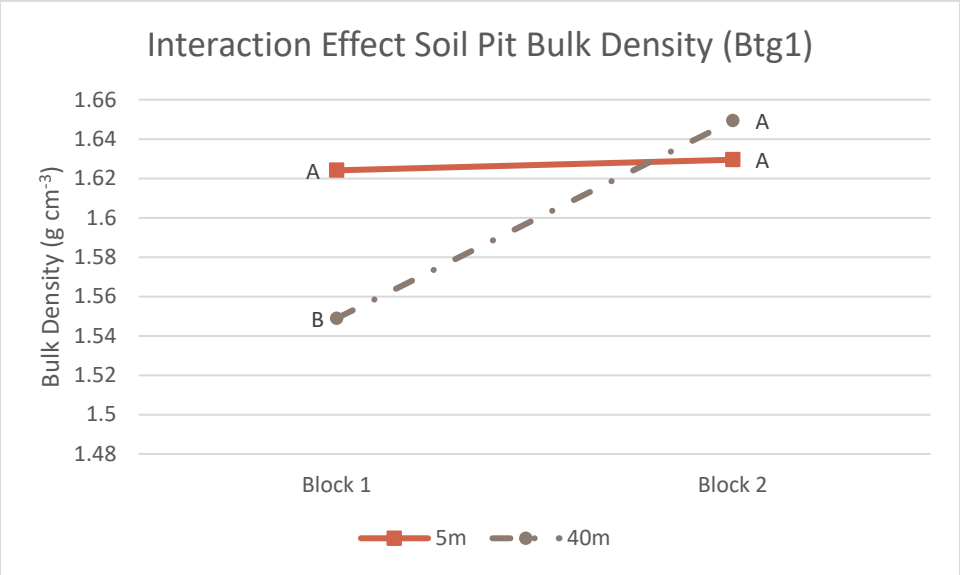


Figure 3.10. Soil pit bulk density spacing*block effect in the Btg1 horizon. Each value represents the mean of 5 subsamples (n=5). Values that contain the same letter are not significantly different as determined by an LSMeans test ($p \leq 0.10$).

### 3.3 Total Porosity

Total porosity was calculated from the bulk density samples and the results follow the same trends as bulk density in terms of significance (Table 3.8, Figure 3.11). Thus, the 0-5 cm depth increment had a significant spacing*block effect due to Block 1 having no difference but in Block 2, the 10 m spacing had a lower total porosity than all other treatments (Figure 3.12). The differences in Block 2 caused a spacing effect of the 10 m treatment being lower than all other treatments (Table 3.8). At 5-15 cm, the 5 m spacing had a higher total porosity (0.421 $cm^3$ $cm^{-3}$) than the 10 m, 20 m, and 40 m spacings (0.408 $cm^3$ $cm^{-3}$, 0.411 $cm^3$ $cm^{-3}$, and 0.405 $cm^3$ $cm^{-3}$, respectively). At 15-30 cm, the 5 m treatment had a higher total porosity (0.409 $cm^3$ $cm^{-3}$) than the 40 m treatment (0.392 $cm^3$ $cm^{-3}$).

Total porosity calculated from hydraulic probe samples follow the bulk density results from the hydraulic probe (Table 3.9, Figure 3.13). The 5 m spacing had a higher total porosity (0.499 $cm^3$ $cm^{-3}$) than the 10 m and 20 m spacings (0.419 $cm^3$ $cm^{-3}$ and 0.426 $cm^3$ $cm^{-3}$, respectively) but was not different than the 40 m spacing in the 0-15 cm depth range. In the 15-30 cm depth range, the 5 m treatment had a higher total porosity (0.393 $cm^3$ $cm^{-3}$) than the 40 m treatment (0.376 $cm^3$ $cm^{-3}$). The 30-50 cm and 50-75 cm depths did not have any differences, but the 75-100 cm depth had a spacing*block effect. Block 2 had no significant differences among treatments but in Block 1, the 40 m treatment had a lower total porosity than all other treatments (Figure 3.14). The differences in Block 1 along with small differences in Block 2 contributed to the spacing effect that shows the 40 m being lower than the 10 m (Table 3.9).

Once again, the total porosity results for the soil pit samples followed the results for the soil pit bulk density. In the Ap2 horizon, the 5 m treatment had a higher total porosity (0.402 $cm^3$ $cm^{-3}$) than the 40 m treatment (0.388 $cm^3$ $cm^{-3}$) (Table 3.10, Figure 15). The only other significant effect was a spacing*block effect in the Btg1 horizon where the 40 m spacing was higher than the 5 m spacing in Block 1 but there were no differences in Block 2 (Figure 3.16).

Table 3.8. Soil total porosity ($cm^3$ $cm^{-3}$). Each value represents the mean of both blocks and 8 subplots (n=16). Values within the same depth that contain the same letter are not significantly different as determined by an LSMeans test ($p \leq 0.10$). Standard deviations are presented in parentheses.

| **Treatment** | **Depth (cm)** | | |
|---|---|---|---|
| | **0-5** | **5-15** | **15-30** |
| **5 m** | 0.474a (0.028) | 0.421a (0.010) | 0.409a (0.014) |
| **10 m** | 0.435b (0.027) | 0.408b (0.012) | 0.400ab (0.012) |
| **20 m** | 0.474a (0.020) | 0.411b (0.013) | 0.399ab (0.016) |
| **40 m** | 0.461a (0.035) | 0.405b (0.013) | 0.392b (0.012) |

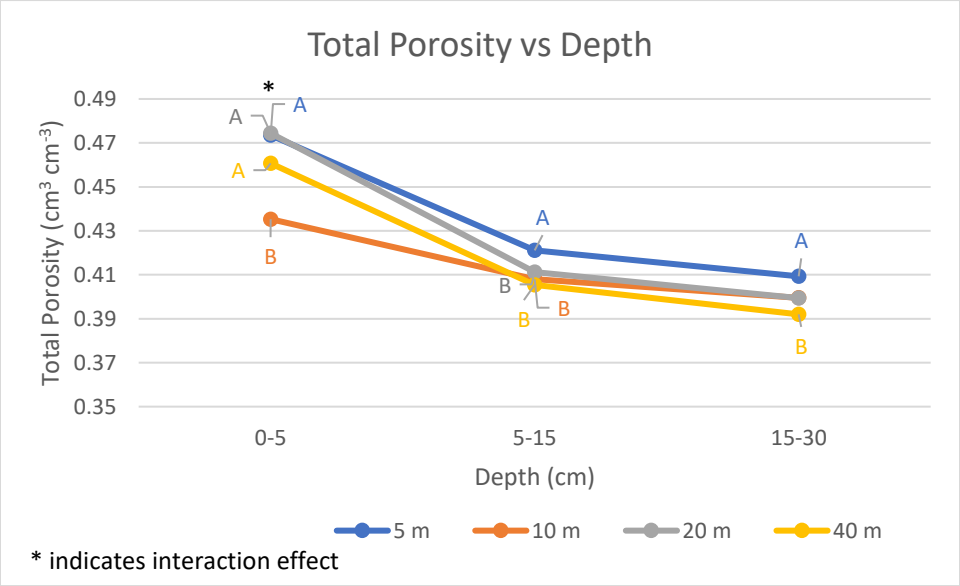


Figure 3.11. Soil total porosity ($cm^3$ $cm^{-3}$). Each data point represents the mean of both blocks and 8 subplots (n=16). Data points within the same depth that contain the same letter are not significantly different as determined by an LSMeans test ($p \leq 0.10$). Data points that do not contain a letter are not significantly different than any other point within that depth.

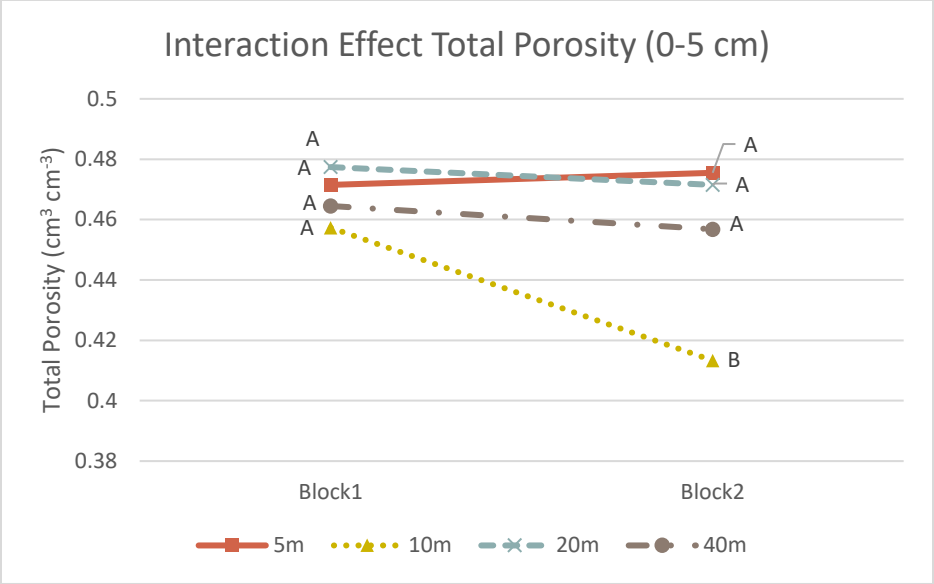


Figure 3.12. Soil total porosity spacing*block effect at 0-5 cm depth increment. Each value represents the mean of 8 subplots (n=8). Values that contain the same letter are not significantly different as determined by an LSMeans test ($p \leq 0.10$).

Table 3.9. Total porosity ($cm^3\ cm^{-3}$) from the hydraulic probe samples. Each value represents the mean of both blocks and 8 subplots (n=16). Values within the same depth that contain the same letter are not significantly different as determined by an LSMeans test ($p \leq 0.10$). Standard deviations are presented in parentheses.

| **Treatment** | **Depth (cm)** | | | | |
|---|---|---|---|---|---|
| | **0-15** | **15-30** | **30-50** | **50-75** | **75-100** |
| **5 m** | 0.449a (0.019) | 0.393a (0.018) | 0.401a (0.021) | 0.409a (0.015) | 0.400ab (0.025) |
| **10 m** | 0.419b (0.014) | 0.384ab (0.015) | 0.400a (0.023) | 0.403a (0.018) | 0.406a (0.021) |
| **20 m** | 0.426b (0.024) | 0.384ab (0.016) | 0.395a (0.018) | 0.405a (0.020) | 0.400ab (0.020) |
| **40 m** | 0.433ab (0.025) | 0.376b (0.016) | 0.389a (0.023) | 0.395a (0.025) | 0.385b (0.020) |

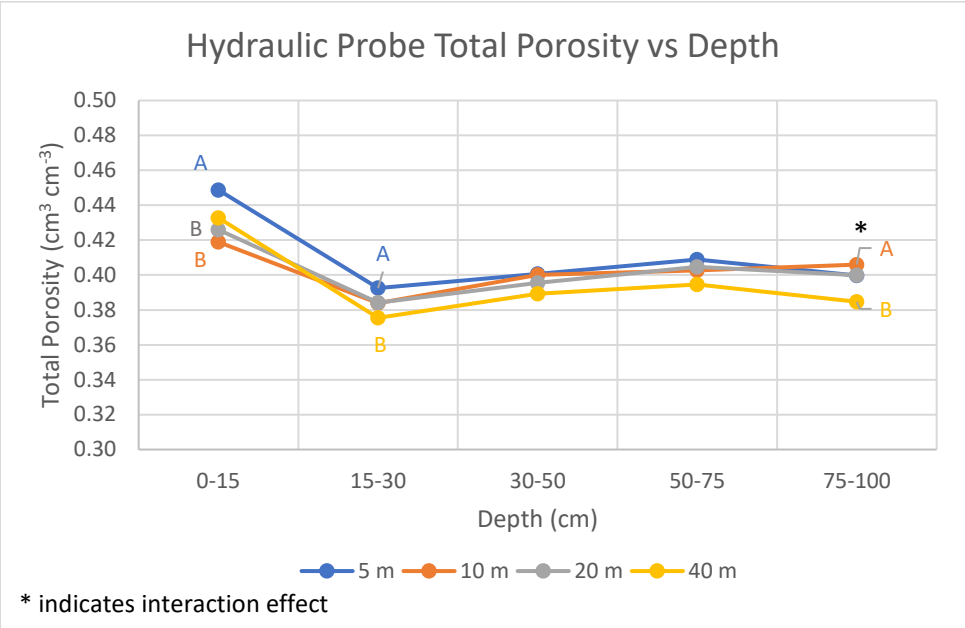


Figure 3.13. Total porosity ($cm^3$ $cm^{-3}$) from the hydraulic probe samples. Each data point represents the mean of both blocks and 8 subplots (n=16). Data points within the same depth that contain the same letter are not significantly different as determined by an LSMeans test ($p \leq 0.10$). Data points that do not contain a letter are not significantly different than any other point within that depth.

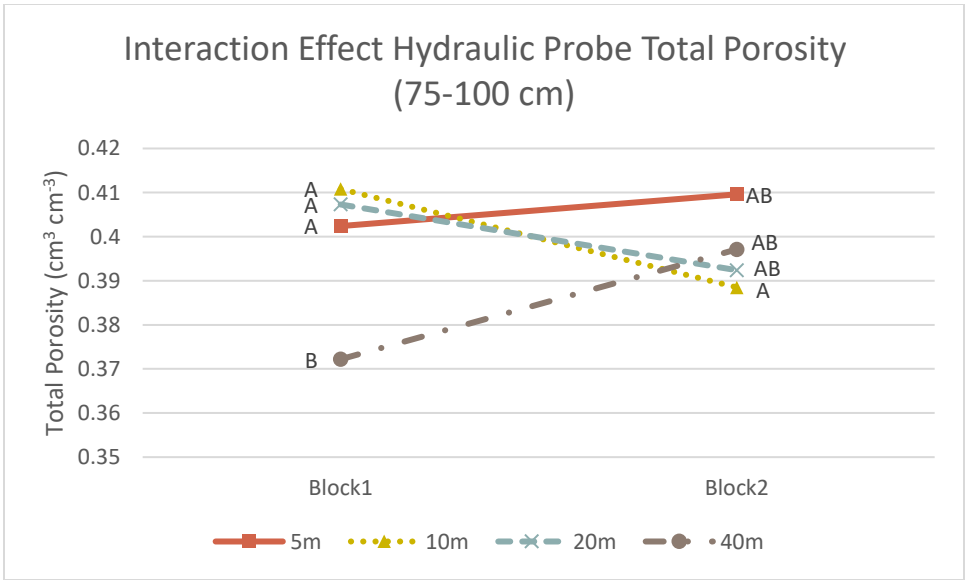


Figure 3.14. Total porosity from the hydraulic probe samples, spacing*block effect at 75-100 cm. Each value represents the mean of 8 subplots (n=8). Values that contain the same letter are not significantly different as determined by an LSMeans test ($p \leq 0.10$).

Table 3.10. Soil pit total porosity ($cm^3$ $cm^{-3}$). Each value represents the mean of both blocks and 5 subsamples (n=10). Values within the same horizon that contain the same letter are not significantly different as determined by an LSMeans test ($p \leq 0.10$). Standard deviations are presented in parentheses.

| **Treatment** | **Horizon** | | | |
|---|---|---|---|---|
| | **Ap2** | **Btg1** | **Btg1/Btg2** | **Btg2/Bt/Btg3** |
| **5 m** | 0.402a (0.012) | 0.386a (0.07) | 0.412a (0.016) | 0.434a (0.015) |
| **40 m** | 0.388b (0.005) | 0.397a (0.026) | 0.410a (0.017) | 0.442a (0.035) |

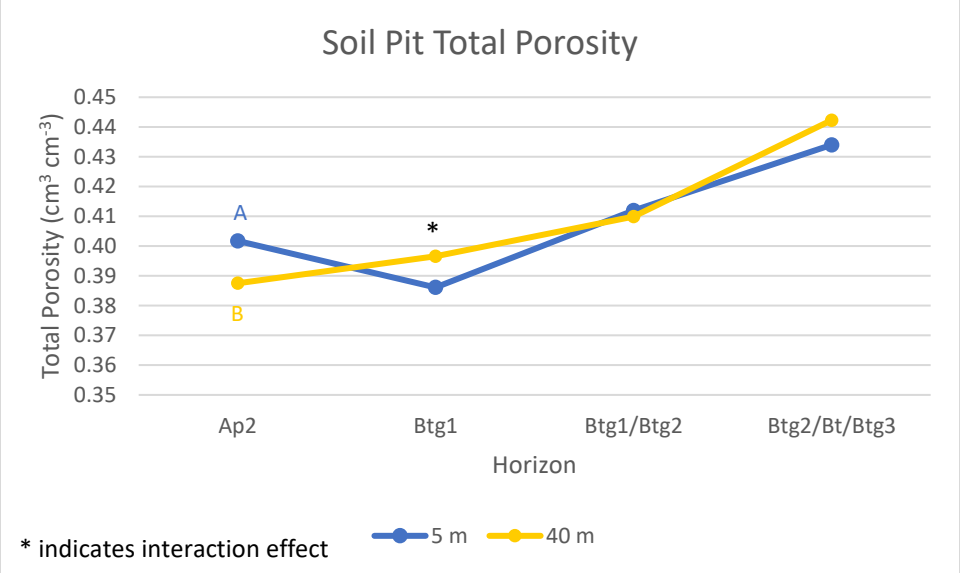


Figure 3.15. Soil pit total porosity ($cm^3$ $cm^{-3}$). Each data point represents the mean of both blocks and 5 subsamples (n=10). Data points within the same horizon that contain the same letter are not significantly different as determined by an LSMeans test ($p \leq 0.10$). Data points that do not contain a letter are not significantly different than any other point within that horizon.

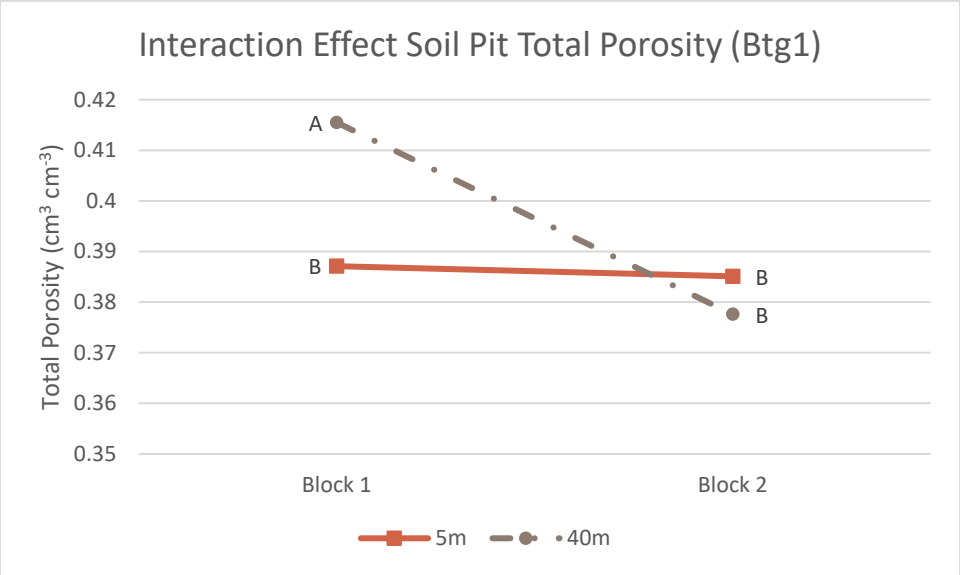


Figure 3.16. Soil pit total porosity spacing*block effect in the Btg1 horizon. Each value represents the mean of 5 subsamples (n=5). Values that contain the same letter are not significantly different as determined by an LSMeans test ($p \leq 0.10$).

## 3.4 Water Retention

### 3.4.1 Samples from 0-5 cm, 5-15 cm, and 15-30 cm

The first set of water retention measurements were taken on the same soil cores as bulk density at depths of 0-5 cm, 5-15 cm, and 15-30 cm on all four spacings, two blocks, and eight subplots. In the 0-5 cm depth range, at 0 kPa water potential, the 10 m spacing had a lower volumetric water content (0.432 $cm^3$ $cm^{-3}$) than the 5 m and 40 m spacings (0.455 $cm^3$ $cm^{-3}$ and 0.453 $cm^3$ $cm^{-3}$, respectively) (Table 3.11, Figure 3.17). Spacing*block, spacing, and block effects occurred at -4.9 kPa, -9.8 kPa, and -33 kPa. In Block 1, the 40 m spacing was lower than the 20 m spacing at all three water potentials but in Block 2, the only significant difference was the 10 m spacing being lower than the 5 m spacing at -33 kPa (Figures 3.18, 3.19, 3.20). The spacing main effect shows the 10 m spacing having a lower volumetric water content than the 5 m and 20 m spacings and the block effect reveals that Block 2 has a higher volumetric water content than Block 1. The spacing effect may be attributed to the 10 m spacing have a higher bulk density at 0-5 cm than the other treatments. A spacing*block effect occurred at -1500kPa because the ranking order and relative differences among treatments changed between Block 1 and Block 2 (Figure 3.21). In Block 1, the 10 m spacing was not significantly different than any other treatments but in Block 2, the 10 m was significantly lower than the 40 m spacing. This resulted in a main spacing effect where the 40 m had a higher volumetric water content than all other treatments. In the 5-15 cm depth range, most water potentials had a block effect where Block 2 was higher than Block 1. For the main effect of spacing at 0 kPa water potential, the 5 m treatment had a higher volumetric water content (0.367 $cm^3cm^{-3}$) than the 10 m treatment (0.356 $cm^3$ $cm^{-3}$) although the difference was small (Table 3.12, Figure 3.22). At -4.9 kPa and -9.8 kPa, the 40 m spacing had a higher volumetric water content than the 10 m spacing. The 40 m spacing had a higher volumetric water content than all other treatments at -33 kPa water potential. At -1500 kPa, there were spacing*block, spacing, and block effects. The spacing*block effect arose from the 40 m spacing being significantly higher than all other treatments in Block 1 but was only significantly higher than the 10 m and 20 m spacings in Block 2 (Figure 3.23). The spacing main effect shows the 40 m treatment had a higher water content than all other treatments and the 5 m treatment had a higher water content than the 10 m and 20 m treatments (Table 3.12) mostly due to Block 2 (Figure 3.23). In the 15-30 cm depth, at 0 kPa, the 5 m spacing had a higher volumetric water content than all other treatments, although

the difference was small (Table 3.13, Figure 3.24). At -4.9 kPa, -9.8 kPa, and -33 kPa, the 40 m spacing had a higher volumetric water content than the 10 m spacing and there was a block effect where Block 2 was higher than Block 1. Spacing*block, spacing, and block effects occurred at -1500 kPa. There were no differences among treatments in Block 1 but in Block 2, the 40 m spacing had a higher volumetric water content than all other treatments (Figure 3.25). The differences in Block 2 caused a spacing main effect where the 40 m treatment had a higher volumetric water content than all other treatments (Table 3.13).

Water holding capacity (WHC) is the difference in volumetric water contents at wilting point, -1500 kPa, and field capacity, -9.8 kPa (Table 3.14, Figure 26). In the 0-5 cm depth increment, a spacing*block effect was observed. Block 2 had no differences among treatments but Block 1 showed the 20 m spacing being higher than the 10 m and 40 m spacings, as well as the 5 m spacing being higher than the 40 m spacing (Figure 3.27). The 20 m spacing had a significantly higher volumetric water content at -9.8 kPa than the 10 m and 40 m spacings as well as a significantly lower volumetric water content than the 40 m spacing and a non-significantly different water content as the 10 m spacing at -1500 kPa resulting in a significantly higher water holding capacity than both the 10 m and 40 m spacings. The 5 m spacing had a non-significantly different water content as the 40 m spacing at -9.8 kPa but had a significantly lower water content than the 40 m spacing at -1500 kPa resulting in a higher WHC for the 5 m spacing. These differences in Block 1 caused a spacing effect where the 5 m and 20 m spacing had a higher water holding capacity than the 10 m and 40 m spacings (Table 3.14). No spacing effects were evident in the 5-15 cm and 15-30 cm depths but there were spacing*block effects in both depths. For the 5-15 cm depth increment, there were no significant differences among spacings within Block 1 or Block 2 but the 10 m spacing had a significantly lower water holding capacity in Block 1 than it did in Block 2 (Figure 3.28). Although the differences were not significant, the 10 m spacing in Block 1 had a slightly lower water content than the 10 m spacing in Block 2 at -9.8 kPa and a slightly higher water content than the 10 m spacing in Block 2 at -1500 kPa resulting in the 10 m spacing in Block1 having a significantly lower WHC than the 10 m spacing in Block 2. For the 15-30 cm depth, Block 2 had no significant differences among treatments but in Block 1, the 5 m spacing had a higher water holding capacity than the 10 m spacing (Figure 3.29). This is a result of the 5 m spacing having a slightly higher, although not significantly different, water content than the 10 m at -9.8 kPa and a slightly lower, although not significantly different, water content than

the 10 m spacing at -1500 kPa in Block 1. With differences among spacings only occurring in Block 1 at 0-5 cm and 15-30 cm and because the differences that did occur are among different treatments at respective depths, it is difficult to say if drain spacing has had any effect on water holding capacity. Frison et al. (2009) detected higher available water contents 0.6 m from the drain compared to 7 m from the drain in an E&Bt horizon. However, there was also a change in minerology that may have contributed to these differences.

### 3.4.2 Samples from soil pit horizons

The second set of water retention measurements were taken from the soil bulk density cores sampled from the soil pits in the 5 m and 40 m treatments. In the Ap2 horizon, Block 2 had higher volumetric water contents than Block 1 at all water potentials but there were no differences among treatments at 0 kPa, -2.45 kPa, -4.9 kPa, and -9.8 kPa (Table 3.15, Figure 30). At -33 kPa, a spacing*block effect occurred because Block 1 had no differences but in Block 2, the 40 m spacing had a higher volumetric water content than the 5 m spacing (Figure 3.31). This resulted in a spacing effect showing the 40 m treatment to be higher than the 5 m treatment (Table 3.15). In the Btg1 horizon (Table 3.16, Figure 32), there was a spacing*block effect at all water potentials. Block 2 did not have any differences among treatments but in Block 1, the 40 m spacing had a higher water content than the 5 m spacing (Figures 3.33, 3.34, 3.35, 3.36, 3.37). This resulted in a spacing effect at all potentials showing the 40 m spacing to have a higher volumetric water content than the 5 m spacing (Table 3.16). This interaction effect and spacing main effect can be related back to bulk density. In the Btg1 horizon, the 40 m spacing had a significantly lower bulk density than the 5 m spacing in Block 1 but Block 2 did not show any differences. A lower bulk density and higher total porosity in Block 1 resulted in the 40 m spacing having more room to store water and a higher water content at all water potentials in Block 1. No spacing*block, spacing, or block effects were evident in the Btg1/Btg2 horizon (Table 3.17, Figure 3.38). In the Btg2/Bt/Btg3 horizon, there were no differences at 0 kPa and -2.45 kPa (Table 3.18, Figure 3.39). There was no main effect of spacing at -4.9 kPa and -9.8 kPa however a spacing*block effect was observed due to the changing of ranking order and relative differences among treatments between Block 1 and Block 2 (Figures 3.40, 3.41). Another spacing*block effect was observed at -33 kPa. Block 1 did not have any differences among treatments but in Block 2, the 5 m treatment had a higher water content than the 40 m treatment (Figure 3.42). No spacing main effect was evident at -33 kPa (Table 3.18).

The -1500 kPa bulk samples were collected from the soil pit in slightly different horizons than the soil cores so the -1500 kPa values could not be converted from gravimetric water content to volumetric water content and available water holding capacity could not be calculated (Table 3.19). The horizons sampled for -1500 kPa measurements were Ap1, Ap2, Btg1/Btg2, and Btg2/Bt/Btg3. In the Ap1 horizon, a spacing*block effect arose from Block 1 not having any differences among treatments but in Block 2, the 5 m spacing had a higher water content than the 40 m spacing (Figure 3.43). The differences in Block 2 caused a main spacing effect where the 5 m treatment is higher than the 40 m treatment. In the Ap2 horizon, the 5 m spacing had a higher gravimetric water content (0.057 g $g^{-1}$) than the 40 m spacing (0.055 g $g^{-1}$), although the difference was small. No differences among treatments were observed in the Btg1/Btg2 or Btg2/Bt/Btg3 horizons (Table 3.19). Frison et al. (2009) found differences in water retention as distance from the drain increased however the differences were too small to be physically meaningful. Lal and Fausey (1993) found undrained plots to have higher available water content as well as higher water retention at several suctions compared to drained plots. However, the authors attribute the differences to changes in pore size distribution caused by changes in organic matter rather than drainage.

### 3.4.3 Water Retention Summary

As discussed earlier, the 15-30 cm depth increment aligns fairly well with the Ap2 horizons. All other horizons from the soil pits are below the depths sampled with the first set of soil cores used for bulk density and water retention measurements. At 15-30 cm and the Ap2 horizon, there is less than a 1.5% water content difference within water potentials between the first set of water retention measurements and the soil pit water retention measurements. The results from both sets of sampling were very similar. Differences among spacings were seen in one block but not the other in several depths and water potentials and because there are only two blocks, it is difficult to interpret if there was an effect due to drainage intensity. Statistically significant differences among spacings at all water potentials were approximately 0.02 $cm^3$ $cm^{-3}$ or less. Although it is statistically significant, a difference that small is not physically meaningful.

Table 3.11. Volumetric water contents ($cm^3$ $cm^{-3}$) at 0-5 cm at multiple water potentials. Each value represents the mean of both blocks and 8 subplots (n=16). Values within the same water potential that contain the same letter are not significantly different as determined by an LSMeans test ($p \leq 0.10$). Standard deviations are presented in parentheses.

| | **Water Potential (kPa)** | | | | |
|---|---|---|---|---|---|
| **Treatment** | **0.0** | **-4.9** | **-9.8** | **-33** | **-1500** |
| **5 m** | 0.455a (0.022) | 0.380a (0.014) | 0.368a (0.017) | 0.338a (0.021) | 0.084b (0.005) |
| **10 m** | 0.432b (0.024) | 0.360b (0.023) | 0.348b (0.022) | 0.317b (0.019) | 0.085b (0.006) |
| **20 m** | 0.451ab (0.023) | 0.382a (0.017) | 0.369a (0.016) | 0.340a (0.019) | 0.087b (0.006) |
| **40 m** | 0.453a (0.024) | 0.369ab (0.024) | 0.355ab (0.025) | 0.327ab (0.026) | 0.093a (0.005) |

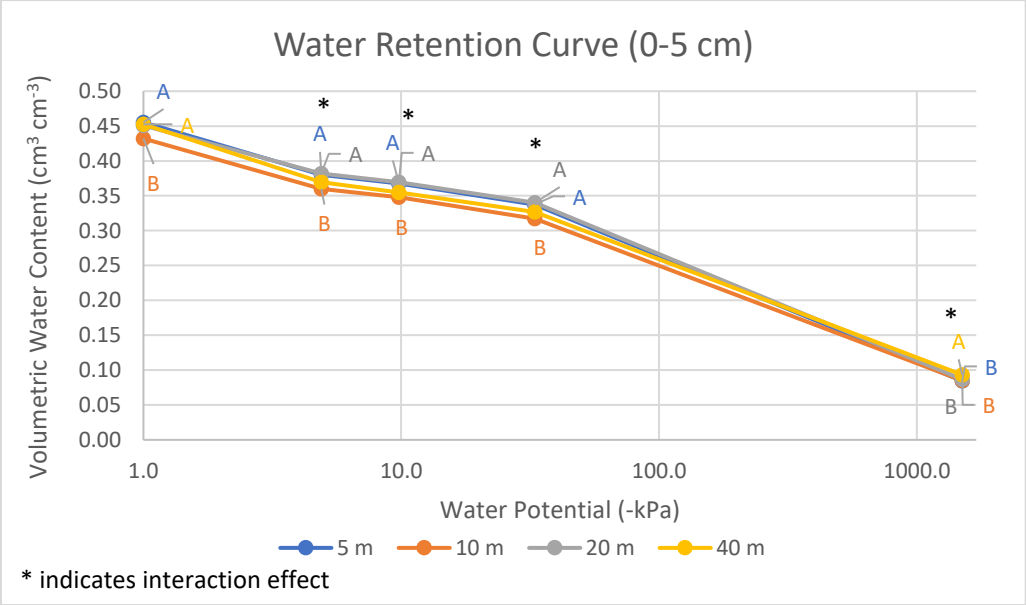


Figure 3.17. Water retention curves at 0-5 cm at multiple water potentials. Each data point represents the mean of both blocks and 8 subplots (n=16). Data points within the same water potential that contain the same letter are not significantly different as determined by an LSMeans test ($p \leq 0.10$). Data points that do not contain a letter are not significantly different than any other point within that water potential.

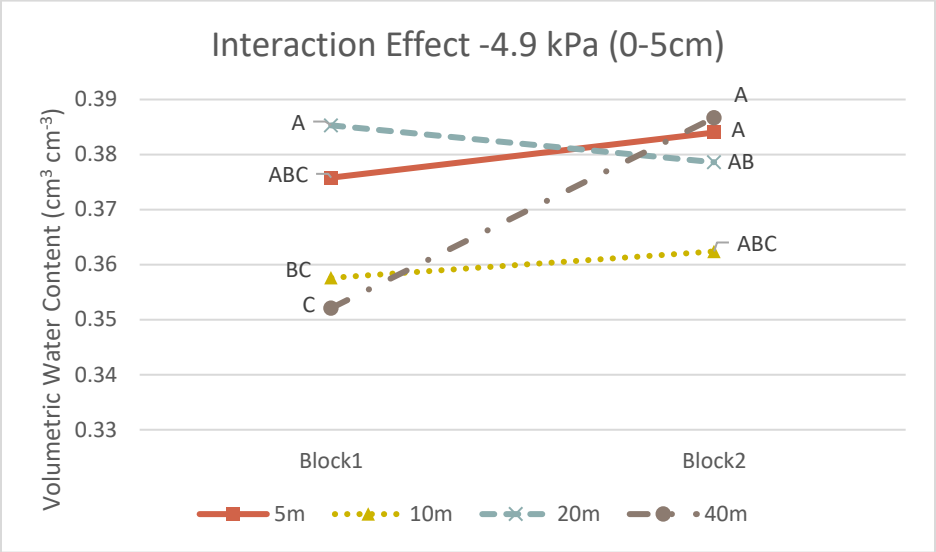


Figure 3.18. Water retention at -4.9 kPa spacing*block effect at 0-5 cm depth. Each value represents the mean of 8 subplots (n=8). Values that contain the same letter are not significantly different as determined by an LSMeans test (p≤0.10).

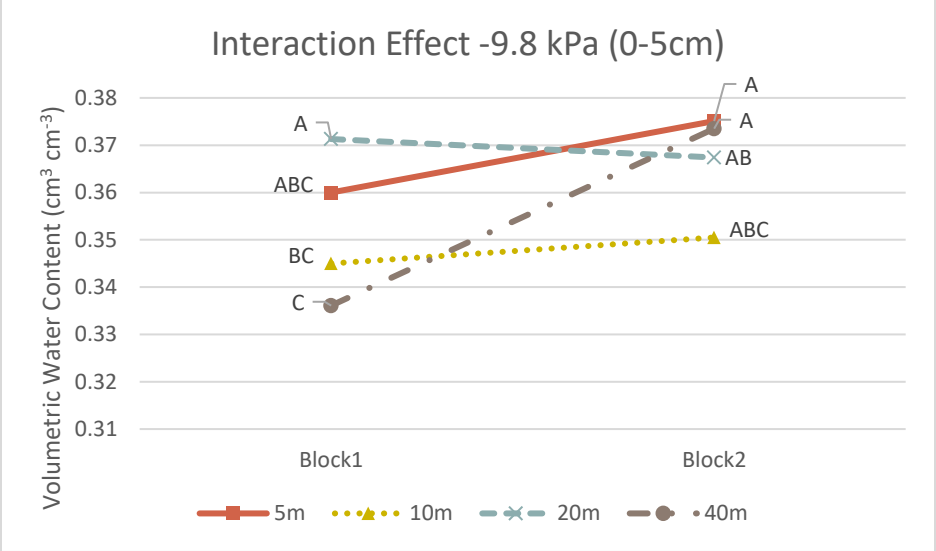


Figure 3.19. Water retention at -9.8 kPa spacing*block effect at 0-5 cm depth. Each value represents the mean of 8 subplots (n=8). Values that contain the same letter are not significantly different as determined by an LSMeans test (p≤0.10).

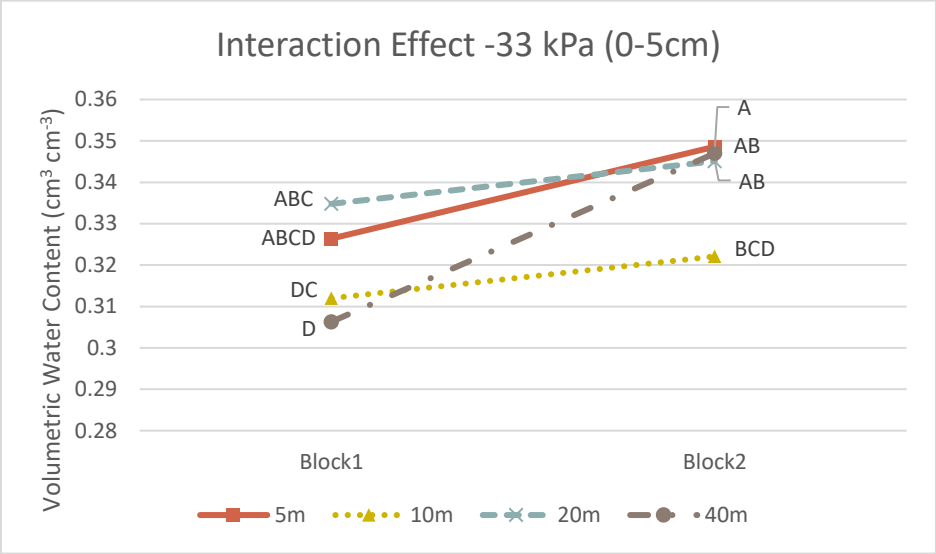


Figure 3.20. Water retention at -33 kPa spacing*block effect at 0-5 cm depth. Each value represents the mean of 8 subplots (n=8). Values that contain the same letter are not significantly different as determined by an LSMeans test (p≤0.10).

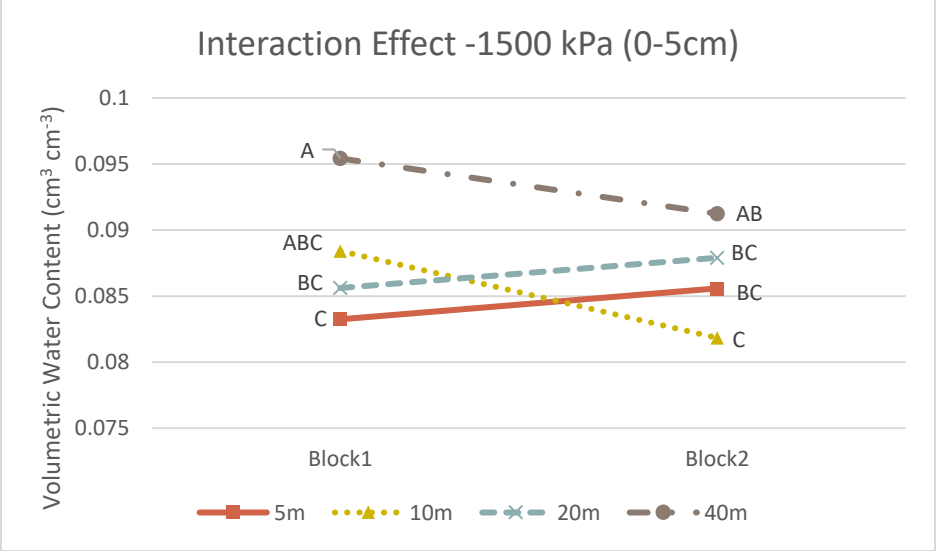


Figure 3.21. Water retention at -1500 kPa spacing*block effect at 0-5 cm depth. Each value represents the mean of 8 subplots (n=8). Values that contain the same letter are not significantly different as determined by an LSMeans test (p≤0.10).

Table 3.12. Volumetric water contents ($cm^3$ $cm^{-3}$) at 5-15 cm at multiple water potentials. Each value represents the mean of both blocks and 8 subplots (n=16). Values within the same water potential that contain the same letter are not significantly different as determined by an LSMeans test ($p \leq 0.10$). Standard deviations are presented in parentheses.

| | **Water Potential (kPa)** | | | | |
|---|---|---|---|---|---|
| **Treatment** | **0.0** | **-4.9** | **-9.8** | **-33** | **-1500** |
| **5 m** | 0.367a (0.012) | 0.307ab (0.009) | 0.295ab (0.008) | 0.276b (0.007) | 0.085b (0.007) |
| **10 m** | 0.356b (0.011) | 0.302b (0.009) | 0.290b (0.009) | 0.273b (0.008) | 0.080c (0.004) |
| **20 m** | 0.361ab (0.009) | 0.306ab (0.009) | 0.294ab (0.010) | 0.276b (0.010) | 0.078c (0.005) |
| **40 m** | 0.360ab (0.011) | 0.312a (0.008) | 0.301a (0.009) | 0.284a (0.009) | 0.090a (0.006) |

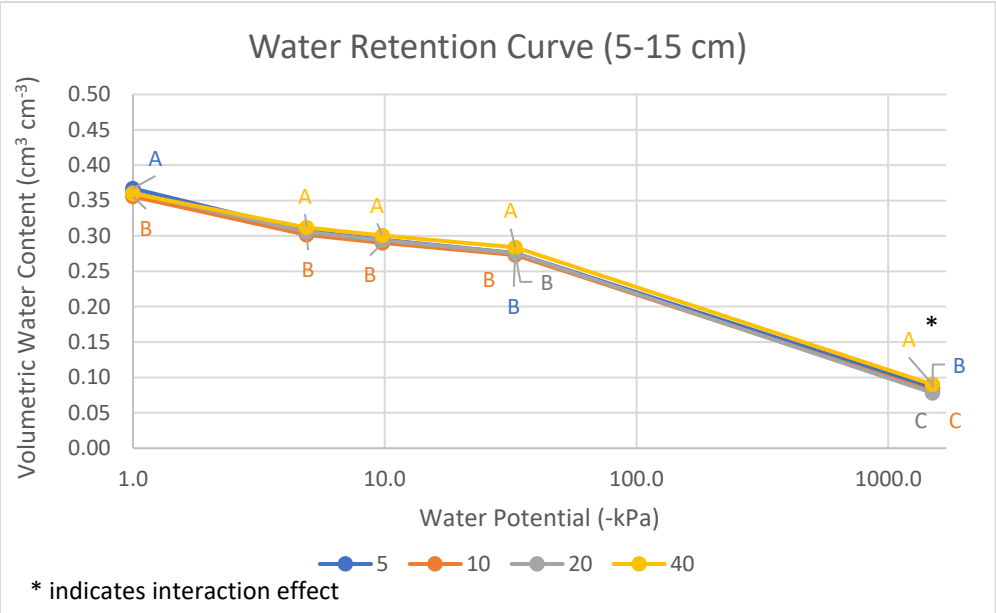


Figure 3.22. Water retention curves at 5-15 cm at multiple water potentials. Each data point represents the mean of both blocks and 8 subplots (n=16). Data points within the same water potential that contain the same letter are not significantly different as determined by an LSMeans test ($p \leq 0.10$). Data points that do not contain a letter are not significantly different than any other point within that water potential.

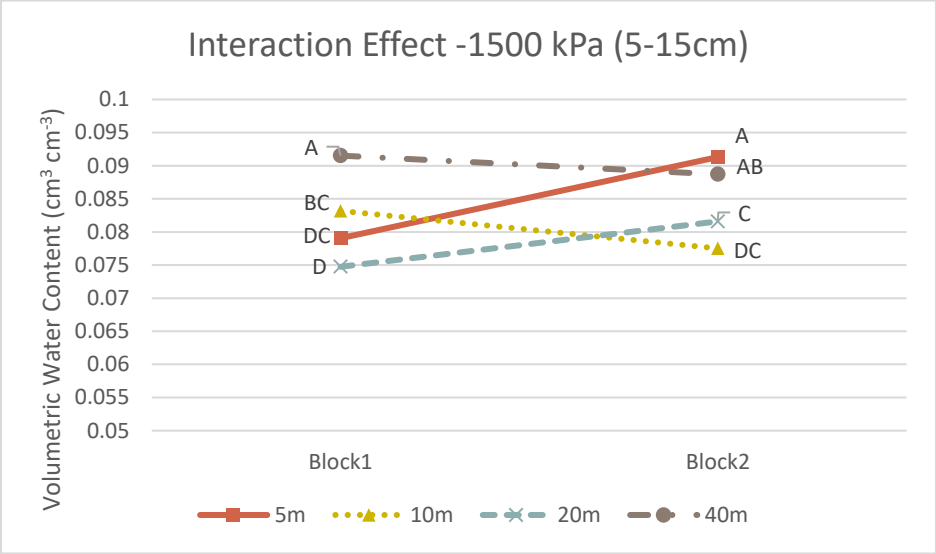


Figure 3.23. Water retention at -1500 kPa spacing*block effect at 5-15 cm depth. Each value represents the mean of 8 subplots (n=8). Values that contain the same letter are not significantly different as determined by an LSMeans test ($p \leq 0.10$).

Table 3.13. Volumetric water contents ($cm^3\ cm^{-3}$) at 15-30 cm at multiple water potential. Each value represents the mean of both blocks and 8 subplots (n=16). Values within the same water potential that contain the same letter are not significantly different as determined by an LSMeans test ($p \leq 0.10$). Standard deviations are presented in parentheses.

| | **Water Potential (kPa)** | | | | |
|---|---|---|---|---|---|
| **Treatment** | **0.0** | **-4.9** | **-9.8** | **-33** | **-1500** |
| **5 m** | 0.365a (0.012) | 0.311ab (0.009) | 0.302ab (0.009) | 0.287ab (0.008) | 0.091b (0.007) |
| **10 m** | 0.352b (0.010) | 0.306b (0.006) | 0.296b (0.008) | 0.282b (0.009) | 0.090b (0.006) |
| **20 m** | 0.354b (0.012) | 0.308ab (0.010) | 0.300ab (0.010) | 0.287ab (0.010) | 0.090b (0.010) |
| **40 m** | 0.355b (0.008) | 0.312a (0.006) | 0.304a (0.007) | 0.292a (0.008) | 0.099a (0.009) |

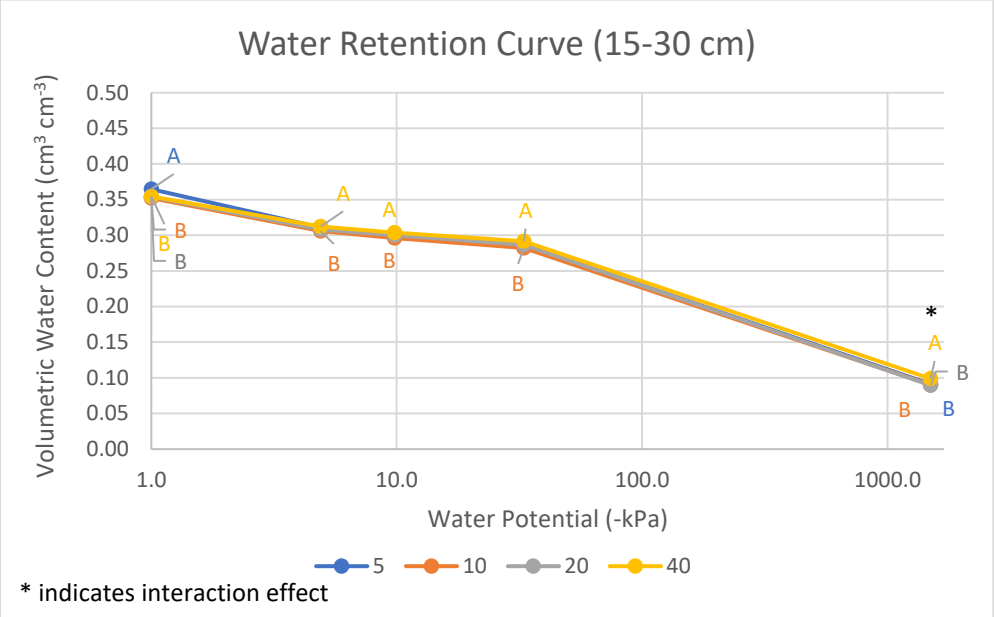


Figure 3.24. Water retention curves at 15-30 cm at multiple water potentials. Each data point represents the mean of both blocks and 8 subplots (n=16). Data points within the same water potential that contain the same letter are not significantly different as determined by an LSMeans test ($p \leq 0.10$). Data points that do not contain a letter are not significantly different than any other point within that water potential.

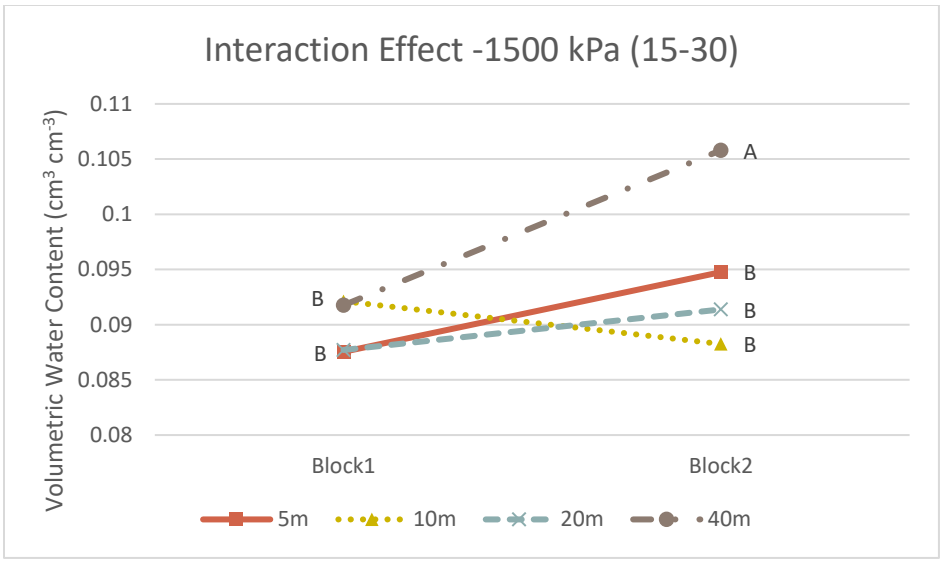


Figure 3.25. Water retention at -1500 kPa spacing*block effect at 15-30 cm depth. Each value represents the mean of 8 subplots (n=8). Values that contain the same letter are not significantly different as determined by an LSMeans test ($p \leq 0.10$).

Table 3.14. Water holding capacity ($cm^3$ $cm^{-3}$) at 0-5 cm, 5-15 cm, and 15-30 cm. Each value represents the mean of both blocks and 8 subplots (n=16). Values within the same depth that contain the same letter are not significantly different as determined by an LSMeans test ($p \leq 0.10$). Standard deviations are presented in parentheses.

| | **Depth (cm)** | | |
|---|---|---|---|
| **Treatment** | **0-5** | **5-15** | **15-30** |
| **5 m** | 0.283a (0.017) | 0.210a (0.007) | 0.211a (0.009) |
| **10 m** | 0.263b (0.023) | 0.210a (0.010) | 0.206a (0.010) |
| **20 m** | 0.283a (0.013) | 0.215a (0.009) | 0.211a (0.010) |
| **40 m** | 0.261b (0.027) | 0.211a (0.013) | 0.205a (0.009) |

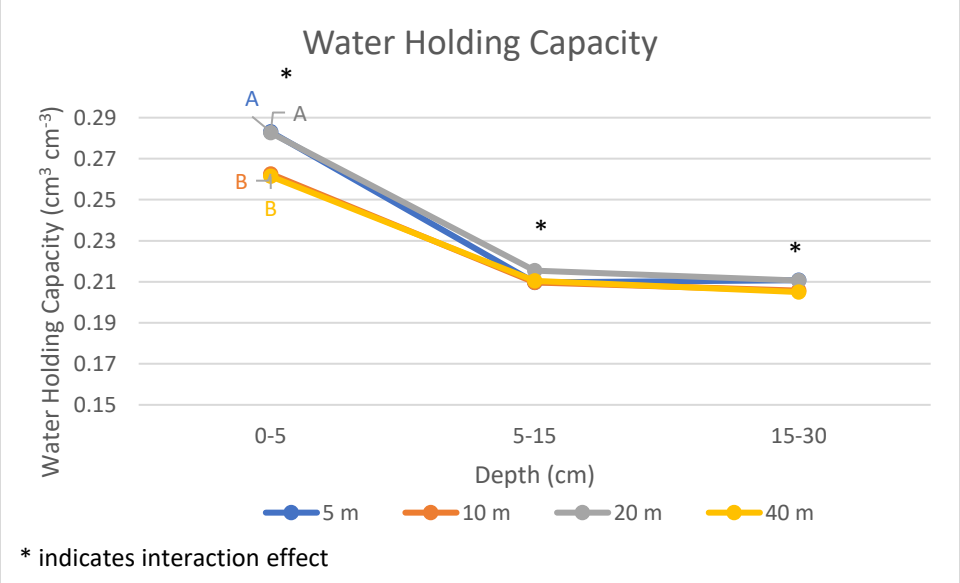


Figure 3.26. Water holding capacity ($cm^3$ $cm^{-3}$) at 0-5 cm, 5-15 cm, and 15-30 cm. Each data point represents the mean of both blocks and 8 subplots (n=16). Data points within the same depth that contain the same letter are not significantly different as determined by an LSMeans test ($p \leq 0.10$). Data points that do not contain a letter are not significantly different than any other point within that depth.

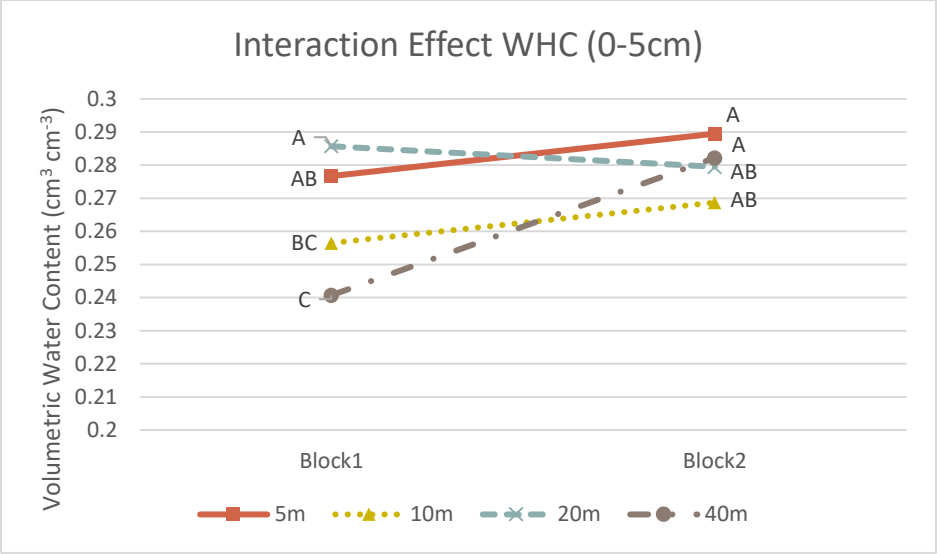


Figure 3.27. Water holding capacity spacing*block effect at 0-5 cm depth. Each value represents the mean of 8 subplots (n=8). Values that contain the same letter are not significantly different as determined by an LSMeans test (p≤0.10).

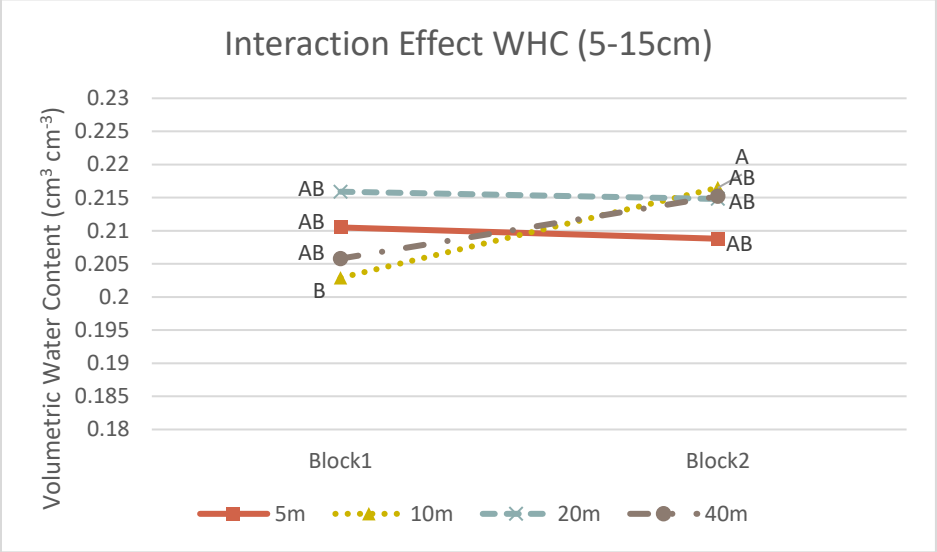


Figure 3.28. Water holding capacity spacing*block effect at 5-15 cm depth. Each value represents the mean of 8 subplots (n=8). Values that contain the same letter are not significantly different as determined by an LSMeans test (p≤0.10).

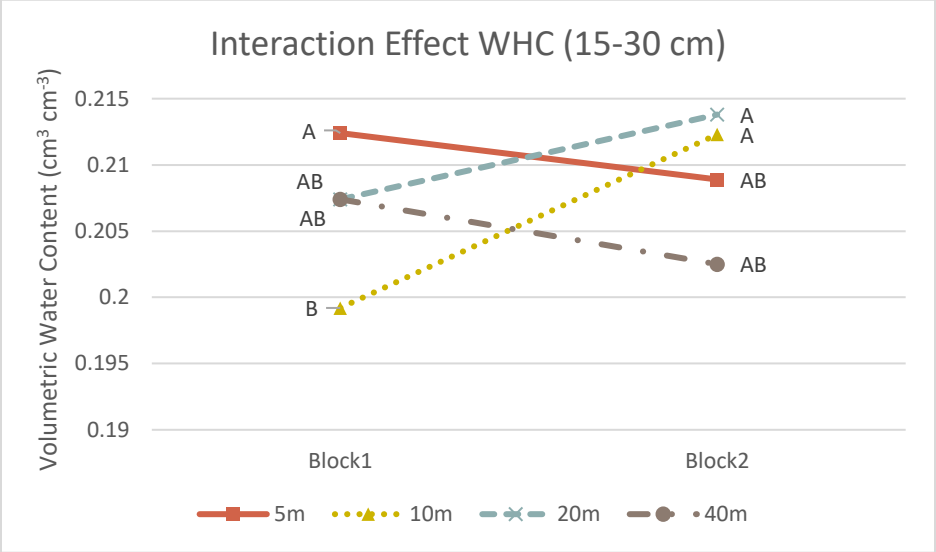


Figure 3.29. Water holding capacity spacing*block effect at 15-30 cm depth. Each value represents the mean of 8 subplots (n=8). Values that contain the same letter are not significantly different as determined by an LSMeans test ($p \leq 0.10$).

Table 3.15. Soil pit volumetric water contents ($cm^3\ cm^{-3}$) in the Ap2 horizon at multiple water potentials. Each value represents the mean of both blocks and 5 subsamples (n=10). Values within the same water potential that contain the same letter are not significantly different as determined by an LSMeans test ($p \leq 0.10$). Standard deviations are presented in parentheses.

| | **Water Potential (kPa)** | | | | |
|---|---|---|---|---|---|
| **Treatment** | **0.0** | **-2.5** | **-4.9** | **-9.8** | **-33.0** |
| **5 m** | 0.350a (0.015) | 0.323a (0.009) | 0.308a (0.008) | 0.297a (0.006) | 0.280b (0.004) |
| **40 m** | 0.352a (0.011) | 0.324a (0.008) | 0.311a (0.009) | 0.299a (0.008) | 0.284a (0.008) |

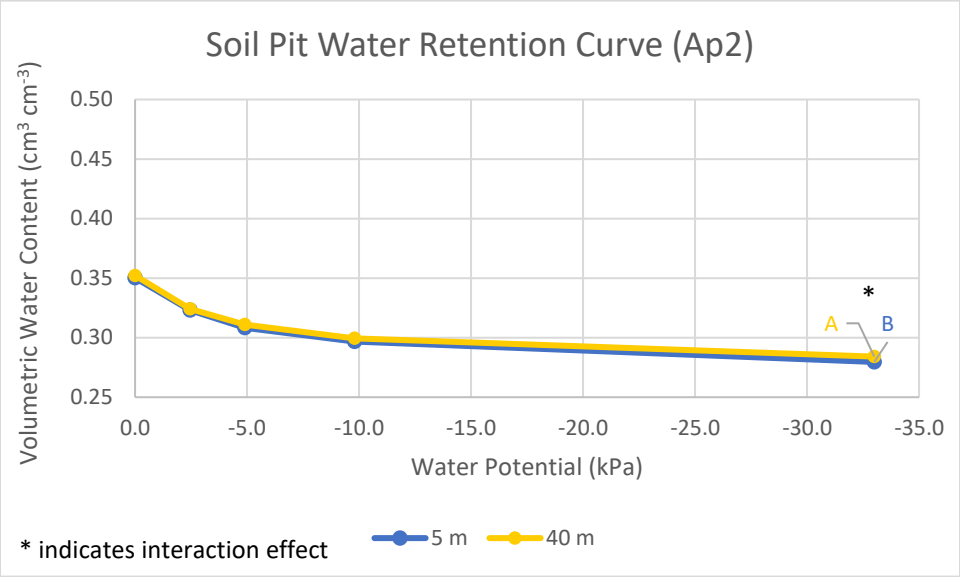


Figure 3.30. Water retention curves in the Ap2 horizon at multiple water potentials. Each data point represents the mean of both blocks and 5 subsamples (n=10). Data points within the same water potential that contain the same letter are not significantly different as determined by an LSMeans test (p≤0.10). Data points that do not contain a letter are not significantly different than any other point within that water potential.

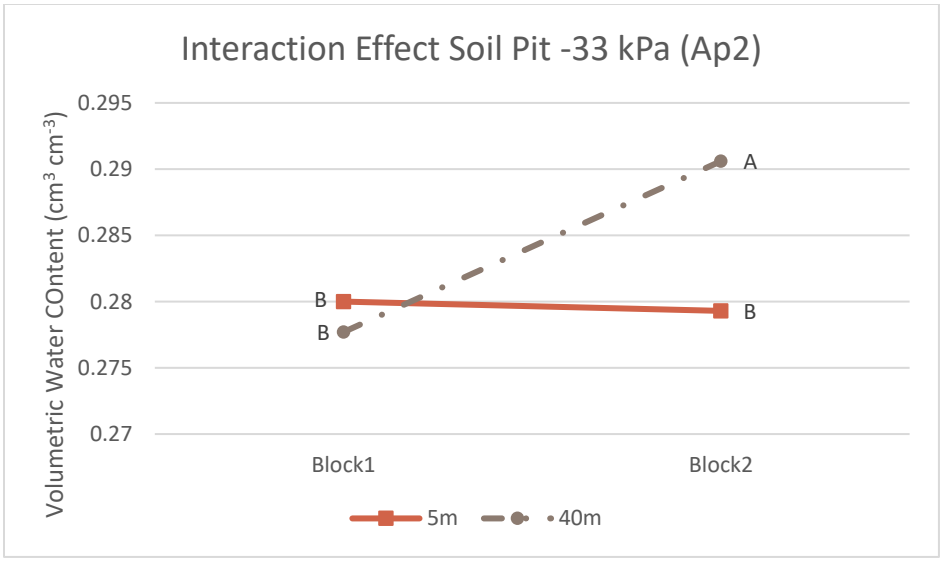


Figure 3.31. Water retention at -33 kPa spacing*block effect in the Ap2 horizon. Each value represents the mean of 5 subsamples (n=5). Values that contain the same letter are not significantly different as determined by an LSMeans test (p≤0.10).

Table 3.16. Soil pit volumetric water contents ($cm^3$ $cm^{-3}$) in the Btg1 horizon at multiple water potentials. Each value represents the mean of both blocks and 5 subsamples (n=10). Values within the same water potential that contain the same letter are not significantly different as determined by an LSMeans test ($p \leq 0.10$). Standard deviations are presented in parentheses.

| | **Water Potential (kPa)** | | | | |
|---|---|---|---|---|---|
| **Treatment** | **0.0** | **-2.5** | **-4.9** | **-9.8** | **-33.0** |
| **5 m** | 0.357b (0.007) | 0.345b (0.010) | 0.336b (0.011) | 0.327b (0.011) | 0.314b (0.010) |
| **40 m** | 0.371a (0.016) | 0.359a (0.014) | 0.350a (0.012) | 0.339a (0.010) | 0.323a (0.006) |

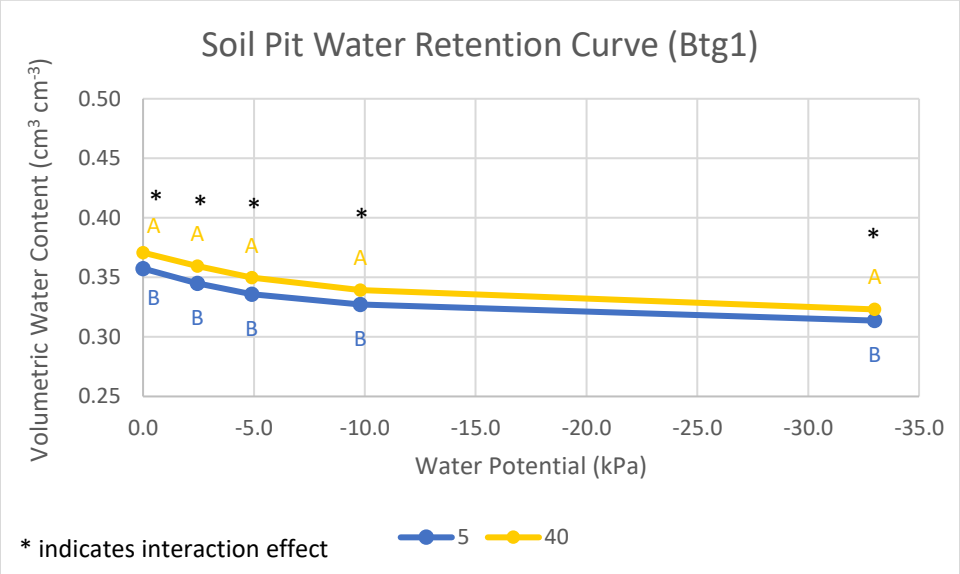


Figure 3.32. Water retention curves in the Btg1 horizon at multiple water potentials. Each data point represents the mean of both blocks and 5 subsamples (n=10). Data points within the same water potential that contain the same letter are not significantly different as determined by an LSMeans test ($p \leq 0.10$). Data points that do not contain a letter are not significantly different than any other point within that water potential.

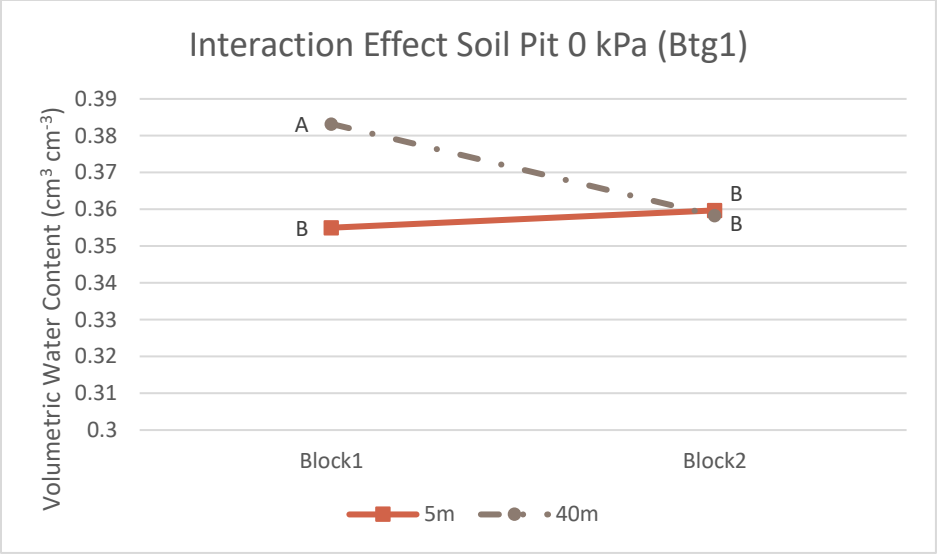


Figure 3.33. Water retention at 0 kPa spacing*block effect in the Btg1 horizon. Each value represents the mean of 5 subsamples (n=5). Values that contain the same letter are not significantly different as determined by an LSMeans test (p≤0.10).

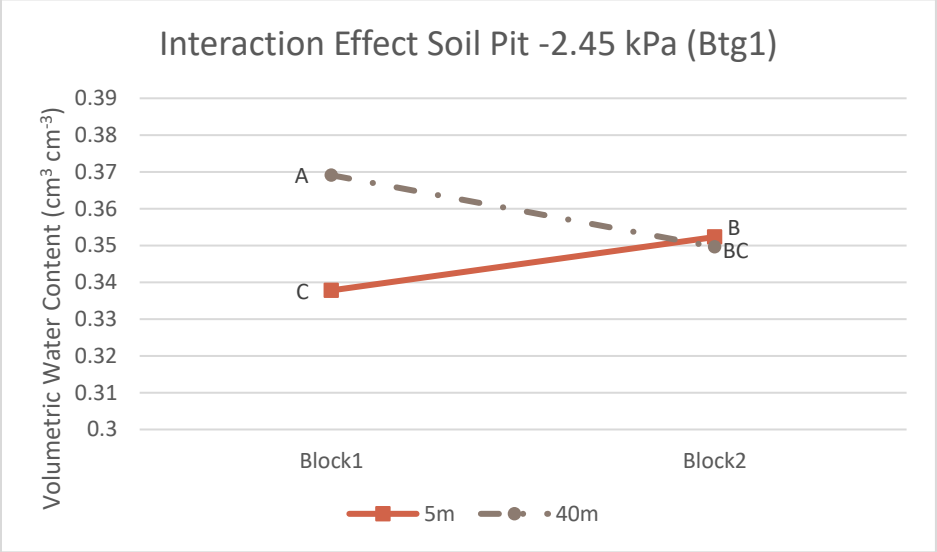


Figure 3.34. Water retention at -2.45 kPa spacing*block effect in the Btg1 horizon. Each value represents the mean of 5 subsamples (n=5). Values that contain the same letter are not significantly different as determined by an LSMeans test (p≤0.10).

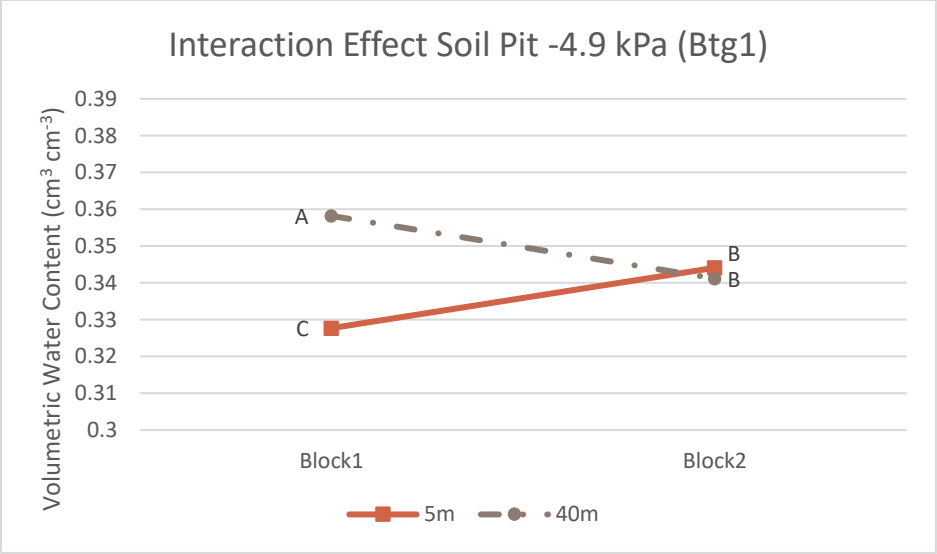


Figure 3.35. Water retention at -4.9 kPa spacing*block effect in the Btg1 horizon. Each value represents the mean of 5 subsamples (n=5). Values that contain the same letter are not significantly different as determined by an LSMeans test (p≤0.10).

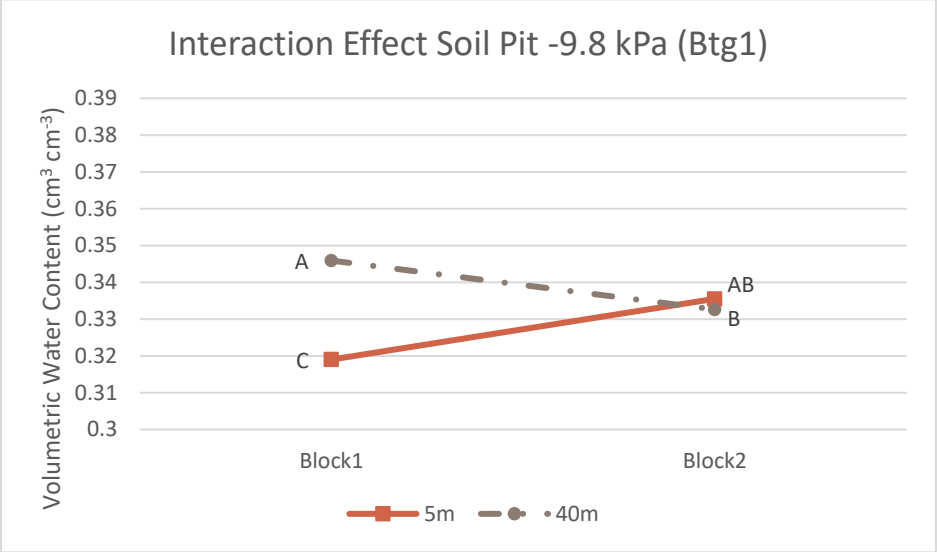


Figure 3.36. Water retention at -9.8 kPa spacing*block effect in the Btg1 horizon. Each value represents the mean of 5 subsamples (n=5). Values that contain the same letter are not significantly different as determined by an LSMeans test (p≤0.10).

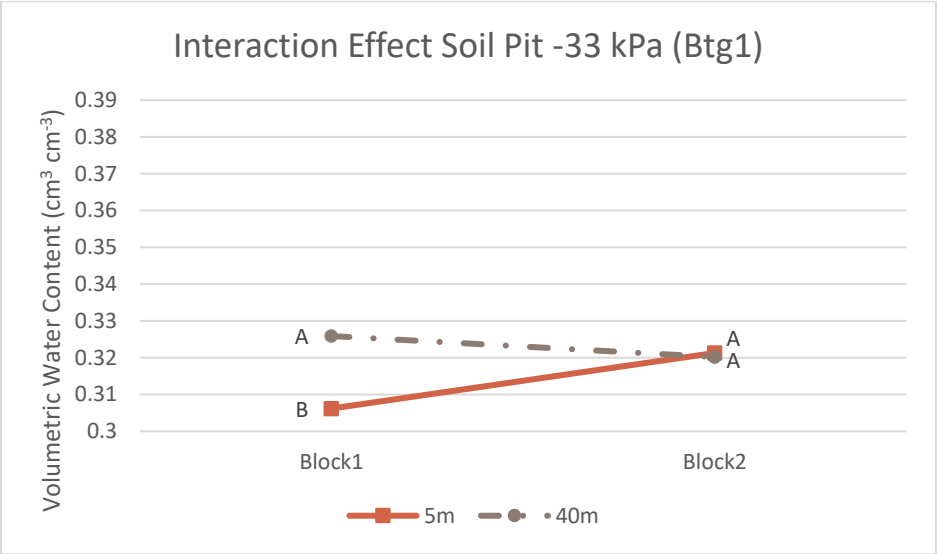


Figure 3.37. Water retention at -33 kPa spacing*block effect in the Btg1 horizon. Each value represents the mean of 5 subsamples (n=5). Values that contain the same letter are not significantly different as determined by an LSMeans test ($p \leq 0.10$).

Table 3.17. Soil pit volumetric water contents ($cm^3\ cm^{-3}$) in the Btg1/Btg2 horizon at multiple water potentials. Each value represents the mean of both blocks and 5 subsamples (n=10). Values within the same water potential that contain the same letter are not significantly different as determined by an LSMeans test ($p \leq 0.10$). Standard deviations are presented in parentheses.

| | **Water Potential (kPa)** | | | | |
|---|---|---|---|---|---|
| **Treatment** | **0.0** | **-2.5** | **-4.9** | **-9.8** | **-33.0** |
| **5 m** | 0.375a (0.015) | 0.360a (0.010) | 0.348a (0.010) | 0.339a (0.009) | 0.323a (0.009) |
| **40 m** | 0.374a (0.012) | 0.359a (0.017) | 0.348a (0.017) | 0.335a (0.017) | 0.317a (0.016) |

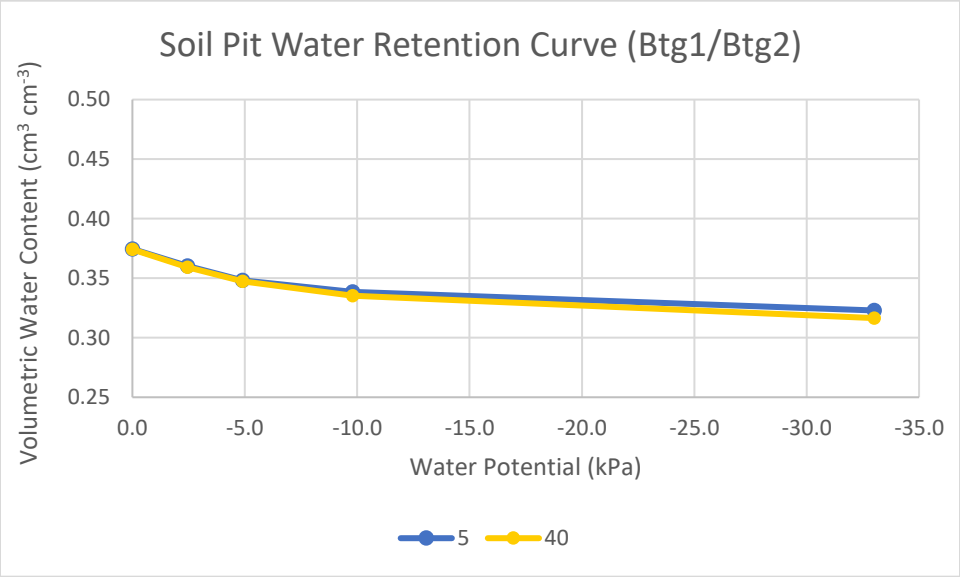


Figure 3.38. Water retention curves in the Btg1/Btg2 horizon at multiple water potentials. Each data point represents the mean of both blocks and 5 subsamples (n=10). Data points within the same water potential that contain the same letter are not significantly different as determined by an LSMeans test ($p \leq 0.10$). Data points that do not contain a letter are not significantly different than any other point within that water potential.

Table 3.18. Soil pit volumetric water contents ($cm^3\ cm^{-3}$) in the Btg2/Bt/Btg3 horizon at multiple water potentials. Each value represents the mean of both blocks and 5 subsamples (n=10). Values within the same water potential that contain the same letter are not significantly different as determined by an LSMeans test ($p \leq 0.10$). Standard deviations are presented in parentheses.

| | **Water Potential (kPa)** | | | | |
|---|---|---|---|---|---|
| **Treatment** | **0.0** | **-2.5** | **-4.9** | **-9.8** | **-33.0** |
| **5 m** | 0.393a (0.013) | 0.373a (0.011) | 0.366a (0.010) | 0.359a (0.010) | 0.349a (0.010) |
| **40 m** | 0.391a (0.031) | 0.371a (0.030) | 0.360a (0.030) | 0.351a (0.031) | 0.335a (0.030) |

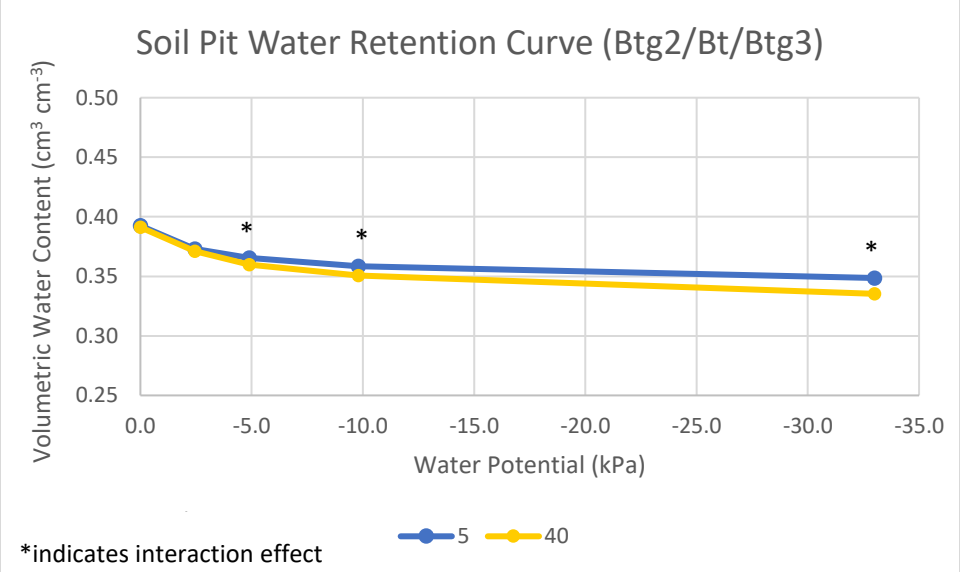


Figure 3.39. Water retention curves in the Btg2/Bt/Btg3 horizon at multiple water potentials. Each data point represents the mean of both blocks and 5 subsamples (n=10). Data points within the same water potential that contain the same letter are not significantly different as determined by an LSMeans test ($p \leq 0.10$). Data points that do not contain a letter are not significantly different than any other point within that water potential.

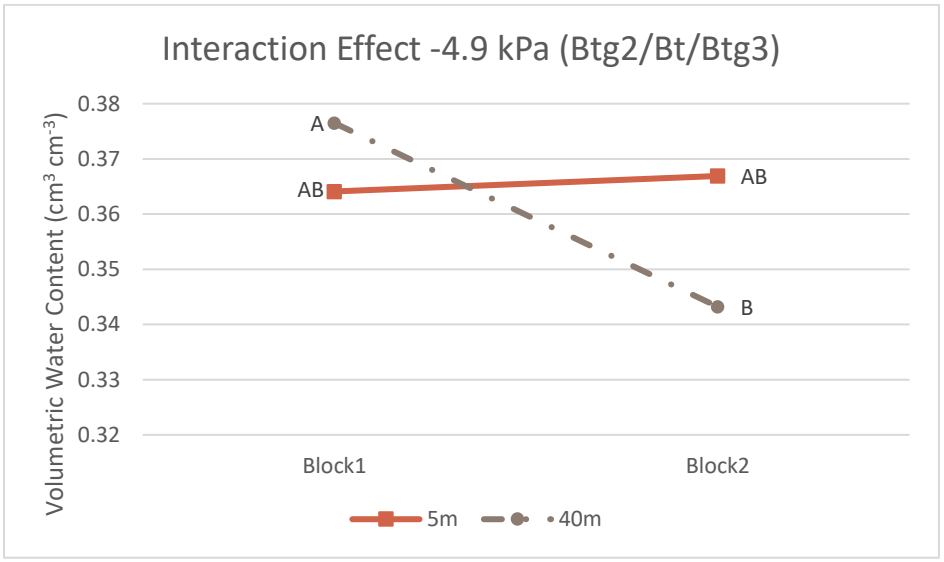


Figure 3.40. Water retention at -4.9 kPa spacing*block effect in the Btg2/Bt/Btg3 horizon. Each value represents the mean of 5 subsamples (n=5). Values that contain the same letter are not significantly different as determined by an LSMeans test ($p \leq 0.10$).

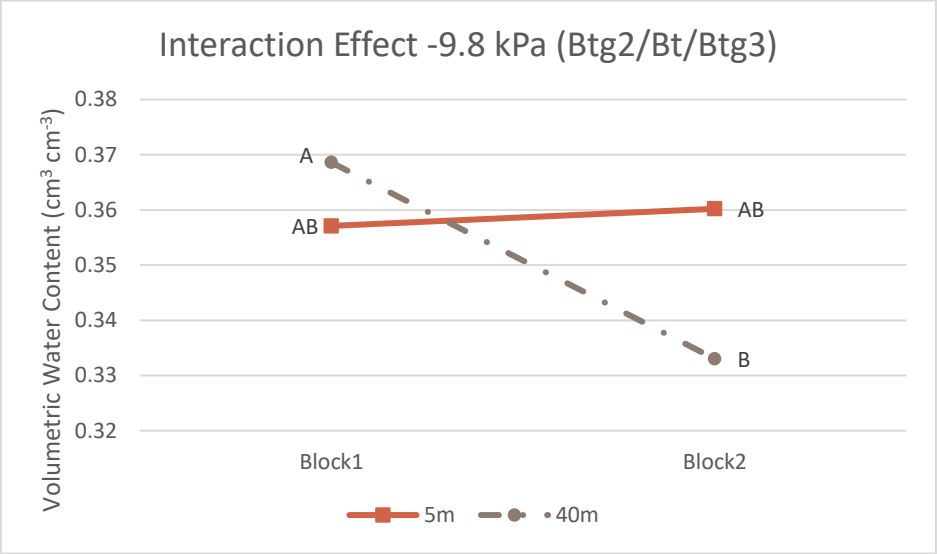


Figure 3.41. Water retention at -9.8 kPa spacing*block effect in the Btg2/Bt/Btg3 horizon. Each value represents the mean of 5 subsamples (n=5). Values that contain the same letter are not significantly different as determined by an LSMeans test (p≤0.10).

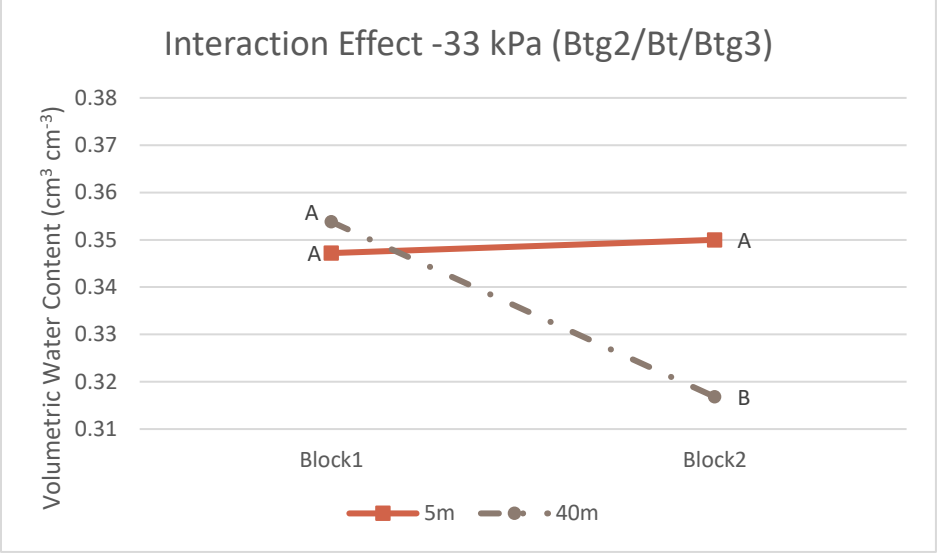


Figure 3.42. Water retention at -33 kPa spacing*block effect in the Btg2/Bt/Btg3 horizon. Each value represents the mean of 5 subsamples (n=5). Values that contain the same letter are not significantly different as determined by an LSMeans test (p≤0.10).

Table 3.19. Soil pit gravimetric water contents (g $g^{-1}$) in the Ap1, Ap2, Btg1/Btg2, and Btg2/Bt/Btg3 horizons at -1500 kPa water potential. Each value represents the mean of both blocks and 2 subsamples (n=4). Values within the same depth that contain the same letter are not significantly different as determined by an LSMeans test (p≤0.10). Standard deviations are presented in parentheses.

| | Horizon | | | |
|---|---|---|---|---|
| **Treatment** | **Ap1** | **Ap2** | **Btg1/Btg2** | **Btg2/Bt/Btg3** |
| **5 m** | 0.085a (0.009) | 0.057a (0.0003) | 0.077a (0.004) | 0.143a (0.018) |
| **40 m** | 0.071b (0.006) | 0.055b (0.001) | 0.083a (0.016) | 0.145a (0.011) |

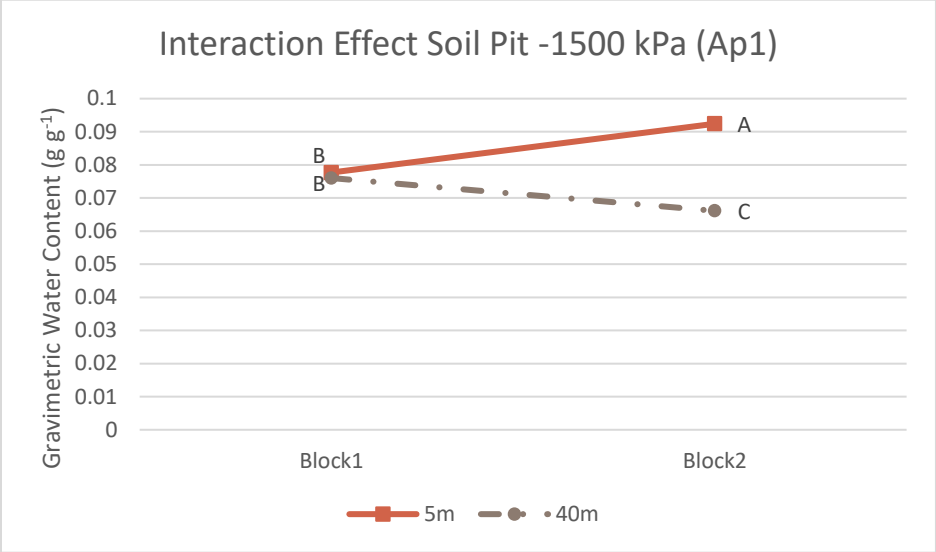


Figure 3.43. Water retention at -1500 kPa spacing*block effect in the Ap1 horizon. Each value represents the mean of 2 subsamples (n=2). Values that contain the same letter are not significantly different as determined by an LSMeans test (p≤0.10).

## 3.5 Saturated Hydraulic Conductivity

Saturated hydraulic conductivity measured with the auger hole method was only conducted on the 40 m spacing, so statistical analyses were not performed on the data. Auger holes were dug to 100 cm depth and when measurements were taken, the four auger holes in Block 1 had depths to the water table of 29.5 cm, 34.5 cm, 40 cm, and 30 cm. This means that the part of the soil profile contributing to the hydraulic conductivity was the silt loam Btg1 horizon, the silty clay loam Btg2 horizon, and the silt loam/silty clay loam 2Btg/2Bx horizon, assuming that the soil profiles where measurements were taken are similar to the soil profile where profile descriptions were done. Auger holes 1, 2, 3, and 4 in Block 2 had depths to the water table of 28 cm, 27.5 cm, 46 cm, and 38 cm, respectively. Auger holes 1 and 2 had the silt loam Btg1 and Btg2 horizons as well as the silty clay loam Btg3 and 2Btg horizons contributing to the hydraulic conductivity. Auger holes 3 and 4 only had the Btg2, Btg3, and 2Btg horizons contributing to water flow. Block 1 had an average Ksat of 30.6 cm $day^{-1}$ and Block 2 had an average of 30.2 cm $day^{-1}$ with standard deviations of 29.5 cm $day^{-1}$ and 11.2 cm $day^{-1}$ respectively (Table 3.20).

Saturated hydraulic conductivity with the Guelph permeameter was measured in the 5 m and 40 m treatments at 63.5 cm depth with a 10 cm and a 25 cm head. At this depth in Block 1, both in the 5 m and 40 m spacings, the silt loam Btg1 horizon was being measured also with some influence from the silty clay loam horizon a couple centimeters below the bottom of the hole. In the 5 m spacing in Block 2, the silt loam Btg1 and Btg2 horizons were being measured while in the 40 m spacing in Block 2, a combination of the silt loam Btg2 and silty clay loam Btg3 horizons were being measured. No spacing, block, or spacing*block effects were observed. The 5 m and 40 m spacings had saturated hydraulic conductivities of 10.1 cm $day^{-1}$ and 9.1 cm $day^{-1}$, respectively (Table 3.21).

The slug test was used to measure Ksat in the 20 m and 40 m treatments as well as the 10 m treatment but only in Block 1. Due to high standard deviation in the data and recognizing that differences among treatments would not be detected, statistical analyses were not performed on the data. The replications within each well were consistent but the values of well 1 and well 2 within the same plot were very different. The average Ksat values for the 20 m and 40 m treatments were 9.0 cm $day^{-1}$ and 12.7 cm $day^{-1}$, respectively, with standard deviations of 8.7 cm $day^{-1}$ and 8.5 cm $day^{-1}$, respectively. The 10 m treatment in Block 1 had an average Ksat value of 2.5 cm $day^{-1}$ and a standard deviation of 0.5 cm $day^{-1}$ (Table 3.22). Although the 10 m treatment has

a lower average for Block 1, it is not fair to compare it to the 20 m and 40 m treatments averages for two reasons. First, Block 2 measurements were not acquired for the 10 m spacing. For both the 20 m and 40 m spacings, Block 2 was higher than Block 1. If Block 2 measurements were to be taken for the 10 m, it would probably raise the average closer to that of the 20 m and 40 m treatments. Second, the water table depth at the time of measurement in the 10 m treatment was approximately 65 cm while it was considerably higher in the 20 m and 40 m treatments. If the 10 m soil profile is similar to the 5 m and 40 m profiles described in the soil pits, 65 cm is approximately where the clay content increases and the texture turns into a silty clay loam. A decrease in saturated hydraulic conductivity would be expected with an increase in clay content. The 10 m spacing's water table was completely in this silty clay loam Btg2 horizon while the 20 m and 40 m spacings' water table was higher and had water coming from the silt loam Btg1 horizons as well. Therefore, it is not a fair evaluation to directly compare the 10 m slug test Ksat value to the 20 m and 40 m values. Taking into consideration the variation within the averages and which Blocks were measured, the slug test Ksat values for the 10 m, 20 m, and 40 m, spacings are not different from one another.

The last set of Ksat measurements were done in the laboratory using the constant head method on the soil pit cores from the 5 m and 40 m treatments (Table 3.23). No spacing or spacing*block effects were detected at any of the horizons sampled. Similarly, Jia et al. (2008) did not find differences in saturated hydraulic conductivity among drained and undrained fields on a silty clay loam and clay loam soil. On the contrary, Hundal et al. (1976) was able to detect a higher hydraulic conductivity at 0-15 cm and 15-30 cm in subsurface drained plots compared to undrained plots in a silty clay soil. A block effect was significant for the Btg1/Btg2 horizon, with Block 2 being higher than Block 1, and also for the Btg2/Bt/Btg3 horizon with Block 1 being higher than Block 2. Extreme variation in the data, most notably from the Ap2 horizon in the 5 m Block 1 soil pit, resulted in skewed averages and no significant differences among treatments (Table 3.24). However, these data points with high values that caused the extreme variation may be noteworthy. Macropores that conduct preferential flow may only comprise a very small portion of the total soil porosity and may be located in relatively few areas. When sampling soil horizons with cores 5.4 cm in diameter, these preferential flow macropores may or may not be sampled with the cores. It is possible that some of the cores intercepted one of these macropores resulting in preferential flow, high Ksat values, and variation in the data even though large earthworm burrows exposed at the

sampling surface were intentionally avoided. A pore was visibly exposed at the surface of only one core that had an extremely high conductivity. Other cores with high conductivities may have had a macropore in the core but it may have been barely sealed at the very surface due to the trimming of the cores during preparation for water retention measurements. There were also some very low Ksat values. Two cores did not have any water move through them after the three hours of constant head applied. Another two cores had Ksat values less than 1 cm $day^{-1}$. These cores may have been sampled in a random pocket of high clay content soil which could have had some slight swelling properties or maybe it was taken in a spot that had an abnormally dense matrix. The five cores with the highest Ksat values, all higher than 266 cm $day^{-1}$, came from the 5 m treatment. In the Block 1, 5 m spacing, two cores were in the Ap2 horizon, one core in the Btg1 horizon, and one core in the Btg1/Btg2 sampling horizon (lower part of the Btg1 horizon for Block 1). The Block 2, 5 m spacing had one of the fastest cores in the Ap2 horizon. However, the two cores that did not have any water move through them and recorded a Ksat of 0 cm $day^{-1}$ came from the Block 2, 5 m spacing Ap2 and Btg1 horizons. The two cores with Ksat values less than 1 cm $day^{-1}$ came from the 40 m spacing in Block 2 in the Btg1 and Btg2/Bt/Btg3 sampling horizons (Btg3 horizon for 40 m Block 2). Although the five highest Ksat values came from the 5 m treatment which possibly suggests more preferential flow occurring in the 5 m treatment than the 40 m treatment, both of the 0 cm $day^{-1}$ values also came from the 5 m treatment. The extremely high and low Ksat values demonstrate the natural variability of the soil across the field.

The auger-hole method and the slug test both primarily measure lateral hydraulic conductivity whereas the soil cores from the soil pits measure vertical hydraulic conductivity. The Guelph permeameter measures both lateral and vertical hydraulic conductivity due to the shape of the saturated zone created in the soil during measurements. At the midplane, water flow is predominately vertical and shifts towards predominately lateral flow as distance to the tile drain decreases. Water flow through the matrix may be similar for both directions but if macropores and preferential flow paths form in the direction of predominate water flow, vertical hydraulic conductivity measurements may be higher at the midplane. After aligning different Ksat methods results by depth increment of the soil profile sampled, all of the methods revealed similar values. The Guelph permeameter depth corresponds best with the Btg1/Btg2 horizon depths. The Guelph permeameter and the Btg1/Btg2 soil pit horizon had Ksat values of approximately 10 cm $day^{-1}$ and 9 cm $day^{-1}$, respectively, for the 5 m spacing and 9 cm $day^{-1}$ and 13 cm $day^{-1}$, respectively, for the

40 m spacing. The slug test and auger hole methods resulted in saturated hydraulic conductivities for the 40 m spacing of 13 cm $day^{-1}$ and 30 cm $day^{-1}$, respectively. Considering the large amount of variation in all the methods and the different depths sampled, no differences were observed among treatments or methods. When sampling volume increases and it begins to capture and average more of the soil variability, variability among samples may decrease. Our Ksat results both agree and disagree with this logic. The soil cores taken from the soil pits have the smallest sampling volume and the highest standard deviation. However, the auger hole method samples the largest volume of soil but the data has larger standard deviations than the slug test and the Guelph permeameter data. Perhaps the auger-hole method sampling volume was not large enough to capture most of the soil variability and be considered a representative elementary volume. The auger-hole method samples were still exposed to areas of soil with high Ksat values and areas with low Ksat values. Each auger-hole may have had different proportions of the sampling volume exhibiting high and low Ksat values resulting in high variability.

Table 3.20. Auger hole method Ksat (cm day$^{-1}$). Statistical analyses were not performed on the data due to measurements only taken in the 40 m treatment.

| | | Saturated hydraulic conductivity | | | | | |
|---|---|---|---|---|---|---|---|
| **40 m Spacing** | **Soil Surface to initial water table (cm)** | **Rep 1** | **Rep 2** | **Rep 3** | **Hole Average** | **Block Average** | **Standard Deviation** |
| **Block 1 Hole 1** | 29.5 | 59.9 | 92.4 | | 76.2 | 30.6 | 29.5 |
| **Block 1 Hole 2** | 34.5 | 20.9 | 33.2 | 20.6* | 24.8 | | |
| **Block 1 Hole 3** | 40.0 | 0.0 | 0.0 | | 0.0 | | |
| **Block 1 Hole 4** | 30.0 | 24.8 | 18.0 | | 21.4 | | |
| **Block 2 Hole 1** | 28.0 | 33.9 | 48.6 | | 41.3 | 30.2 | 11.2 |
| **Block 2 Hole 2** | 27.5 | 38.8 | 30.4 | | 34.6 | | |
| **Block 2 Hole 3** | 46.0 | 34.1 | 22.6 | | 28.3 | | |
| **Block 2 Hole 4** | 38.0 | 17.8 | 15.2 | | 16.5 | | |

*A third rep was done on Block 1 Hole 2 because the initial 25% rise calculation for rep 2 was done incorrectly so it did not rise a full 25% before stopping measurements. The calculation was corrected and rep 3 was taken.

Table 3.21. Saturated hydraulic conductivity (cm day$^{-1}$) measured with the Guelph permeameter at a depth of 63.5 cm. Each value represents the mean of both blocks and 5 subsamples (n=10). Values that contain the same letter are not significantly different as determined by an LSMeans test ($p \leq 0.10$). Standard deviations are presented in parentheses.

| **Treatment** | **Saturated hydraulic conductivity** |
|---|---|
| **5 m** | 10.1a (4.6) |
| **40 m** | 9.1a (4.5) |

Table 3.22. Saturated hydraulic conductivity (cm $day^{-1}$) measured by the slug test. Statistical analyses were not performed on the data due to the high variation and recognizing that differences among treatments would not be detected.

| | | Saturated hydraulic conductivity | | | | | |
|---|---|---|---|---|---|---|---|
| **Treatment/Well** | **Soil Surface to initial water table (cm)** | **Rep 1** | **Rep 2** | **Well Average** | **Plot Average** | **Treatment Average** | **Standard Deviation** |
| **10m Block 1 Well 1** | 67.5 | 2.1 | 2.1 | 2.1 | 2.5 | 2.5 | 0.5 |
| **10m Block 1 Well 2** | 63.5 | 2.8 | 2.9 | 2.9 | | | |
| **20m Block 1 Well 1** | 40.5 | 12.9 | 14.0 | 13.4 | 6.9 | 9.0 | 8.7 |
| **20m Block 1 Well 2** | 36.5 | 0.3 | 0.3 | 0.3 | | | |
| **20m Block 2 Well 1** | 40.5 | 2.5 | 1.8 | 2.1 | 11.1 | | |
| **20m Block 2 Well 2** | 50.0 | 19.8 | 20.5 | 20.1 | | | |
| **40m Block 1 Well 1** | 9.0 | 4.4 | 4.3 | 4.4 | 10.3 | 12.7 | 8.5 |
| **40m Block 1 Well 2** | 14.0 | 17.2 | 15.2 | 16.2 | | | |
| **40m Block 2 Well 1** | 14.5 | 24.5 | 23.5 | 24.0 | 15.1 | | |
| **40m Block 2 Well 2** | 9.0 | 6.0 | 6.5 | 6.3 | | | |

Table 3.23. Arithmetic mean, standard deviation (SD), and inter-quartile range (IQR) of saturated hydraulic conductivity (cm $day^{-1}$) measured using the constant head method on the soil pit cores. Each value represents both blocks and 5 subsamples (n=10).

| | **5 m Treatment** | | | **40 m Treatment** | | |
|---|---|---|---|---|---|---|
| **Horizon** | **Mean** | **SD** | **IQR** | **Mean** | **SD** | **IQR** |
| **Ap2** | 220.0 | 336.1 | 360.5 | 33.4 | 34.8 | 43.3 |
| **Btg1** | 124.3 | 346.0 | 31.8 | 9.3 | 9.2 | 11.2 |
| **Btg1/Btg2** | 125.3 | 312.0 | 54.4 | 14.5 | 12.5 | 23.4 |
| **Btg2/Bt/Btg3** | 24.0 | 31.7 | 28.4 | 11.9 | 9.8 | 14.9 |

Table 3.24. Statistical analysis of saturated hydraulic conductivity data presented in the previous table. Data were transformed for the analysis but are presented in back-transformed units (cm $day^{-1}$). LSMeans are presented. Each value represents the mean of both blocks and 5 subsamples (n=10). Values within the same horizon that contain the same letter are not significantly different as determined by an LSMeans test ($p \leq 0.10$).

| **Treatment** | **Horizon** | | | |
|---|---|---|---|---|
| | **Ap2** | **Btg1** | **Btg1/Btg2** | **Btg2/Bt/Btg3** |
| **5 m** | 86.6a | 17.9a | 9.1a | 13.5a |
| **40 m** | 22.4a | 6.4a | 13.4a | 8.1a |

## 3.6 Summary

Bulk density was lower in the 5 m treatment than in the 40 m treatment at depths above 30 cm. Although the 0-5 cm depth increment did not show a significant difference between the 5 m and 40 m spacings, this may be attributed to other factors obscuring the changes caused by drainage intensity such as foot and wheel traffic causing compaction, physical disturbance caused by the planting equipment, solar radiation and evaporation at the surface, and many others. These bulk density results agree with our hypothesis of bulk density decreasing as drain spacing decreases. As the water table is lowered by the tile drains, increased aeration creates a more hospitable environment for soil organisms and plant roots. The burrows created by soil organisms and root channels created by plants decrease bulk density. Soil organisms and plant roots also help decrease bulk density by releasing compounds that support soil aggregation and structural stability which creates stable pore space. The small difference in bulk density was not observed below 30 cm possibly because of the reduced amount of organic matter, soil organisms, and plant roots. Even though the tile drains may have created a more aerated environment in the subsoil, there is probably a lower population of soil organisms than above 30 cm due to less organic matter for the soil organisms to feed on at these depths. The amount of plant roots in the subsoil may also be less than in the top 30 cm due to slightly restrictive bulk densities. With less soil organism activity and fewer plant roots, the effects of drainage on bulk density will be less. The difference in bulk density among treatments in the top 30 cm was 0.06 g $cm^{-3}$ or less. A difference this small is probably physically insignificant. In the top 30 cm of the soil profile descriptions, where a change in bulk density was measured, there was no apparent change in soil structure. The soil profile descriptions did not reveal any evident differences in the soil of the 5 m treatment and the 40 m treatment other than the 40 m treatments having slightly more redoximorphic concentrations which may be attributed to soil variation and estimations of redoximorphic feature abundance rather than direct measurements. The results of no visibly obvious differences in soil structure in the soil profile descriptions disagrees with our hypothesis of soil structure improving with a decrease in drain spacing. The inherent weak structure, low organic matter, and low clay content of this soil may be at fault for drainage intensity not having a bigger effect on bulk density and structure. With soils that already have moderately strong structure, higher amounts of organic matter, and higher clay contents, the processes responsible for aggregation, stabilization of structure, and decreasing bulk density are already active. Subsurface drainage in this case may enhance those processes and lead

to a large effect while in soils with poor structure, low organic matter, and low clay content, those processes are inherently low and may require a much longer time of artificial drainage to produce the same amount of change. Chieng and Hughes-Games (1995) reported subsurface drained plots to have a lower bulk density than undrained plots on a silty clay loam soil in Canada. Hundal et al. (1976) also reported tile drained plots having a lower bulk density than drained plots on a silty clay soil while Jia et al. (2008) did not find differences in bulk density among drained and undrained plots on a silty clay loam soil.

Water retention results did not show any consistent differences among treatments. The majority of significant differences were very small and seen in one block but not the other. This data disagrees with our hypothesis of water retention and water holding capacity increasing as drain spacing decreases. However, after analyzing the bulk density data, it is not surprising that water retention did not change. The small changes in bulk density and total porosity were not large enough to significantly change water retention and water holding capacity. Perhaps if there was a larger change in bulk density and total porosity, there would also be a change in water retention. One change in water retention that relates back to a change in bulk density is at saturation in the first set of bulk density and water retention samples at the 15-30 cm depth increment. The 5 m spacing had a significantly lower bulk density than the 40 m spacing and as a result the 5 m spacing had a higher water content at saturation. But the majority of water retention differences do not follow trends in bulk density. The water retention differences were very small and could have been caused by small differences in the size of pores in the soil pore network without a significant change in total porosity. Chieng and Hughes-Games (1995) as well as Lal and Fausey (1993) reported tile drained soils to have lower water retention than undrained soils at several water potentials on silty clay loam soils although Lal and Fausey (1993) attribute the differences to organic matter induced changes. Frison et al. (2009) reported water holding capacity was higher 0.6 m from the drain than 7 m from the drain although the authors acknowledge a change in minerology was likely the cause.

Saturated hydraulic conductivity values did not significantly differ among treatments which disagrees with our hypothesis of Ksat increasing as drain spacing decreases. However, the Ksat results do agree with the total porosity results. All of the Ksat measurements, except in the Ap2 horizon of the soil pits, were taken below 30 cm. There were no differences in total porosity below 30 cm as well as no differences in Ksat. The Ap2 horizon Ksat values were too variable to

detect any differences between treatments. The Ksat data from each method of measurement and each sampling depth was highly variable. Poiseuille's law, which can be used to predict the flow rate of water through a cylindrical tube, uses the radius of the tube in the equation and it is raised to the fourth power which means even a small change in the radius will have a large effect on the flow rate. Soil pores can be very diverse in size and be distributed and connected somewhat randomly. This gives some explanation as to why Ksat is highly variable. The extremely high Ksat values in the soil pit samples occurred in the 5 m treatments which might suggest preferential flow in the narrow spacing but these values were also accompanied by two Ksat values of 0 cm $day^{-1}$ in the 5m treatments. Jia et al. (2008) and Frison et al. (2009) were unable to detect differences in hydraulic conductivity among subsurface drained and undrained plots. However, Hundal et al. (1976) provided evidence of higher hydraulic conductivity in drained plots compared to undrained plots in a silty clay soil.

# CHAPTER 4. CONCLUSIONS AND FUTURE WORK

Soil profile descriptions were a valuable tool for gaining an overall understanding of the soil we were studying. Although no obvious differences in structure were detected among the 5 m and 40 m profiles with the profile descriptions, we were able to assess how the soil naturally changes with increasing depth. The profile descriptions allowed us to document which horizons were sampled with the bulk density and water retention cores in the top 30 cm and the bulk density measurements sampled with the hydraulic probe down to 100 cm, to see if changes occurred in some horizons but not others. The depths of horizons were also helpful in comparing which horizons were being measured for Ksat and how that may have affected the results, especially with the auger holes and slug tests because each of the auger holes and wells had a different depth to the water table. Future studies at this experimental site will now have the added resource of a full detailed soil profile description to utilize in the research.

A slightly lower bulk density in the 5 m treatment compared to the 40 m treatment was detected in the top 30 cm of the soil where organic matter, amount of plant roots, and soil organism activity are the highest. The small differences in bulk density were statistically significant but are most likely physically insignificant. Water retention and water holding capacity did not show consistent differences among treatments and any statistically significant differences were not large enough to be physically meaningful. Although the effects of drainage intensity were not large, the process of change may be slow and may require more time. With differences being so small, natural soil variability and error from sampling, preparation, and measurement procedures have a larger effect on statistical analyses than if the effect size was larger. In future studies, increasing sample size as well as sample volume for these measurements may help in detecting differences among treatments by reducing the signal to noise ratio. However, sample size is limited by practicality. Finding a long enough time window when weather and soil conditions permit proper sampling, as well as number of people helping take samples and time allotted for processing of samples, all put a limit on the number that can be taken.

Saturated hydraulic conductivity values were too variable to detect any differences among treatments. The high variability may have been caused by the complex soil pore network due to a small change in pore size having a large effect on water flow. Outliers and variability in data sets can sometimes provide answers to questions that main effects do not capture. The five soil cores

with the highest Ksat values that caused a lot of the variability were all taken from the 5 m spacing. These samples could be evidence of preferential flow occurring more in the narrow drain spacing treatment than the "undrained" control, however the two soil cores with the lowest Ksat values were also taken in the 5 m treatment.

These mostly nonsignificant results do not reveal details about possible changes in the soil that may have caused the observed faster drain flow over the last 35 years (Bowling and Kladivko, 2016). Preferential flow paths may have developed over time in the form of voids between soil peds but also as earthworm burrows and root channels, which may or may not have been included in the small soil core samples. Increased drainage on this naturally poorly drained soil may have led to an improved environment for roots and earthworms, and potentially larger root masses and earthworm populations. When the soil pits were dug, many earthworms and burrows were observed in the field and they were being exposed nearly the full depth of the soil pits, with more being observed in the 5 m treatment than the 40 m treatment. Earthworm burrows can conduct water flow at high rates and can get water deep into the soil profile in a short period of time. Root channels and earthworm burrows may be directly connected to the tile drain or simply move surface water down to the water table quicker, which raises the water table and pressure head, and forces water into the drains. The long-term no-till management of this field may have also helped preserve root channels and earthworm burrows every year in the top 25-30 cm of soil whereas in conventional tillage they would have been destroyed. If preferential flow, which has been previously documented at this site, is the cause of the faster drain flow, it may be too localized and spatially variable to cause large enough changes in the horizon to be detected by common physical property measurements like bulk density, total porosity, water retention, and Ksat. Preferential flow can occur in single macropores and in relatively few areas of the field making it difficult to capture in small samples. While inexpensive, easy, and creating a relatively small destructive footprint in the field, these common physical property measurements may not sample large enough areas to detect preferential flow. One potential way future studies could assess possible effects of preferential flow on drain flow would be to utilize techniques like dye staining experiments that sample larger portions of the field and can show the spatial variability of preferential flow paths. One major downside of dye staining experiments is that they are extremely destructive to large areas of the field and would eliminate the possibility of studying that area again in the future. Documenting earthworm burrow locations and hydraulic activity while conducting a dye staining

experiment as well as analyzing earthworm populations in future studies could also be a way to investigate if earthworms influence preferential flow.

In July 2019 when the soil pits in the 5 m and 40 m treatments were dug, Dr. Daniel Hirmas, from the University of California-Riverside, came to the SEPAC drainage experimental site and took several soil monoliths from each of the soil pit faces. After being transported to the University of California-Riverside, the exposed face of each soil monolith was prepared using a unique method to minimize the number of artificial features and markings created by tools and present a monolith face that was a more naturally structured soil. Each monolith is currently being scanned with a multistripe laser triangulation (MLT) scanner which produces a 3-D image of the soil monolith surface and gives quantitative values for soil structure. A major limitation of traditional soil profile descriptions is that structure is forced into broad categories and detailed differences are hard to distinguish from one another. Technologies like the MLT scanner that give quantitative values to undisturbed soil structure provide an advantage of studying soil structure at a much more detailed level. The data from the MLT scan, when combined with a coefficient of linear extensibility, can be related to saturated hydraulic conductivity and preferential flow. As this work continues, the resulting data may provide a more detailed analysis of differences in soil structure and preferential flow among the 5 m and 40 m treatments.

The small differences and no differences among treatments presented in this study may simply show that the physical properties of this particular soil need more time for them to change. Even though 35 years of drainage is a long period of time when compared to other subsurface drainage experiments, it is still a relatively short period of time when compared to the time frame of soil formation and development. Subsurface drainage research should continue with experimental sites located on different soil types, different environments, and for long periods of time after drain installation to further our understanding of how artificial drainage affects soil physical and hydraulic properties over time.

# REFERENCES


Alakukku, L., Nuutinen, V., Ketoja, E., Koivusalo, H., and Paasonen-Kivekäs, M. (2010). Soil macroporosity in relation to subsurface drain location on a sloping clay field in humid climatic conditions. *Soil and Tillage Research*, *106*(2), 275-284.

Allaire, S. E., Roulier, S., and Cessna, A. J. (2009). Quantifying preferential flow in soils: A review of different techniques. *Journal of Hydrology*, *378*(1-2), 179-204.

Amoozegar, A. (2002). Auger-hole method (Saturated zone). In Dane J.H., and Topp, G.C. (Eds.), *Methods of Soil Analysis: Part 4 Physical Methods* (pp. 859-869). American Society of Agronomy and Soil Science Society of America. Madison, Wisconsin.

Arshad, M. A., and Coen, G. M. (1992). Characterization of soil quality: Physical and chemical criteria. *American Journal of Alternative Agriculture*, *7*(1-2), 25-31.

Assouline, S. (2006). Modeling the relationship between soil bulk density and the hydraulic conductivity function. *Vadose Zone Journal*, *5*(2), 697-705.

Baker, B. J., Fausey, N. R., and Islam, K. R. (2004). Comparison of soil physical properties under two different water table management regimes. *Soil Science Society of America Journal*, *68*(6), 1973-1981.

Beven, K. (2018). A century of denial: Preferential and nonequilibrium water flow in soils, 1864-1984. *Vadose Zone Journal*, *17*(1).

Beven, K., and Germann, P. (1982). Macropores and water flow in soils. *Water Resources Research*, *18*(5), 1311-1325.

Bogner, C., Trancón y Widemann, B., and Lange, H. (2013). Characterizing flow patterns in soils by feature extraction and multiple consensus clustering. *Ecological Informatics*, *15*, 44-52.

Bouma, J. (1991). Influence of soil macroporosity on environmental quality. *Advances in Agronomy*, *46*, 1-37.

Bouma, J., Van Hoorn, J. W., and Stoffelsen, G. H. (1981). Measuring the hydraulic conductivity of soil adjacent to tile drains in a heavy clay soil in The Netherlands. *Journal of Hydrology*, *50*, 371-381.

Bouwer, H., and Rice, R. C. (1976). A slug test for determining hydraulic conductivity of unconfined aquifers with completely or partially penetrating wells. *Water Resources Research*, *12*(3), 423-428.

Bowling, L.C., and E.J. Kladivko. (2016). Trend analysis of the SEPAC 30 year drainage climatology. Proc. 10th International Drainage Symp., Sept. 7-9, 2016, Minneapolis, MN. doi:10.13031/ids.20162515027.

Chieng, S. T. and Hughes-Games, G. A. (1995). Effects of subirrigation and controlled drainage on crop yield, water table fluctuation and soil properties. In D'ltri, F.M. and Belcher, H.W. (Eds.), *Subirrigation and Controlled Drainage* (pp. 231-246). CRC Press. Boca Raton, Florida.

Dane, J.H., and Hopmans, J.W. (2002a). Pressure plate extractor. In Dane J.H., and Topp, G.C. (Eds.), *Methods of Soil Analysis: Part 4 Physical Methods* (pp. 688-690). American Society of Agronomy and Soil Science Society of America. Madison, Wisconsin.

Dane, J.H., and Hopmans, J.W. (2002b). Suction table. In Dane J.H., and Topp, G.C. (Eds.), *Methods of Soil Analysis: Part 4 Physical Methods* (pp. 692-697). American Society of Agronomy and Soil Science Society of America. Madison, Wisconsin.

Eck, D. V., Hirmas, D. R., and Giménez, D. (2013). Quantifying soil structure from field excavation walls using multistripe laser triangulation scanning. *Soil Science Society of America Journal*, *77*(4), 1319-1328.

Eck, D. V., Qin, M., Hirmas, D. R., Giménez, D., and Brunsell, N. A. (2016). Relating quantitative soil structure metrics to saturated hydraulic conductivity. *Vadose Zone Journal*, *15*(1).

Fausey, N. R., and Lal, R. (1989). Drainage-tillage effects on Crosby-Kokomo soil association in Ohio I. Effects on stand and corn grain yield. *Soil Technology*, *2*(4), 359-370.

Fausey, N.R., Doering, E.J., and Palmer, M.L. (1987). Purposes and Benefits of Drainage. In Pavelis, G.A. (Ed.), *Farm Drainage in the United States: History, Status, and Prospects.* Bull. No.1455 (pp. 64–67). Economic Research Services, U.S. Department of Agriculture.

Flury, M., Flühler, H., Jury, W. A., and Leuenberger, J. (1994). Susceptibility of soils to preferential flow of water: A field study. *Water Resources Research*, *30*(7), 1945-1954.

Franzmeier, D. P., and Kladivko, E.J. (2001). Drainage and wet soil management: Wet soils of Indiana. Bull. No. AY-301. Purdue University Extension.

Frey, S. K., and Rudolph, D. L. (2011). Multiscale characterization of vadose zone macroporosity in relation to hydraulic conductivity and subsurface drainage. *Soil Science Society of America Journal*, *75*(4), 1253-1264.

Frey, S. K., Rudolph, D. L., and Parkin, G. W. (2012). Spatial and temporal influences on hydraulic properties in macroporous tile-drained soil. *Soil Science Society of America Journal*, *76*(2), 350-360.

Frison, A., Cousin, I., Montagne, D., and Cornu, S. (2009). Soil hydraulic properties in relation to local rapid soil changes induced by field drainage: A case study. *European Journal of Soil Science*, *60*(4), 662-670.

Grossman, R.B., and Reinsch, T.G. (2002). Bulk density and linear extensibility. In Dane J.H., and Topp, G.C. (Eds.), *Methods of Soil Analysis: Part 4 Physical Methods* (pp. 201-228). American Society of Agronomy and Soil Science Society of America. Madison, Wisconsin.

Gupta, S., and Larson, W. E. (1979). Estimating soil water retention characteristics from particle size distribution, organic matter percent, and bulk density. *Water Resources Research*, *15*(6), 1633-1635.

Hayes, W. A., and Vepraskas, M. J. (2000). Morphological changes in soils produced when hydrology is altered by ditching. *Soil Science Society of America Journal*, *64*(5), 1893-1904.

Hendrickx, J. M., and Flury, M. (2001). Uniform and preferential flow mechanisms in the vadose zone. *Conceptual Models of Flow and Transport in the Fractured Vadose Zone*, 149-187. National Academy Press.

Hirmas, D. R. (2013). A simple method for removing artifacts from moist fine-textured soil faces. *Soil Science Society of America Journal*, *77*(2), 591-593.

Hollis, J. M., Jones, R. J. A., and Palmer, R. C. (1977). The effects of organic matter and particle size on the water-retention properties of some soils in the West Midlands of England. *Geoderma*, *17*(3), 225-238.

Hudson, B. D. (1994). Soil organic matter and available water capacity. *Journal of Soil and Water Conservation*, 49(2), 189-194.

Hundal, S. S., Schwab, G. O., & Taylor, G. S. (1976). Drainage system effects on physical properties of a lakebed clay soil. *Soil Science Society of America Journal, 40*(2), 300-305.

Hvorslev, M. J. (1951). *Time Lag and Soil Permeability in Ground-water Observations*. Bull. No. 36 (pp. 1-50). Waterways Experiment Station, Corps of Engineers, US Army. Vicksburg, Mississippi.

Inoue, H. (1993). Lateral water flow in a clayey agricultural field with cracks. *Geoderma*, *59*(1-4), 311-325.

Jarvis, N., Koestel, J., and Larsbo, M. (2016). Understanding preferential flow in the vadose zone: Recent advances and future prospects. *Vadose Zone Journal*, *15*(12).

Jamison, V. C., and Kroth, E. M. (1958). Available moisture storage capacity in relation to textural composition and organic matter content of several Missouri soils. *Soil Science Society of America Journal*, *22*(3), 189-192.

Jia, X., Scherer, T. F., DeSutter, T. M., and Steele, D. D. (2008). Change of soil hardness and soil properties due to tile drainage in the Red River Valley of the North. Presented at the 2008 ASABE Annual International Meeting, Providence, Rhode Island, June 29–July 2, 2008.

Katuwal, S., Moldrup, P., Lamandé, M., Tuller, M., and De Jonge, L. W. (2015). Effects of CT number derived matrix density on preferential flow and transport in a macroporous agricultural soil. *Vadose Zone Journal*, *14*(7).

Kapilevich, Z.A., Tselishcheva, L.K. and Vysochenko, A.V. (1991). Transformation of soils developing on glacial-lacustrine clays after drainage. *Soviet Soil Science*, 23(8), 9-18.

Kladivko, E. J., Frankenberger, J. R., Jaynes, D. B., Meek, D. W., Jenkinson, B. J., and Fausey, N. R. (2004). Nitrate leaching to subsurface drains as affected by drain spacing and changes in crop production system. *Journal of Environmental Quality*, *33*(5), 1803-1813.

Kladivko, E. J., Grochulska, J., Turco, R. F., Van Scoyoc, G. E., and Eigel, J. D. (1999). Pesticide and nitrate transport into subsurface tile drains of different spacings. *Journal of Environmental Quality*, *28*(3), 997-1004.

Kladivko, E. J., Van Scoyoc, G. E., Monke, E. J., Oates, K. M., and Pask, W. (1991). Pesticide and nutrient movement into subsurface tile drains on a silt loam soil in Indiana. *Journal of Environmental Quality*, *20*(1), 264-270.

Kladivko, E. J., Willoughby, G. L., and Santini, J. B. (2005). Corn growth and yield response to subsurface drain spacing on Clermont silt loam soil. *Agronomy Journal*, *97*(5), 1419-1428.

Klute, A., and Dirksen, C. (1986). Hydraulic conductivity and diffusivity: Laboratory methods. In Klute, A. (Ed.) *Methods of Soil Analysis: Part 1—Physical and Mineralogical Methods* (pp. 687-734). American Society of Agronomy and Soil Science Society of America. Madison, Wisconsin.

Koestel, J. K., Norgaard, T., Luong, N. M., Vendelboe, A. L., Moldrup, P., Jarvis, N. J., Lamande, M., Iversen, B.V., and Wollesen de Jonge, L. (2013). Links between soil properties and steady-state solute transport through cultivated topsoil at the field scale. *Water Resources Research*, *49*(2), 790-807.

Köhne, J. M., and Gerke, H. H. (2005). Spatial and temporal dynamics of preferential bromide movement towards a tile drain. *Vadose Zone Journal*, *4*(1), 79-88.

Kung, K. J., Kladivko, E. J., Gish, T. J., Steenhuis, T. S., Bubenzer, G., and Helling, C. S. (2000). Quantifying preferential flow by breakthrough of sequentially applied tracers: silt loam soil. *Soil Science Society of America Journal*, 64(4), 1296-1304.

Kutílek, M. (2011) Soil water flow. In: Gliński J., Horabik J., Lipiec J. (Eds.) *Encyclopedia of Agrophysics. Encyclopedia of Earth Sciences Series* (pp. 798-801). Springer. Dordrecht, The Netherlands.

Lal, R., and Fausey, N. R. (1993). Drainage and tillage effects on a Crosby-Kokomo soil association in Ohio IV. Soil physical properties. *Soil Technology*, *6*(2), 123-135.

Larney, F. J., Kladivko, E. J., and Monke, E. J. (1988). Subsurface drain spacing effects on soil moisture regime of Clermont silt loam. *Transactions of the ASAE*, *31*(4), 1128-1134.

Libohova, Z., Seybold, C., Wysocki, D., Wills, S., Schoeneberger, P., Williams, C., Lindbo, D., Stott, D., and Owens, P. R. (2018). Reevaluating the effects of soil organic matter and other properties on available water-holding capacity using the National Cooperative Soil Survey Characterization Database. *Journal of Soil and Water Conservation*, *73*(4), 411-421.

Luo, L., and Lin, H. (2009). Lacunarity and fractal analyses of soil macropores and preferential transport using micro-X-ray computed tomography. *Vadose Zone Journal*, *8*(1), 233-241.

Luo, L., Lin, H., and Halleck, P. (2008). Quantifying soil structure and preferential flow in intact soil using X-ray computed tomography. *Soil Science Society of America Journal*, *72*(4), 1058-1069.

Mason, D. D., Lutz, J. F., and Petersen, R. G. (1957). Hydraulic conductivity as related to certain soil properties in a number of Great Soil Groups—Sampling errors involved. *Soil Science Society of America Journal*, *21*(5), 554-560.

Mbagwu, J. S. C. (1994). Saturated hydraulic conductivity in relation to physical properties of soils in the Nsukka plains, SE Nigeria (No. IC--94/98). *International Centre for Theoretical Physics*. Trieste, Italy.

McCoy, E. L., Boast, C. W., Stehouwer, R. C., and Kladivko, E. J. (1994). Macropore hydraulics: Taking a sledgehammer to classical theory. *Soil Processes and Water Quality*, 303-348. Lewis Publishers. Boca Raton, Florida.

Messing, I., and Wesström, I. (2006). Efficiency of old tile drain systems in soils with high clay content: Differences in the trench backfill zone versus the zone midway between trenches. *Irrigation and Drainage: The journal of the International Commission on Irrigation and Drainage*, *55*(5), 523-531.

Minasny, B., and McBratney, A. B. (2018). Limited effect of organic matter on soil available water capacity. *European Journal of Soil Science*, *69*(1), 39-47.

Montagne, D., Cornu, S., Le Forestier, L., and Cousin, I. (2009). Soil drainage as an active agent of recent soil evolution. *Pedosphere*, *19*(1), 1-13.

Montagne, D., Cousin, I., Le Forestier, L., Daroussin, J. and Cornu, S. (2007). Quantification of soil volumes in the Eg and Bt-horizon of an Albeluvisol using image analysis. *Canadian Journal of Soil Science*, 87, 51–59.

Mooney, S. J., and Nipattasuk, W. (2003). Quantification of the effects of soil compaction on water flow using dye tracers and image analysis. *Soil Use and Management*, *19*(4), 356-363.

Mossadeghi-Björklund, M., Arvidsson, J., Keller, T., Koestel, J., Lamandé, M., Larsbo, M., and Jarvis, N. (2016). Effects of subsoil compaction on hydraulic properties and preferential flow in a Swedish clay soil. *Soil and Tillage Research*, *156*, 91-98.

Nuutinen, V., and Butt, K. R. (2003). Interaction of *Lumbricus terrestris* L. burrows with field subdrains: The 7th international symposium on earthworm ecology, Cardiff, Wales, 2002. *Pedobiologia*, *47*(5-6), 578-581.

Nuutinen, V., Pöyhönen, S., Ketoja, E., and Pitkänen, J. (2001). Abundance of the earthworm *Lumbricus terrestris* in relation to subsurface drainage pattern on a sandy clay field. *European Journal of Soil Biology*, *37*(4), 301-304.

Oygarden, L., Kvaerner, J., and Jenssen, P. D. (1997). Soil erosion via preferential flow to drainage systems in clay soils. *Geoderma*, *76*(1-2), 65-86.

Petersen, C. T., Nielsen, M. H., and Hansen, S. (2012). Quantification of drain-connected macroporous flow pathways by smoke injection. *Soil Science Society of America Journal*, *76*(2), 331-341.

Petersen, G. W., Cunningham, R. L., and Matelski, R. P. (1968a). Moisture characteristics of Pennsylvania soils: I. Moisture retention as related to texture. *Soil Science Society of America Journal*, *32*(2), 271-275.

Petersen, G. W., Cunningham, R. L., and Matelski, R. P. (1968b). Moisture characteristics of Pennsylvania soils: II. Soil factors affecting moisture retention within a textural class—Silt loam. *Soil Science Society of America Journal*, *32*(6), 866-870.

Reeve, M. J., Smith, P. D., and Thomasson, J. (1973). The effect of density on water retention properties of field soils. *Journal of Soil Science*, *24*(3), 355-367.

Reynolds, W. D., and Elrick, D. E. (1986). A method for simultaneous in situ measurement in the vadose zone of field-saturated hydraulic conductivity, sorptivity and the conductivity-pressure head relationship. *Groundwater Monitoring and Remediation*, *6*(1), 84-95.

Salter, P. J., Berry, G., and Williams, J. B. (1966). The influence of texture on the moisture characteristics of soils: III. Quantitative relationships between particle size, composition, and available-water capacity. *Journal of Soil Science*, *17*(1), 93-98.

Sammartino, S., Lissy, A. S., Bogner, C., Van Den Bogaert, R., Capowiez, Y., Ruy, S., and Cornu, S. (2015). Identifying the functional macropore network related to preferential flow in structured soils. *Vadose Zone Journal*, *14*(10).

SAS Institute Int. 2013. SAS® 9.4 SAS Institute Inc. Cary, NC, USA.

Sharma, M. L., and Uehara, G. (1968). Influence of soil structure on water relations in low humic Latosols: I. Water retention. *Soil Science Society of America Journal*, *32*(6), 765-770.

Shipitalo, M. J., Nuutinen, V., and Butt, K. R. (2004). Interaction of earthworm burrows and cracks in a clayey, subsurface-drained, soil. *Applied Soil Ecology*, *26*(3), 209-217.

Šimůnek, J., Jarvis, N. J., Van Genuchten, M. T., and Gärdenäs, A. (2003). Review and comparison of models for describing non-equilibrium and preferential flow and transport in the vadose zone. *Journal of Hydrology*, *272*(1-4), 14-35.

Soil Moisture Equipment Corp, 2012. Model 2800K1 Guelph permeameter: Operating instructions. Santa Barbara, CA.

Sugg, Z. (2007). Assessing US farm drainage: Can GIS lead to better estimates of subsurface drainage extent. *World Resources Institute*, Washington, DC.

Thomas, G. W., and Phillips, R. E. (1979). Consequences of water movement in macropores. *Journal of Environmental Quality*, *8*(2), 149-152.

USDA Natural Resources Conservation Service. (2008). *Soil quality indicators: Bulk density.* Retrieved from https://www.nrcs.usda.gov/Internet/FSE_DOCUMENTS/nrcs142p2_053256.pdf

Van Beers, W. F. J. (1958). *The auger-hole method*. International Institute for Land Reclamation and Improvement. Wageningen, The Netherlands.

# APPENDIX AUGER HOLE METHOD

Equation A.1. Shape factor, C, calculation (Amoozegar, 2002).

$$C = 4000r/[y(20 + H/r)(2 - y/H)]$$

Equation A.2. Ksat calculation in m/day (Amoozegar, 2002).

$$Ksat = C(\Delta y/\Delta t)$$

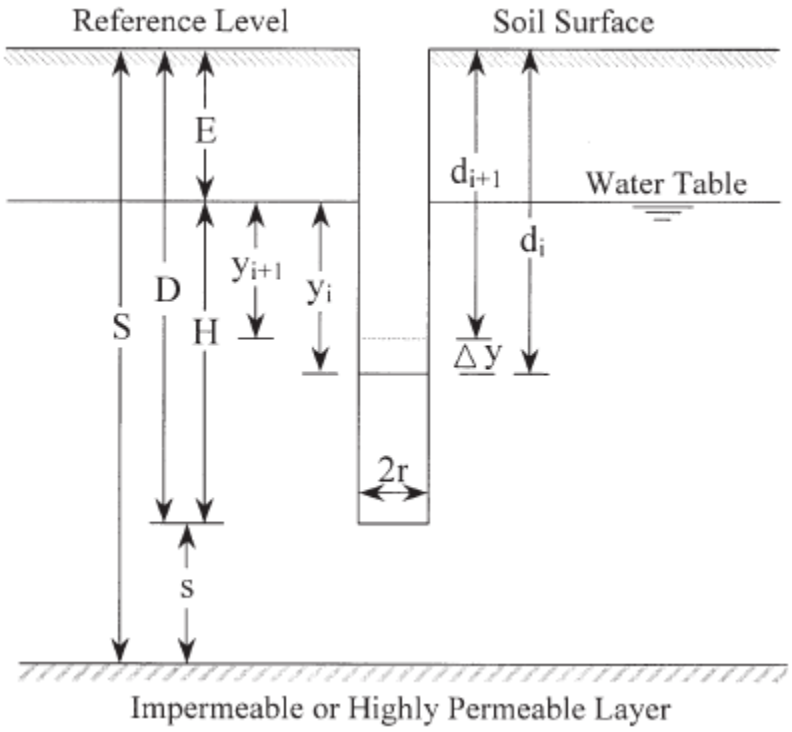


Figure A.1. Diagram of the auger hole method variables (Amoozegar, 2002).

Table A.1. Example data sheet for auger hole measurements.

| Plot 208 Hole 1 Rep 1 | | | | | |
|---|---|---|---|---|---|
| Hole diameter (cm)(2r)= | 9 | | | | |
| Measuring point above soil surface (cm)(T)= | 23.5 | | Allowable total length of water rise: (D-E)*0.25 = | 17.63 | |
| Depth of hole (cm)(D)= | 100 | | Distance between static water level and bottom of hole (H) = (D-E) = | 70.5 | |
| Soil Surface to initial water table (cm) (E)= | 29.5 | | H/r = | 15.6667 | |
| Observation number | Depth to water from measuring point (cm) | time (sec) | Distance between static water table and water in hole(di-T-E)=(yi) | Change in y (Δy) | Average y [(yi + yi+1)/2] |
| 1 | 123 | 0 | 70 | | |
| 2 | 119 | 30 | 66 | 4 | 68 |
| 3 | 116.4 | 60 | 63.4 | 2.6 | 64.7 |
| 4 | 113.8 | 90 | 60.8 | 2.6 | 62.1 |
| 5 | 111.3 | 120 | 58.3 | 2.5 | 59.55 |
| 6 | 109.2 | 150 | 56.2 | 2.1 | 57.25 |
| 7 | 107.4 | 180 | 54.4 | 1.8 | 55.3 |
| 8 | 105.8 | 210 | 52.8 | 1.6 | 53.6 |
| 9 | 104.4 | 240 | Measurements past 25% rise not included in calculations | | |
| 10 | 103 | 270 | | | |

Table A.1 continued.

| Observation number | Change in time (Δt) | Δy/Δt | y/H | C factor | Ksat (m/day) | Ksat (cm/day) |
|---|---|---|---|---|---|---|
| 1 | | | | | | |
| 2 | 30 | 0.133333 | 0.964539 | 7.1674938 | 0.9556658 | 95.56658 |
| 3 | 30 | 0.086667 | 0.91773 | 7.2072615 | 0.6246293 | 62.46293 |
| 4 | 30 | 0.086667 | 0.880851 | 7.2615695 | 0.629336 | 62.9336 |
| 5 | 30 | 0.083333 | 0.844681 | 7.3354413 | 0.6112868 | 61.12868 |
| 6 | 30 | 0.07 | 0.812057 | 7.4205961 | 0.5194417 | 51.94417 |
| 7 | 30 | 0.06 | 0.784397 | 7.5074621 | 0.4504477 | 45.04477 |
| 8 | 30 | 0.053333 | 0.760284 | 7.5949143 | 0.4050621 | 40.50621 |
| | | | | **Average=** | 0.5994099 | 59.94099 |

**Guelph Permeameter**

Table A.2. Calculation formulas related to shape factor ($C$). Where $H_1$ is the first water head height (cm), $H_2$ is the second water head height (cm), α is borehole radius (cm) and α* is microscopic capillary length factor which is decided according to the soil texture-structure category. For one-head method, only $C_1$ needs to be calculated while for two-head method, $C_1$ and $C_2$ are calculated (Soil Moisture Equipment Corp, 2012). A α* value of 0.12 was selected for this study.

| Soil Texture-Structure Category | $\alpha^*(cm^{-1})$ | Shape Factor |
|---|---|---|
| Compacted, Structure-less, clayey or silty materials such as landfill caps and liners, lacustrine or marine sediments, etc. | 0.01 | $C_1 = \left(\frac{H_2/a}{2.081 + 0.121\left(H_2/a\right)}\right)^{0.672}$ |
| Soils which are both fine textured (clayey or silty) and unstructured; may also include some fine sands. | 0.04 | $C_1 = \left(\frac{H_1/a}{1.992 + 0.091\left(H_1/a\right)}\right)^{0.683}$<br>$C_2 = \left(\frac{H_2/a}{1.992 + 0.091\left(H_2/a\right)}\right)^{0.683}$ |
| Most structured soils from clays through loams; also includes unstructured medium and fine sands. The category most frequently applicable for agricultural soils. | 0.12 | $C_1 = \left(\frac{H_1/a}{2.074 + 0.093\left(H_1/a\right)}\right)^{0.754}$<br>$C_2 = \left(\frac{H_2/a}{2.074 + 0.093\left(H_2/a\right)}\right)^{0.754}$ |
| Coarse and gravely sands; may also include some highly structured soils with large and/or numerous cracks, macro pores, etc. | 0.36 | $C_1 = \left(\frac{H_1/a}{2.074 + 0.093\left(H_1/a\right)}\right)^{0.754}$<br>$C_2 = \left(\frac{H_2/a}{2.074 + 0.093\left(H_2/a\right)}\right)^{0.754}$ |

Table A.3. Calculation formulas related to one-head and two-head methods. Where $\overline{R}$ is steady-state rate of fall of water in reservoir (cm/s), $K_{fs}$ is Soil saturated hydraulic conductivity (cm/s), $\phi_m$ is Soil matric flux potential ($cm^2/s$), α* is Macroscopic capillary length parameter (from Table 1), α is Borehole radius (cm), $H_1$ is the first head of water established in borehole (cm), $H_2$ is the second head of water established in borehole (cm), and $C$ is shape factor (from Table 1) (Soil Moisture Equipment Corp, 2012).

| | | |
|---|---|---|
| One Head, Combined Reservoir | $Q_1 = \bar{R}_1 \times 35.22$ | $K_{fs} = \frac{C_1 \times Q_1}{2\pi H_1^2 + \pi a^2 C_1 + 2\pi\left(\frac{H_1}{a^*}\right)}$<br>$\Phi_m = \frac{C_1 \times Q_1}{(2\pi H_1^2 + \pi a^2 C_1)a^* + 2\pi H_1}$ |
| One Head, Inner Reservoir | $Q_1 = \bar{R}_1 \times 2.16$ | |
| Two Head, Combined Reservoir | $Q_1 = \bar{R}_1 \times 35.22$<br>$Q_2 = \bar{R}_2 \times 35.22$ | $G_1 = \frac{H_2 C_1}{\pi(2H_1H_2(H_2 - H_1) + a^2(H_1C_2 - H_2C_1))}$<br>$G_2 = \frac{H_1 C_2}{\pi(2H_1H_2(H_2 - H_1) + a^2(H_1C_2 - H_2C_1))}$<br>$K_{fs} = G_2Q_2 - G_1Q_1$<br>$G_3 = \frac{(2H_2^2 + a^2C_2)C_1}{2\pi(2H_1H_2(H_2 - H_1) + a^2(H_1C_2 - H_2C_1))}$<br>$G_4 = \frac{(2H_1^2 + a^2C_1)C_2}{2\pi(2H_1H_2(H_2 - H_1) + a^2(H_1C_2 - H_2C_1))}$<br>$\Phi_m = G_3Q_1 - G_4Q_2$ |
| Two Head, Inner Reservoir | $Q_1 = \bar{R}_1 \times 2.16$<br>$Q_2 = \bar{R}_2 \times 2.16$ | |

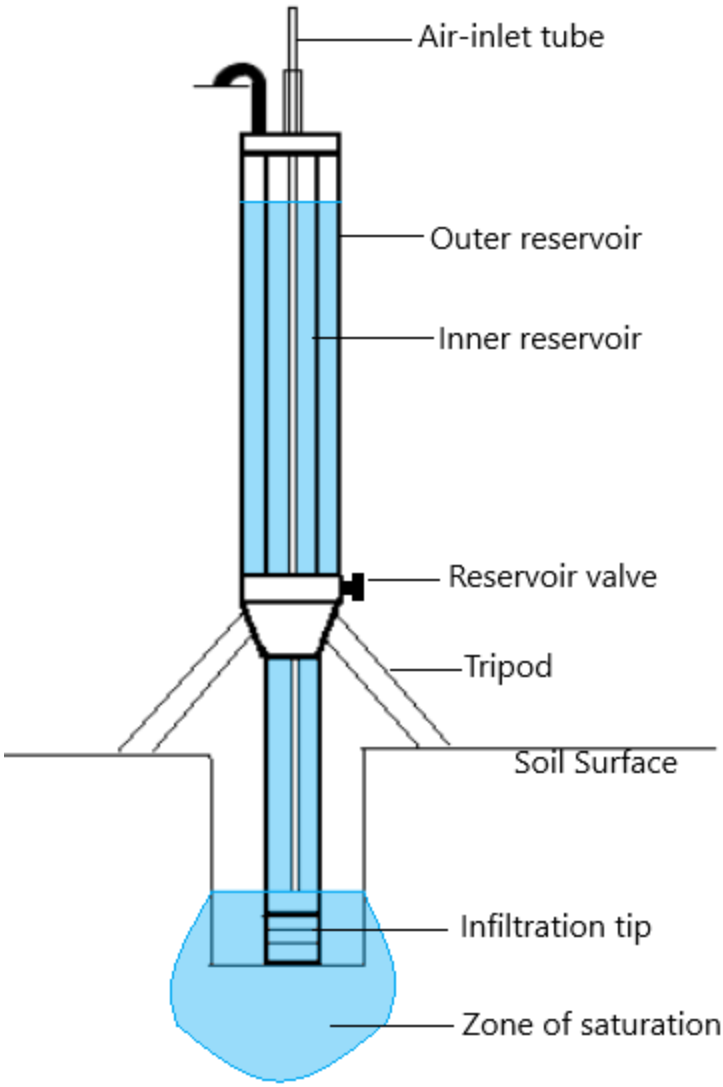


Figure A.2. Guelph Permeameter diagram.

Table A.4. Example data sheet for the Guelph permeameter measurements.

| **Date:** | 8/12/2019 | **Plot/Rep:** | 5 m Block 1 |
|---|---|---|---|
| **Depth of Hole:** | 63.5 cm | **Head Height:** | 25 cm |
| **Hole Radius:** | 3 cm | | |
| **Combined (X)** or Inner (Y) Reservoir | | | |
| Time (min) | Water Level in Reservoir (cm) | Water Level Change (cm) | Rate of Change, R (cm/min) |
| 0 | 23.5 | ----- | ----- |
| 2 | 24.8 | 1.3 | 0.65 |
| 4 | 26.2 | 1.4 | 0.7 |
| 6 | 27.2 | 1 | 0.5 |
| 8 | 28.4 | 1.2 | 0.6 |
| 10 | 29.4 | 1 | 0.5 |
| 12 | 30.5 | 1.1 | 0.55 |
| 14 | 31.5 | 1 | 0.5 |
| 16 | 32.4 | 0.9 | 0.45 |
| 18 | 33.3 | 0.9 | 0.45 |
| 20 | 34.2 | 0.9 | 0.45 |

**Slug Test**

Equation A.3. Hvorselve's expression of hydraulic conductivity where K = hydraulic conductivity, r = radius of the well, R = radius of the well boring, L = length of perforated zone, $T_O$ = time it takes for the water level to rise to 0.37 on the y axis (y = $H_T/H_O$ = 0.37).

$$K = \frac{r^2 \ln(\frac{L}{R})}{2LT_0}$$

Table A.5. Example data sheet for the slug test.

| Plot 202 Well 1 Rep 1 | | |
|---|---|---|
| Hole diameter (cm)(2r)= | 2.54 | |
| Measuring point above soil surface (cm)(X)= | 20 | |
| Depth of hole (cm)(D)= | 150 | |
| Depth of water pumped out (cm) (Hto) = | 100 | |
| Soil Surface to intitial water table (cm) (Hs)= | 67.5 | |
| Allowable total length of water rise: (D-Hs)*0.25 = | 8.125 | |

| Observation number | Depth to water from measuring point (cm) (Ht) | time (min:sec) | Distance between static water table and water in hole (HT = Ht-Hs-X) | HO = Hto - Hs | HT/HO |
|---|---|---|---|---|---|
| 1 | 120 | 0 | 32.5 | 32.5 | 1 |
| 2 | 119.4 | 0:30 | 31.9 | 32.5 | 0.98153846 |
| 3 | 118.9 | 1:00 | 31.4 | 32.5 | 0.96615384 |
| 4 | 118.3 | 1:30 | 30.8 | 32.5 | 0.94769230 |
| 5 | 117.9 | 2:00 | 30.4 | 32.5 | 0.93538461 |
| 6 | 117.3 | 2:30 | 29.8 | 32.5 | 0.91692307 |
| 7 | 116.8 | 3:00 | 29.3 | 32.5 | 0.90153846 |
| 8 | 116.2 | 3:30 | 28.7 | 32.5 | 0.88307692 |
| 9 | 115.7 | 4:00 | 28.2 | 32.5 | 0.86769230 |
| 10 | 115.2 | 4:30 | 27.7 | 32.5 | 0.85230769 |
| 11 | 114.5 | 5:00 | 27 | 32.5 | 0.83076923 |
| 12 | 114.1 | 5:30 | 26.6 | 32.5 | 0.81846153 |
| 13 | 113.6 | 6:00 | 26.1 | 32.5 | 0.80307692 |
| 14 | 113.2 | 6:30 | 25.7 | 32.5 | 0.79076923 |
| 15 | 112.9 | 7:00 | 25.4 | 32.5 | 0.78153846 |
| 16 | 112.5 | 7:30 | 25 | 32.5 | 0.76923076 |
| 17 | 112 | 8:00 | 24.5 | 32.5 | 0.75384615 |
| 18 | 111.6 | 8:30 | 24.1 | 32.5 | 0.74153846 |

Table A.5 continued.

| TO (time on graph when y= 0.37) | L (length of perforated zone) (D-Hs) | R (radius of the well boring) (cm)* | K (cm/day) |
|---|---|---|---|
| 1248 | 82.5 | 3.81 | 2.08109381 |

*We are assuming a 3.81 cm radius of the well boring because the actual value has been lost to antiquity. The calculations were also conducted with a well boring radius of 2.54 cm and while the absolute values changed very slightly, the trends among treatments did not change.

Figure A.3. Graph of slug test data used to find TO.